U. S. DEPARTMENT OF COMMERCE
Charles Sawyer, Secretary
NATIONAL BUREAU OF STANDARDS
E. U. Condon, Director

JUNE 1950
VOLUME • 44
NUMBER 6

JOURNAL OF RESEARCH

of the

NATIONAL BUREAU OF STANDARDS

Contents

RP		Page
2103	A suggested relocation and respacing of the Union colorimeter scale for lubricating oil and petrolatum. Deane B. Judd, Lorenzo Plaza, and Marion A. Belknap. (Price 10 cents)	559
2104	Measurement of the proton moment in absolute units. Harold A. Thomas, Raymond L. Driscoll, and John A. Hipple. (Price 10 cents)	569
2105	Measurement of sixty-degree specular gloss. Harry K. Hammond, III, and Isadore Nimeroff. (Price 10 cents)	585
2106	Rate of shrinkage of tendon collagen: Further effects of tannage and liquid environment on the activation constants of shrinkage. C. E. Weir and J. Carter. (Price 10 cents)	599
2107	Molecular microwave spectra tables. Paul Kisliuk and Charles H. Townes. (Price 20 cents)	611
	Index to volume 44 (January to June 1950, Research Papers RP2053 to RP2107).	643

For sale by the Superintendent of Documents, U. S. Government Printing Office, Washington 25, D. C. • Price 60 cents
$4.50 per year on subscription

UNITED STATES GOVERNMENT PRINTING OFFICE, WASHINGTON : 1950

U. S. Department of Commerce
National Bureau of Standards

Research Paper RP2103
Volume 44, June 1950

Part of the Journal of Research of the National Bureau of Standards

A Suggested Relocation and Respacing of the Union Colorimeter Scale for Lubricating Oil and Petrolatum

By Deane B. Judd, Lorenzo Plaza, and Marion A. Belknap

At the request of Research Division IX, Committee D–2 of the American Society for Testing Materials, a study of the chromaticities and daylight transmittances of petroleum products has been carried out. From the results of this study a recommended relocation of the ASTM Union colorimeter scale has been derived that is intended to minimize the difficulties frequently experienced in the color-grading of off-color petroleum products. This study also revealed in some detail discrepancies in color-grading between laboratories ascribable to failure of the glass color standards of the various Union colorimeters to conform to the master standards. It has been found possible to respace the color standards along the relocated locus by changes smaller than these interlaboratory discrepancies so as to yield uniform color steps as perceived by the eye under the conditions of observation prescribed by the method of test in ASTM D 155–45T. This relocation and respacing of the Union colorimeter scale is presented as a suggestion for possible adoption by the industry.

I. Introduction

Since 1923 it has been customary to measure and specify the color of lubricating oil and petrolatum by means of the ASTM Union colorimeter.[1] This colorimeter consists of an artificial daylight assembly with flashed-opal diffuse light transmitter; a jar of internal diameter between 32.5 and 33.4 mm to hold the test sample; a series of 12 glass color standards ranging from pale greenish yellow to dark red and mounted in a vertical slide that may be raised or lowered to permit one or another of the standards to be viewed; a light shield to prevent extraneous light from falling on sample or standard; and an arrangement of partitions and diaphragms permitting the observer to view the color of the glass standard and the color of the test sample as filling two circles subtending at the eye of the observer about 2° with their centers separated by about 6°, the surrounding field being dark. The glass color standards are combinations of Lovibond glasses obtained from Tintometer, Ltd.

The spectral transmittances of the master standards for the Union color scale were determined at this Bureau,[2] and their luminous transmittances, T_0, and chromaticity coordinates, x, y, were computed in accord with the ICI standard observer and coordinate system for colorimetry[3] by Scofield, Judd, and Hunter.[4] Table 1 repeats the Lovibond analysis of these master standards given in D 155–45T (see footnote 1), and gives the luminous transmittances and the chromaticity coordinates both on the ICI system (x, y) and on the UCS system (r, g).[5]

[1] ASTM Tentative method of tests for color of lubricating oil and petrolatum by means of ASTM colorimeter, ASTM Designation: D 155-45T, ASTM standards, part III-A, p. 839 (1946).

[2] Report of NBS Test No. 57968, issued December 18, 1929, to ASTM Committee D-2 on Petroleum Products and Lubricants.

[3] Proceedings, Eighth Session, Commission Internationale de L'Éclairage, Cambridge, England, September 1931, p. 19–29; also A. C. Hardy, Handbook of colorimetry (Cambridge, Technology Press, 1936); also D. B. Judd, The 1931 ICI standard observer and coordinate system for colorimetry, J. Opt. Soc. Am. **23**, 359 (1933).

[4] F. Scofield, D. B. Judd, and R. S. Hunter, A proposed method of designating color, ASTM Bulletin, p. 19 (May 1941).

[5] D. B. Judd, A Maxwell triangle yielding uniform chromaticity scales, J. Research NBS **14**, 41 (1935) RP756; J. Opt. Soc. Am. **25**, 24 (1935).

TABLE 1. *Colorimetric specifications of the 12 glasses comprising the Union color scale; illuminant: ICI standard C (average daylight)*

ASTM color numbers	Lovibond analysis			Luminous transmittance	Chromaticity coordinates			
	Red	Yellow	Blue		ICI system		UCS system	
				T_3	x	y	r	g
1	0.12	2.4	.....	0.751	0.3488	0.3815	0.462	0.476
1½	.60	8.0	.....	.654	.3995	.4460	.491	.477
2	2.5	26.0	.....	.443	.4724	.4765	.542	.448
2½	4.6	27.0	.....	.365	.4985	.4570	.570	.421
3	6.9	32.0	.....	.287	.5252	.4402	.600	.393
3½	9.4	45.0	.....	.211	.5561	.4234	.636	.360
4	14.0	50.0	0.55	.086	.5908	.3995	.683	.315
4½	21.0	56.0	.55	.065	.6199	.3758	.729	.270
5	35.0	93.0	.....	.036	.6528	.3467	.789	.210
6	60.0	60.0	.55	.017	.6764	.3234	.841	.159
7	60.0	106.0	1.8	.0066	.6841	.3155	.860	.140
8	166.0	64.0	.....	.0020	.7140	.2860	.938	.062

To determine the ASTM color number of an oil, the oil is put into the standard jar, and the jar is placed in the right-hand compartment. In the other compartment is placed a 4-ounce sample bottle of distilled water. The jar and bottle are covered with the light shield, and the artificial daylight lamp is lighted. The color of the oil is obtained by determining the glass color standard that most nearly matches the color of the oil under examination. The colors of oils that are intermediate to the standard colors are expressed in terms of the darker as "lighter than" or "minus". For example, an oil that has a color between 7 and 8 is expressed as "lighter than 8" or "8 minus". In determining the darker colors, the daylight lamp is sometimes moved closer to the opal-glass diffuser.

For many oils the Union colorimeter is quite satisfactory. The results are obtained rapidly, and one observer can repeat his own results or those of another observer without trouble. This indicates that the glass color standards have been chosen with some care so as to cover the color range of these oils with good precision. Other oils, however, depart considerably from the locus of colors defined by the 12 standards of the Union color scale. For such oils, the observer finds that none of the standards yields a color match, nor does it seem to him that the oil color is intermediate between any two of the standard colors.

II. Committee Deliberations on Relocation

Color is a three-dimensional quantity; it requires for its specification at least three independent scales. The simplicity of the Union color scale is based upon the fact that it describes a one-dimensional variation. That is, the Union color scale corresponds to a single (curved) line in the color solid, and it serves well for those colors represented on (or near) that one line. Relocation of the one-dimensional color scale cannot make it applicable to all oils, but by choosing color standards that correspond to the average color of oils it is possible to minimize the difficulties introduced by off-color oils.

Another source of error in grading oils by ASTM Method D 155–45T arises from the difficulty of obtaining precise duplicates of the master standards of the Union color scale. At its Detroit meeting in June 1948, Subcommittee VI on Color, ASTM Committee D–2 on Petroleum Products, decided to cooperate with the C. J. Tagliabue Manufacturing Co., maker of the ASTM Union colorimeter, in an attempt to make possible the procurement of color standards from an American source of supply, procurement of satisfactory duplicates from the present foreign source of supply (Tintometer, Ltd., Salisbury, England) having become increasingly difficult, due primarily to shortage in the supply of Lovibond glasses. It was proposed first that the master standards, or duplicates of certain of them that have become scratched or chipped, be submitted to the Corning Glass Works as a guide in the preparation of a set of glasses that should give a visual match for the colors of the master standards. Second, it was proposed that these matching color glasses be submitted to a referee laboratory, such as the National Bureau of Standards, so that their spectral transmittances might be determined and the luminous transmittances and chromaticity coordinates for illuminant C calculated. Third, it was suggested that tolerances in the procurement of duplicates from Corning Glass Works be set at ± 0.006 in chromaticity coordinates (r, g) on the UCS system and either at ± 10 percent of the luminous transmittance or at 10 percent for the darker glasses with smaller tolerances on a sliding scale for the lighter glasses, the differences between the approved matching color glasses and the duplicates to be evaluated by visual colorimetry.

Following the Detroit meeting, a summary of available colorimetric data (transmittance and chromaticity coordinates on the UCS system) of

the master standards and certain approximate duplicates of them prepared before 1939 by the Jena Glass Works of Germany was drawn up by H. M. Hancock, Chairman, and circulated on October 11, 1948, to the members of the subcommittee. This summary included remarks on the goodness of match judged by visual comparison of the Jena approximate duplicates with the respective master standards. This comparison corroborated the proposed tolerance on chromaticity coordinates (r, g, b) of ± 0.006, and suggested that the transmittance tolerance be set at ± 10 percent for the darkest glass (Union No. 8) and progressively reduced to about ± 4 percent for the lightest (Union No. 1).

On November 5, 1948, a meeting of representatives of the C. J. Tagliabue Co., the Weston Electric Instrument Co., the Corning Glass Works, and Subcommittee VI, ASTM D–2, was held to discuss feasibility of procuring from Corning Glass Works duplicates of the master standards within these suggested tolerances. The representative of the Corning Glass Works (A. J. Werner) reported that the present glasses available through Corning would permit two-component combinations, one component being amethyst glass, to be made that would satisfy the tolerances above Union No. 3½, but that those below 3½ exhibited a consistent shift toward yellow. A number of sets of these glasses have been made up and sold. Mr. Werner agreed to investigate the possibility of using a different combination of glasses that would satisfy the tolerances for glasses below 3½ also.

Following this preliminary meeting, the November 1948 meeting of Subcommittee VI was held in Chicago. It was pointed out in discussion of Mr. Werner's difficulty with glasses to duplicate the lighter standards (less than 3½) that measurements of 22 petroleum products by Diller, De Gray, and Wilson [6] indicated that they departed from the Union locus in the same range and direction. It was voted that the subcommittee undertake to determine the average colors of oils in the range of Union 1 to 3½ based upon a more adequate sampling than is afforded by the 22 products measured by Diller, De Gray, and Wilson. Accordingly, the various members of the subcommittee submitted representative samples of finished and processed petroleum products up to and including Union No. 3½ to H. M. Hancock, Chairman A selection of 49 representative samples of this group of petroleum products was then made, and the 49 samples were sent to this Bureau for measurement of luminous transmittance and chromaticity coordinates. One purpose of this paper is to give the method and results of these measurements and to recommend a relocation of the Union color scale based upon them.

[6] M. Diller, R. J. De Gray, and J. W. Wilson, Jr., Photoelectric color description, and mensuration of the color of petroleum products, Ind. Eng. Chem. 14, 607 (1942).

III. Committee Deliberations on Respacing

At the Chicago meeting, the question of whether the present spacing of the color standards of the Union scale ought to be duplicated was also raised. It was pointed out that the scale proceeds by half steps up to 5, then by whole steps up to 8. Furthermore, the perceptual difference between Union No. 6 and 7 is much smaller than that between 7 and 8. This is shown by the spectrophotometric determinations (see table 1, $r_6=0.841$, $r_7=0.860$, $r_8=0.938$) and by visual inspection of the master standards. Would it not be better, it was argued, if we are going to relocate the Union locus anyway, to request Corning Glass Works to supply duplicates of a master set of standards having as close an approximation as is possible to uniform perceptual spacing? Is it not foolish to reproduce with great care all of the defects of a choice of color scale made in 1923? Some members of the subcommittee viewed with discomfort the prospect of changing the meaning of the various Union numbers. This would cause confusion between the old and the new meanings and would give rise to disputes and dislocations of present practice in writing purchase specifications of petroleum products, they thought. It was pointed out by Mr. Hancock, however, that a great improvement in uniformity of spacing could be achieved by making changes that would be less than the spread between color standards of the same Union color number in the different colorimeters now in use. He presented two tentative suggestions, one at the meeting, one soon after, in a letter of November 24, 1948, showing that only relatively small changes might be required. Table 2 gives these tentative suggestions in terms of the r-coordinate of the UCS-system.

TABLE 2. *Suggestions by H. M. Hancock for respacing of the Union color scale*

Union standard			Suggestion at Chicago meeting			Suggestion of November 24, 1948		
N	r	$\frac{\Delta r}{\Delta N}$	r	$\frac{\Delta r}{\Delta N}$	Equivalent on present Union scale	r	$\frac{\Delta r}{\Delta N}$	Equivalent on present Union scale
2	0.542		0.528		1.8	0.542		2.0
		0.056		0.072			0.068	
2.5	.570		.564		2.4	.576		2.6
		.060		.072			.076	
3	.600		.600		3.0	.614		3.2
		.072		.072			.066	
3.5	.636		.636		3.5	.647		3.6
		.094		.062			.072	
4	.683		.667		3.8	.683		4.0
		.092		.080			.064	
4.5	.729		.707		4.2	.715		4.3
		.120		.064			.068	
5	.789		.739		4.6	.749		4.7
		.052		.067			.067	
6	.841		.806		5.3	.816		5.5
		.019		.068			.068	
7	.860		.874		7.2	.884		7.3
		.078		.064			.070	
8	.938		.938		8.0	.954		8.2

It may be seen from table 2 that the chromaticity spacing ($(\Delta r/\Delta N)$ of the revisions suggested by Mr. Hancock is indeed much more constant than that of the present Union scale. The variation in step size has been reduced from 0.100 in the Union scale to 0.018 in the Chicago suggestion and to 0.012 in the suggestion of November 24. These marked improvements in chromaticity spacing have been obtained by shifts that average about 0.2 of a step in the Union scale. In criticism of Mr. Hancock's suggestions, however, it was remarked at the Chicago meeting that the perceptual size of the steps in the color scale might not be correctly indicated by spacing of the r-coordinate of the colors. The UCS system gives a close approach to uniform chromaticity spacing only when the luminance of the fields being compared remains substantially at the same level. Since the luminous transmittance of the standards varies from 75 percent down to 0.2 percent, there is some question whether there is enough light available to permit the eye to distinguish the chromaticity differences between the darker members of the set of color standards with as much facility as those between the lighter members. Since the method permits moving the daylight lamp closer to the diffuser for the darker colors, it would seem that a lack of sufficient light is to be admitted and that some account should be taken of the luminance of the fields being compared by spacing out the darker members of the color scale more than would be indicated by a uniform spacing of chromaticity alone.

Another possibility that ought to be taken into account is the fact that the members of each pair of neighboring color standards in the set differ appreciably in luminous transmittance. Although the separation of the two fields to be compared by a sizable dark area tends to obscure the luminance difference between them, it is possible that the perceptual size of the step depends appreciably on the luminance difference as well as the chromaticity difference.

It was agreed at the Chicago meeting that suitable account should be taken of these two factors, and one of us (DBJ) was requested to derive a respacing of the Union scale that should appear uniform under the conditions of viewing embodied in the ASTM Union colorimeter. It is the second purpose of this paper to give the results of the derivation made.

IV. Measurement of Luminous Transmittance, T, and Chromaticity Coordinates, x, y, of 49 Samples of Petroleum Products

Each of the 49 samples was compared by the substitution method with two glass standards of known spectral transmittance by means of a photoelectric colorimeter with tristimulus filters[7] belonging to the Henry A. Gardner Laboratory, Bethesda, Md. This colorimeter is designed especially for the measurement of liquids in cylindrical cells and permitted one of us (MAB) to make the measurements of the samples without removing them from the sample bottles, which conform closely to the requirements of ASTM Method D 155–45T for the standard jar. Thanks are due to R. S. Hunter of the Henry A. Gardner Laboratory for his courtesy in permitting us to bring the oil samples to his laboratory for these measurements. The glass standards used are the master standards developed to check photoelectric colorimeters used to determine a color index for

[7] R. S. Hunter, Photoelectric tristimulus colorimetry with three filters, NBS Circular C429 (July 30, 1942).

petroleum products.[8] These glasses resemble petroleum products closely in spectral characteristics. The luminous transmittances of these glass standards for ICI illuminant C (average daylight) have been computed, together with the chromaticity coordinates (x, y) by routine methods (see footnote 3). The reduction of the data to yield these quantities for the 49 samples of petroleum products was likewise carried out by routine methods (see footnote 7). From the agreement obtained between results by way of different standards it is estimated that the values of chromaticity coordinates (x, y) are uncertain by not more than 0.005. Table 3 shows the results; figure 1 is a portion of the (x, y)-chromaticity diagram showing how the chromaticity coordinates of these oils compare with the master standards of the Union color scale. The curve is the recommended relocation of the Union color scale; it is intended to be a smooth average of the chromaticity variation shown by the petroleum products. Note that with three exceptions all of the oil samples between Union 2 and 3½ deviate from the Union locus in the direction of the spectrum locus. This corroborates the report by Diller, De Gray, and Wilson (see footnote 6), although these deviations average less than those for the petroleum products studied by them. It would appear from figure 1 that an appreciable reduction of trouble from off-color oils is to be obtained by this relocation of the Union color scale.

In addition to accomplishing their chief purpose of supplying information basic to relocation of the Union color scale, these data also constitute an interlaboratory comparison of grading by the ASTM Union colorimeter. This comes about from the fact that 46 out of the 49 oil samples were marked with the ASTM (or NPA) number when submitted.[9] From figure 1 it is possible to estimate with a maximum uncertainty of 0.2 Union step what this number would be if the judgment had been made on the basis of nearest chromaticity. These estimates are given in the third column of table 1. It is seen that on the average the ASTM number reported by the re-

TABLE 3. *Luminous transmittance, T, and chromaticity coordinates x, y of 49 petroleum products*

Serial number	ASTM or NPA color number		Laboratory and sample number	Chromaticity coordinates		Daylight transmittance, T
	Reported by refiner	From nearest chromaticity match		x	y	
1	1	0.7	C	0.342	0.357	0.820
2	1 Dk	.8	E-6	.343	.366	.848
3	¾	.2	A-1	.317	.327	.804
4	1 Dk	.9	E-1	.346	.375	.866
5	1	1.0	B-1	.352	.386	.847
6	1 Lt	.4	E-7	.326	.344	.897
7	1	.8	F	.343	.365	.850
8	1	1.0	D-222	.352	.379	.819
9	1	1.1	D-227	.363	.392	.824
10	1½	1.6	D-228	.414	.454	.735
11	1½	1.5	F	.402	.445	.784
12	1½ Dk	1.6	E-10	.418	.462	.700
13	---	1.1	48-54	.363	.397	.838
14	1¾	1.6	D-218	.422	.444	.634
15	---	1.5	A-2	.404	.434	.717
16	1½	1.5	C	.407	.432	.700
17	---	2.1	48-56	.485	.477	.533
18	1½	1.5	B-2	.404	.445	.782
19	1½	1.6	D-223	.411	.455	.741
20	1½	2.0	A-4	.466	.466	.568
21	---	1.5	48-55	.407	.448	.768
22	1¾	2.0	A-5	.482	.503	.635
23	2	2.0	F	.474	.495	.626
24	2	2.2	D-224	.491	.486	.530
25	2	2.2	D-229	.487	.482	.546
26	2	2.2	D-219	.489	.476	.429
27	2 Dk	2.0	E-4	.473	.496	.650
28	2	1.9	C	.464	.491	.656
29	2	2.1	B-3	.479	.472	.560
30	2½ Lt	2.2	E-8	.488	.474	.518
31	2½	2.6	B-4A	.519	.468	.440
32	2½	2.8	D-230	.528	.460	.392
33	2½	2.5	B-4	.513	.460	.422
34	2½	3.0	F	.511	.478	.508
35	2½	2.9	D-225	.532	.460	.367
36	2½ Dk	2.5	E-11	.494	.456	.486
37	2½	2.7	D-220	.525	.462	.310
38	2½	2.7	A-6	.524	.465	.442
39	2½	3.0	A-7	.538	.457	.392
40	2¾	3.0	A-8	.538	.456	.363
41	3	3.0	B-5A	.540	.452	.349
42	3	3.0	B-5	.536	.457	.390
43	3	3.2	D-231	.550	.443	.289
44	3	3.3	D-226	.553	.440	.267
45	3	3.5	D-221	.561	.431	.177
46	3	3.0	F	.537	.457	.374
47	3 Lt	2.7	E-9	.521	.470	.366
48	3¼	4.0	A-9	.592	.403	.127
49	3½	3.2	E-12	.549	.444	.271

[8] A proposed method for determination of a color index for petroleum products, Appendix IV, 1947 Report of ASTM Committee D-2.

[9] Acknowledgment is made to the following laboratories supplying these data: Shell Development Co., Atlantic Refining Co., Socony-Vacuum Oil Co., Inc., Sun Oil Co., Esso Standard Oil Co., and Phillips Petroleum Co.

finer agrees closely with those indicated by this colorimetric study. However, one oil (Serial No. 48) is graded lower by 0.7 than our measurements would place it, and another similar oil (Serial No. 49) is graded higher by 0.3. This suggests that there is a serious discrepancy between the Union 3½ glasses used in the two laboratories.

Table 4 gives a breakdown of this sort of difference according to laboratory. It will be noted that there is a remarkably consistent tendency for one laboratory to read high by about 0.2, for two laboratories to read low by 0.2 and 0.3, respectively, and for one laboratory to yield agreement with the present results.

TABLE 4. *Interlaboratory comparison of grading by the ASTM Union Colorimeter*

ASTM Union no. reported by refiner	ASTM number reported by the laboratory of the refiner minus the ASTM number obtained in the present test					
	Lab. A	Lab. B	Lab. C	Lab. D	Lab. E	Lab. F
¼	0.0	----	----	----	----	----
1 Lt (=0.8)	----	----	----	----	+0.4	----
1	----	0.0	+0.3	0.0	----	+0.2
				−.1	----	----
1 Dk (=1.2)	----	----	----	----	+.4	----
					+.3	----
1¼	−.2	----	----	----	----	----
1½	−.5	.0	.0	−.1	----	.0
				−.1	----	----
				−.1	----	----
1½ Dk (=1.7)	−.3	----	----	----	+.1	----
2	----	−.1	+.1	−.2	----	.0
				−.2	----	----
				−.2	----	----
2 Dk (=2.2)	----	----	----	----	+.2	----
2½ Lt (=2.3)	----	----	----	----	+.1	----
2½	−.2	−.1		−.3	----	.5
	−.5	.0	----	−.4	----	----
				−.2	----	----
2½ Dk (=2.7)	----	----	----	----	+.2	----
2¾	−.2	----	----	----	----	----
3 Lt (=2.8)	----	----	----	----	+.1	----
3	----	.0		−.2	----	.0
		.0	----	−.3	----	----
				−.5	----	----
3¼	−.7	----	----	----	----	----
3½	----	----	----	----	+.3	----
Average	−0.3	0.0	+0.1	−0.2	+0.2	−0.1

V. Respacing of the Union Color Scale

By reference to ASTM D 155–45T (see footnote 1), it may be seen that the observer views two circular spots of color (9/16 inch in diameter at a distance of 15 inches) subtending about 2° at his eye with their centers separated by about 6°, both surrounded by a dark field. The light source (60-watt bulb of about 13 lumens per watt) supplies a luminous flux of 780 lumens nearly all of which, because of the reflector, is fairly uniformly distributed over the hemisphere viewed

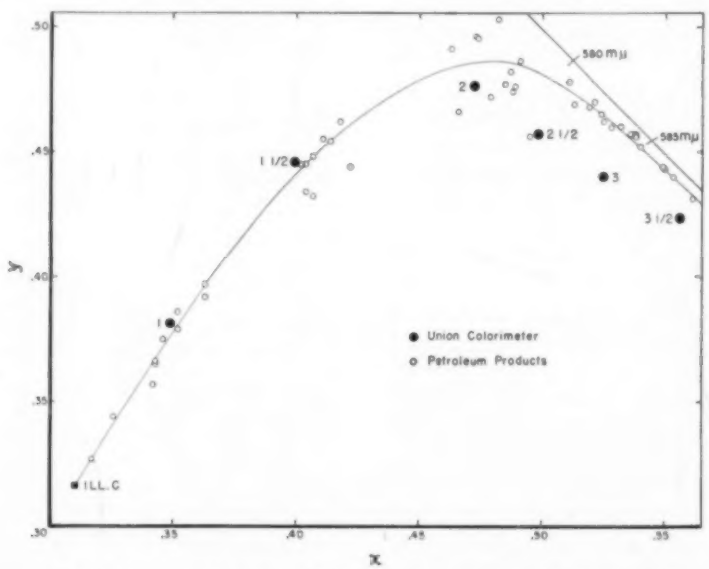

FIGURE 1. *Comparison of the chromaticities of the Union colorimeter standards with those of representative petroleum products collected by Subcommittee VI (now Research Division IX), ASTM Committee D–2.*

The curved line on this (*x,y*)-chromaticity diagram, running from the point representing illuminant C (average daylight) to a region near the spectrum locus at 585 mμ and beyond, corresponds closely to the average of these petroleum products, and is recommended as a relocation of the Union colorimeter scale

toward the opal-glass diffuser, except that there is a bright spot corresponding to the lamp filament located close to the axis of the instrument. The portion of the diffuser viewed in either of the observing fields subtends at a distance of 4 inches about one-twentieth of the hemisphere. The useful light flux striking the diffuser is about 60 lumens. This flux would light up a perfectly transmitting, perfectly diffusing plate to a luminance (photometric brightness) of about 45 foot-Lamberts. Counting the transmittance of the flashed-opal diffuser as 30 percent and the transmittance of the daylight filter as 16 percent, we find the luminance of the field without any oil sample or glass color standard interposed to be about 2 foot-Lamberts. This is about double the least luminance required to permit the eye to detect chromaticity differences with an approach to maximum efficiency; so it may be concluded that the lighting unit is all that could be asked for if used for samples that transmit more than 50 percent (Union No. 2 and lower), but that darker samples would be more easily distinguished in chromaticity if more light were provided.

Consider then three types of spacings of the Union color range: (1) that intended to be uniform for oils of the Union color range viewed in the standard bottles (1 5/16-inch inside diameter) against the sky (as on a shelf in front of a window), (2) that intended to be uniform for the Union colorimeter specified in D 155–45T, and (3) that intended to be uniform for fields maintained at more than 1 foot-Lambert over the whole range. In all of these scales, set the end points to correspond to a clear glass with standard source C ($r=0.439, g=0.465, b=0.086$) as zero and to a dark-red glass whose chromaticity is represented by the point ($r=0.956$, $g=0.044$, $b=0.000$) at 8.0, as in Mr. Hancock's suggestion of November 24, 1948 (see table 2). The chromaticity locus to be covered is that corresponding to the average curve drawn on figure 1 of the present report for the 49 representative samples of petroleum products, and the variation of daylight transmittance with chromaticity is based upon the values in tables 3 of the present report, supplemented for the darker parts of the scale by data given by Diller, De Gray, and Wilson (see footnote 6).

The spacing (1), intended to appear uniform if the oils are viewed in bottles against the sky, may be derived with good reliability from the formula for color difference, ΔE, published by Judd [10] in 1939 and subjected to numerous checks since that time:

$$\Delta E=600\left[T^{1/2}\overline{\Delta S}^2+0.02\overline{\Delta(T^{1/2})}^2\right]^{1/2} \qquad (1)$$

where $\overline{\Delta S}^2=\overline{\Delta r}^2+\overline{\Delta g}^2+\overline{\Delta b}^2$, r, g, b, being chromaticity coordinates on the UCS triangle (see footnote 5), and T being luminous transmittance for standard source C. The factor used to weight the lightness difference relative to the chromatic difference has been taken at 0.02 rather than the published value of 0.04, because the color produced by the oils in bottles side by side are not juxtaposed but are separated by areas of contrasting color (daylight passing between the bottles). Although this interferes slightly with the perception of chromatic differences, it interferes importantly with the perception of lightness differences. This spacing (1) is of value to the present discussion because, as will appear presently, spacing (2), which it is our purpose to derive, must necessarily lie between spacing (1) and spacing (3).

Spacing (3), intended to appear uniform under the viewing conditions of the Union colorimeter except that the field luminance is to be maintained (such as by a higher wattage source and a system of condensing lenses) in excess of 1 foot-Lambert, can be computed from the analogous formula

$$\Delta E=600\left[T^{0}\overline{\Delta S}^2+0.02\overline{\Delta(T^{1/2})}^2\right]^{1/2}. \qquad (3)$$

It differs from the formula for spacing (1) by substitution of the term $T^0(=1)$, for the term, $T^{1/2}$, applying to $\overline{\Delta S}^2$. The factor, 0.02, applies to the Union colorimeter field because here too the color fields are separated by an area of contrasting color (much darker). Because of the low value, 0.02, of this constant factor, spacing (3) agrees essentially with spacing by uniform chromaticity alone much as was suggested by Mr. Hancock in his letter of November 24, 1948 (see table 2).

Spacings of type (2) intended to yield steps of equal visual importance under the viewing conditions now specified by the Union colorimeter must space out the darker colors (Union Nos. 6, 7, and 8) more than spacing (3) because not enough light is provided to distinguish these dark colors effi-

[10] D. B. Judd, Specification of color tolerances at the National Bureau of Standards, Am. J. Psychol. 52, 418 (July 1939).

ciently. The colorimeter field becomes much darker for some samples than the field to which the observer is adapted, in a way similar to viewing dark samples surrounded by the background (sky) supplying the illumination. Since the colorimeter screens the observer's eye from direct light from the source by providing a dark surrounding field, however, spacing (1) based on unshielded viewing must give steps in the dark-color range too large to apply to the Union colorimeter.

Exactly what spacing applies to the conditions of use of the colorimeter might depend importantly on whether room light is customarily excluded from the eyes of the observer, or whether he looks at the colorimeter field for two or three minutes to become adapted to it before making a reading on a dark sample, and on whether he moves the daylight-lamp assembly closer to the opal-glass diffusing plate for dark samples as is permitted by ASTM D 155–45T. Since there is probably no well-defined procedure in these respects, it must be admitted that any scale developed by setting the exponent of T between $\frac{1}{4}$ and $\frac{1}{16}$ would conform essentially to uniform spacing under the range of conditions permitted by ASTM D 155–45T.

Preliminary study [11] of the scales resulting from various choices of exponents within this range resulted in the tentative recommendation of the exponent, $\frac{1}{8}$, first, because it corresponds to the best estimate of the conditions under which the ASTM Union colorimeter is used, and second, because it departs by nearly the least amount possible from the present Union colorimeter standards. No considerations have arisen since this tentative recommendation was made that indicate any change. Accordingly, it is our present recommendation that the respacing of the Union color scale be based upon the formula

$$\Delta E = 600\left[T^{1/8}\overline{\Delta S}^2 + 0.02\overline{\Delta(T^{1/2})}^2\right]^{1/2} \quad (2)$$

Table 5 shows the specification of 16 points uniformly spaced by formula 2 between the end points $r=0.439, g=0.465, b=0.096$ (standard source C) and $r=0.956$, $g=0.044$, $b=0.000$, as in Mr. Hancock's suggestion of November 24, 1948 (see table 2). This scale follows the relocation of the Union locus indicated by the curve drawn in figure 1. The chromaticity coordinates (x, y) for a number of points on this curve were read from figure 1, and these coordinates were transformed to chromaticity coordinates (r, g, b) on the UCS system (see footnote 5) according to the transformation formulas

$$\left.\begin{aligned} r &= \frac{2.7760x + 2.1543y - 0.1192}{-1.0000x + 6.3553y + 1.5405} \\ g &= \frac{-2.9446x + 5.0323y + 0.8283}{-1.0000x + 6.3553y + 1.5405} \\ b &= 1.0000 - 1.0000r - 1.0000g \end{aligned}\right\}. \quad (4)$$

These points were plotted in triangular coordinates to form figure 2, and the smooth curve joining them indicates this relocation of the Union color scale in the UCS system. The points on this curve corresponding to uniform spacing by the above formula were found by trial and error by one of us (LP), and table 5 gives the details of the check of this trial-and-error solution showing to what

[11] Letter, Judd to Hancock, December 23, 1948.

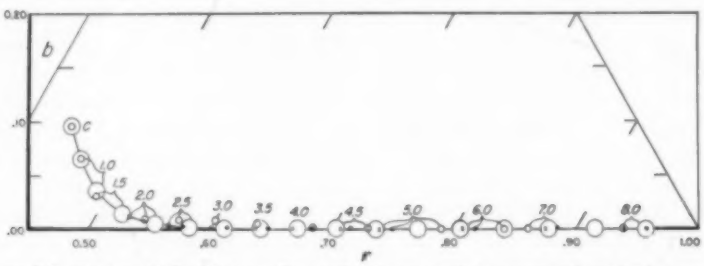

FIGURE 2. *Recommended spacing of the Union color scale (large circles) compared with the present Union scale (small circles) and with two suggestions for respacing by H. M. Hancock (dots and crosses).*

The UCS chromaticity diagram, formed by plotting at 60° the b-coordinate against the r-coordinate, is used. Uniform steps on this diagram are known to correspond, to a good approximation, to chromaticity scales that are perceptually uniform at constant luminance. Note that the darker colors (5 to 8) of the recommended spacing are spaced out more than the lighter colors (1 to 4). Note also the good agreement between the recommended scale derived by formula and the two suggestions made by Hancock from practical considerations alone.

degree the spacing is uniform according to the formula adopted (eq 2). It will be noted that the degree of uniformity indicated by this check cannot be improved unless the chromaticity coordinates are given to four decimals instead of to three. This recommended relocation and respacing of the Union color scale is compared in figure 2 with the present scale and with Mr. Hancock's two suggestions (see table 2). The open circles defining the chromaticities of the recommended standards have a radius of 0.006 so as to indicate the proposed tolerance.

TABLE 5. *Definition of the recommended scale (eq 2), comparison of its daylight transmittance with that of the Union scale, and check of its conformity to the defining equation*

Number	Definition of scale (2)				Union scale, T_b	Check of the scale (2) against the defining equation: $\Delta E = 600[T^{1/3}\overline{\Delta S^2} + 0.02\overline{\Delta(T^{1/3})^2}]^{1/2}$							
	Chromaticity coordinates			Daylight transmittance, T		$T^{1/3}$	$\overline{\Delta r^2}\times10^4$	$\overline{\Delta g^2}\times10^4$	$\overline{\Delta b^2}\times10^4$	$\overline{\Delta S^2}\times10^4$	$T^{1/3}\overline{\Delta S^2}\times10^4$	$0.02\overline{\Delta(T^{1/3})^2}$	NBS units, ΔE
	r	g	b										
0.0	0.439	0.465	0.096	0.922	.....	0.990	5.29	0.64	9.61	15.54	15.3	0.2	24
.5	.462	.473	.065	.856	.....	.981	7.29	.04	8.41	15.74	15.3	.4	24
1.0	.489	.475	.036	.774	0.751	.969	10.24	1.21	4.41	15.86	15.2	.7	24
1.5	.521	.464	.015	.672	.654	.954	9.61	4.84	0.81	15.26	14.3	1.3	24
2.0	.552	.442	.006	.548	.443	.928	9.00	6.76	.16	15.92	14.5	1.3	24
2.5	.582	.416	.002	.436	.365	.901	8.41	7.84	.01	16.26	14.4	2.0	24
3.0	.611	.388	.001	.314	.287	.865	8.41	8.41	.00	16.82	14.2	1.9	24
3.5	.640	.359	.001	.215	.211	.825	9.61	9.61	.00	19.22	15.5	1.1	24
4.0	.671	.328	.001	.152	.096	.790	10.24	10.24	.00	20.48	15.9	.7	24
4.5	.703	.296	.001	.109	.065	.758	10.89	10.24	.01	21.14	15.7	.4	24
5.0	.736	.264	.000	.081	.036	.730	11.56	11.56	.00	23.13	16.5	.4	25
5.5	.770	.230	.000	.058	.....	.700	12.25	12.25	.00	24.50	16.8	.3	25
6.0	.805	.195	.000	.040	.017	.669	12.96	12.96	.00	25.92	16.9	.3	25
6.5	.841	.159	.000	.026	.....	.634	12.96	12.96	.00	25.92	15.9	.3	24
7.0	.877	.123	.000	.016	.0066	.596	14.44	14.44	.00	28.88	16.4	.3	24
7.5	.915	.085	.000	.0081	.....	.548	16.81	16.81	.00	33.62	17.2	.3	25
8.0	.956	.044	.000	.0025	.0020	.473	.....	.....	.....	.....	.....	.....	.....

It will be noted from figure 2 that the chromaticity spacing of the recommended scale decreases regularly from the dark colors to the light, the total decrease in spacing being by about 50 percent. This decrease in spacing arises primarily from the factor, $T^{1/3}$, in the equation defining color difference for the conditions of the ASTM Union colorimeter. The recommended tolerances of ± 0.006 correspond to about 0.1 step in the respacing of the Union color scale. The relocation of the scale is seen from figure 2 to amount in maximum also to 0.006 in r, g, or b.

Figure 2 also shows that the recommended scale corresponds within the tolerance of ± 0.006 either to Mr. Hancock's Chicago suggestion or to his suggestion of November 24, 1948 with the single exception of the No. 2 standard. Since practical considerations led Mr. Hancock to such

a close correspondence with our best determination of a perfectly uniform scale, it is to be presumed that this recommendation is worthy of adoption by industry.

There remains, of course, the important question of whether industry will become reconciled to any change in definition of the Union scale at all. Perhaps it would avoid confusion if the recommended scale be given a new name and a different number of steps. If such a procedure is decided upon, formula (2) is recommended for use in development of specifications for standard glasses unless an important change in viewing conditions is also made.

VI. Summary

In response to a request from Subcommittee VI on Color, of ASTM Committee D–2 on Petroleum Products, a study of the colors of typical petroleum products supplied by members of the subcommittee has been carried out, and a relocation and respacing of the Union color scale has been derived from these measurements and from an analysis of the viewing conditions of the ASTM Union colorimeter used in accordance with ASTM D 155–45T. The recommended colors and tolerances for 17 glass color standards are given in table 6.

TABLE 6. *Recommended color specifications and tolerances for 17 glass color standards comprising a relocation and respacing of the ASTM Union color scale*

Number	Chromaticity coordinates (UCS system, footnote 5)[a]			Luminous transmittance (ICI standard source C)	
	r	g	b	T	
0.0	0.439	0.465	0.096	0.92	±0.03
0.5	.462	.473	.065	.86	± .03
1.0	.489	.475	.036	.77	± .03
1.5	.521	.464	.015	.67	± .03
2.0	.552	.442	.006	.55	± .03
2.5	.582	.416	.002	.44	± .02
3.0	.611	.388	.001	.31	± .02
3.5	.640	.359	.001	.22	± .02
4.0	.671	.328	.001	.152	± .011
4.5	.703	.296	.001	.109	± .008
5.0	.736	.264	.000	.081	± .006
5.5	.770	.230	.000	.058	± .005
6.0	.805	.195	.000	.040	± .004
6.5	.841	.159	.000	.026	± .003
7.0	.877	.123	.000	.016	± .002
7.5	.915	.085	.000	.0081	± .0008
8.0	.956	.044	.000	.0025	± .0003

[a] Tolerances on the chromaticity coordinates (r, g, b) are ±0.006.

WASHINGTON, March 15, 1950.

U. S. Department of Commerce
National Bureau of Standards

Research Paper RP2104
Volume 44, June 1950

Part of the Journal of Research of the National Bureau of Standards

Measurement of the Proton Moment in Absolute Units

By Harold A. Thomas, Raymond L. Driscoll, and John A. Hipple

By measuring the absolute value of the magnetic field and the frequency required for nuclear resonance absorption in a water sample, the gyromagnetic ratio of the proton has been determined to be $\gamma_p = (2.67528 \pm 0.00006) \times 10^4$ sec^{-1} gauss^{-1}. Using this value with Planck's constant, the value of the magnetic moment of the proton in absolute units becomes $\mu_p = (1.4100 \pm 0.0002) \times 10^{-23}$ dyne cm/gauss.

A combination of our result with recent measurements of the proton moment in Bohr magnetons gives a value of $e/m = (1.75890 \pm 0.00005) \times 10^7$ emu gram^{-1}.

I. Introduction

Since the development of molecular beam [1],[1] nuclear induction [2], and nuclear resonance absorption [3, 4] techniques, considerable work has been done on the determination of nuclear gyromagnetic ratios. From this ratio and the nuclear spin, the magnetic moment of the nucleus can be calculated.

The measurement of a gyromagnetic ratio γ involves the measurement of the frequency, ν, and magnetic field of induction B_0 required for resonance as indicated by the condition for resonance, $\omega = 2\pi\nu = \gamma B_0$. The comparison of either gyromagnetic ratios or magnetic moments requires only frequency determinations, and for this reason much of the data on magnetic moments now available is of this type. A few direct measurements of gyromagnetic ratios in absolute units have been made with accuracies of the order of 0.5 percent, which is about the best that can be done with the ordinary techniques of measuring magnetic fields. In the experiment reported here, the proton gyromagnetic ratio has been determined with much greater accuracy by using more elaborate methods of measuring the magnetic field and frequency. This precise measurement will allow previous relative determinations to be recalculated in absolute units, and will also provide a convenient standard of magnetic field for the measurement of other atomic constants.

[1] Figures in brackets indicate the literature references at the end of this paper.

The nuclear absorption method of Purcell [3, 4] was used for detecting resonance, because the field involved lends itself more readily to precise measurement than that used in the molecular beam method, and the apparatus appeared somewhat simpler to construct than that employed by Bloch in the nuclear induction experiment.

The use of a solenoid of known dimensions would provide the most accurately known magnetic field, but this possibility was discarded, because the maximum field available would only be of the order of 20 gausses. The signal-to-noise ratio becomes very low in such a weak field, and at the time this experiment was planned no attempt had yet been made to work in this range.[2] An iron-cored electromagnet with a relatively strong field was used, which reduced the signal-to-noise problem but required auxiliary apparatus for measuring the field.

To measure the field, a Pellat electrodynamometer [6] could be used but would require a large gap and a correspondingly large magnet. The method finally chosen is one similar to that previously described in the literature [7, 8, 9] for measuring magnetic fields. In this method one measures the force on a known length of wire carrying a known current in the magnetic field to be determined. A long rectangular coil is suspended vertically from an analytical balance

[2] The recent success of Brown and Purcell [5] in working in fields as low as 11 gausses now makes the solenoid method appear more attractive than when the present work was undertaken; as a means of eliminating systematic errors and possibly improving the accuracy, it is important that the measurements described here be repeated with this method. This is now being done.

with the lower end in the gap of the magnet. The vertical sides of the coil act as the connecting leads to the "force conductors", which are formed by the lower horizontal portion of the coil. The fringing field at the upper end of the coil may be reduced to a negligible value by means of Helmholtz coils. Figure 1 is a photograph of the over-all experimental setup showing the magnet, coil, balance, current measuring apparatus, and

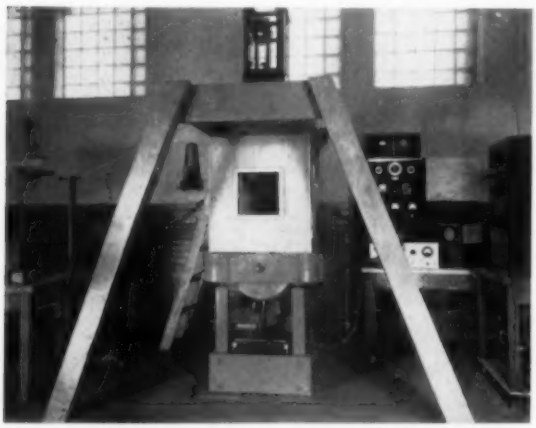

FIGURE 1. *General view of magnet, balance, and proton resonance equipment.*

electronic equipment for regulating the magnet and detecting the resonance absorption.

Since it is the average field over the region occupied by the force conductors that is measured by the force method, it is essential that the field distribution be precisely determined, and that the field in this region be reasonably uniform. Then, from the value of the average field and the field distribution, one can determine the value of the field at the proton sample, which may be located just below the coil.

The value of the field was adjusted so that the resonance frequency would be 20 Mc, which can be heterodyned directly with the Bureau's radio station WWV for the frequency measurement.

II. Magnet Design

Since the method of field measurement employed requires a homogeneous field of considerable extent, quite large pole faces are required. This limits the maximum field intensity available if the magnet is to be held to a reasonable size and cost. For proton resonance at 20 Mc, the maximum field must be about 5,000 gausses. The coil, being suspended from a balance, is quite sensitive to air currents, and for this reason particular care was used in the design of the magnet to insure that all exposed surfaces of the windings and pole faces would be sufficiently close to room temperature to minimize the effect of thermal air currents. These considerations led to a magnet design shown in some detail in figure 2.

Performance tests showed the magnet to operate satisfactorily up to 5,000 gausses; however, beyond this point the leakage flux from the sides of the poles to the yoke was great enough to produce partial saturation of the yoke. At 5,000 gausses the magnet requires 6.7 amp at 150 v, and the temperature rise in the hottest point of the windings is 30° C with a water flow of 1.6 liters a minute. The time constant of the magnet is 2.7 sec.

While the yoke is operating near saturation at the maximum value of field, the usable portion of the pole faces is operating at only about 5,000 gausses, which is sufficiently low to insure a stable field distribution.

III. Nuclear Resonance Techniques

For the detection of the proton resonance absorption, a radio frequency bridge similar to that used by Purcell and his collaborators [4] was constructed. This arrangement, however, had two serious drawbacks for this application. It was quite sensitive to microphonics so that it could not be easily used to probe the field for determining its distribution; and, since it shows the dispersion as well as the absorption, there would be greater uncertainty involved in determining the exact center of resonance. For these reasons, this method was finally rejected and a new amplitude bridge arrangement for detecting nuclear resonance was developed [10]. As its name implies, this bridge detects only amplitude changes in the radio-frequency voltage across the absorption coil and does not respond to phase changes. As a result, response to microphonic disturbances, which are largely reactive, is reduced by several orders of magnitude. Similarly, the reactive or dispersion component of the nuclear absorption signal is reduced to a negligible second-order correction, and only the resistive or absorption component is detected.

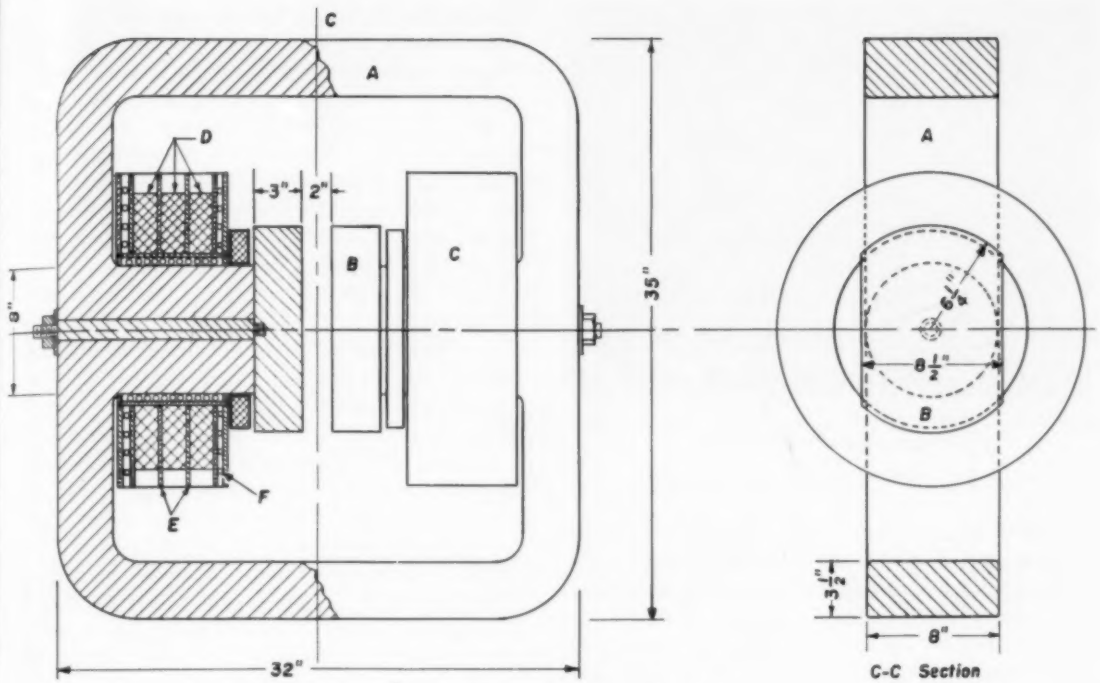

FIGURE 2. *Magnet design details.*

Figure 3 shows the essential details of an amplitude bridge for operating at 20 Mc. The proton sample is placed in L_1, which is tuned to resonance by C_1 and fed from a radio-frequency generator through a resistance, R_1, much higher than the resonant impedance of L_1-C_1. The field is modulated locally a few tenths of a gauss by applying a 20-c/s voltage to the small Helmholtz coils located on either side of the sample. As the magnetic field passes through the value required for nuclear resonance, the nuclear absorption lowers the Q, causing the voltage across L_1 to change. This change in the amplitude of the radio-frequency voltage is detected by a diode detector, D_1, and the resulting audio resonance signal can be amplified by a high-gain audio amplifier and displayed on an oscilloscope. To eliminate noise and hum modulation present in the radio-frequency source, a capacitance voltage divider and diode rectifying in the reverse phase to D_1 are used and the outputs combined in an audio bridge network. Audio modulation in the radio frequency is thus balanced out, but the nuclear absorption signal, detected by only one diode, appears at the output reduced by a factor of two. Sufficient cancellation of the noise modulation is usually obtained by merely adjusting C_3.

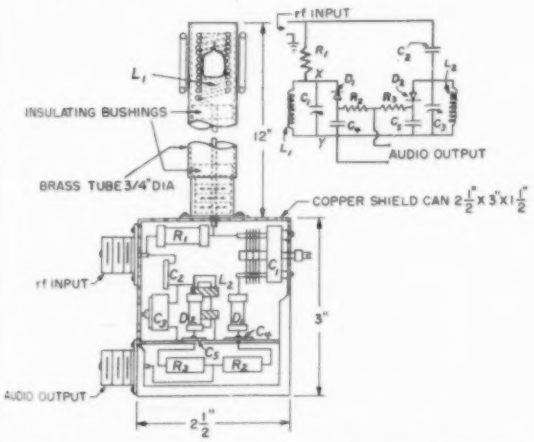

FIGURE 3. *Amplitude bridge for detecting nuclear resonance.*

R_1=25,000 ohms; R_2, R_3=50,000 ohms; C_1=120 mmf; C_2=2 mmf mica; C_3=7 mmf ceramic trimmer; C_4, C_5=500 mmf feed through condenser; L_2=1 millihenrie r-f choke; D_1, D_2=1N34 crystal diodes.

The signal-to-noise ratio obtainable with this circuit depends largely on the type of diodes used, approaching the theoretical maximum for pure

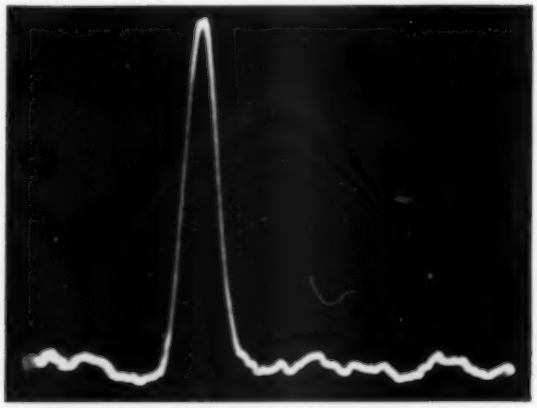

FIGURE 4. *Proton resonance line detected with amplitude bridge using crystal detectors.*

The field intensity was 4,700 gausses, and line width is 0.3 gauss.

tungsten filament diodes, and being much lower for oxide-coated cathode or crystal diodes. The flicker noise of the oxide-coated diode is quite similar in magnitude and frequency distribution to the contact noise of the crystal diode, and at the low frequencies it predominates over shot and thermal noise. In spite of the higher noise figure, the crystal diodes work quite satisfactorily for detecting the relatively strong proton signal at fields above a few thousand gausses and were used exclusively throughout this experiment because of the circuit simplicity gained by their use. Figure 4 shows a typical proton resonance line using a water sample with the relaxation time [2] T_1 adjusted with a dilute solution of ferric nitrate [4]. The line width shown in figure 4 is 0.3 gauss, and the field is 4,700 gausses. During the experiment the line width was somewhat less than this. A comparison of the sample used with oil samples containing no ferric nitrate indicated that the change in susceptibility of the sample due to the ferric salt was not detectable and could not have caused an error of more than 4 parts per million in the final result.

IV. Magnet Regulator Employing Proton Resonance

Stabilization of the magnetic field was accomplished by using the signal from a resonance detector in a feedback circuit, as shown in figure 5. If the field at the sample is modulated by an amount considerably less than the resonance line width as shown, the output signal is essentially sinusoidal, and its phase and amplitude depend upon the value of the steady field as indicated. After amplification in a narrow-band amplifier, the sinusoidal voltage from the resonance detector is mixed in the phase detector with a signal from the oscillator supplying the coils modulating the magnetic field. The output of the phase detector is the d-c voltage shown in figure 5, which goes through zero as B passes through the value required for the center of the resonance line. This d-c voltage is applied to a power amplifier that excites the auxiliary regulating coils on the magnet. Hunting was eliminated by adding a large RC time constant to the output of the phase detector. The main exciting coils were energized by storage batteries. Because of the large time constant of the magnet (2.7 sec), it is not necessary for the regulator to compensate for rapid fluctuations of exciter current.

The resonance detector used is the same as shown in figure 3, and again water was used for the sample. Both the resonance probe for displaying the resonance line on the oscilloscope and the one for the regulator were excited from the same 20-Mc crystal oscillator. The frequency from this crystal oscillator varied less than 1 part per million (ppm) after a 3-hr warm-up period, as shown in figure 6. This curve was checked a number of times by heterodyning with WWV and measuring the difference frequency.

Figure 7 shows the circuit details of the magnet regulator. By observing the shift in the proton line from one probe, it was found that the regulator reduced the effect of a 2-percent change in

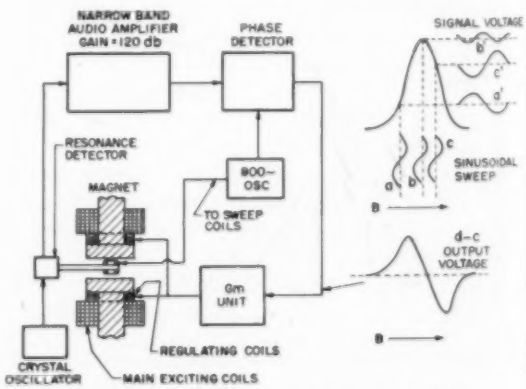

FIGURE 5. *Proton-resonance magnet regulator*

main exciting current to 0.02 gauss in 4,700 gausses.

V. Field Distribution

To shim the magnetic field and determine the field distribution, one resonance probe was used to regulate the magnetic field, and another resonance probe was mounted on a movable carriage so that it could be moved easily in the magnetic field while watching the proton pip. As the field does not vary with time, variations in the field as a function of position could be observed as a shift in the position of the proton pip on the oscilloscope screen. The oscilloscope sweep voltage was obtained from the sinusoidal voltage applied to the field sweep coils located on either side of the sample (see fig. 3). This voltage was also put through a peak-clipping and differentiating circuit, and the resulting pulses mixed with the resonance signal so that vertical marking lines would also appear on the scope. The shift of the resonance pip with change in field could then be observed relative to these markers with good precision.

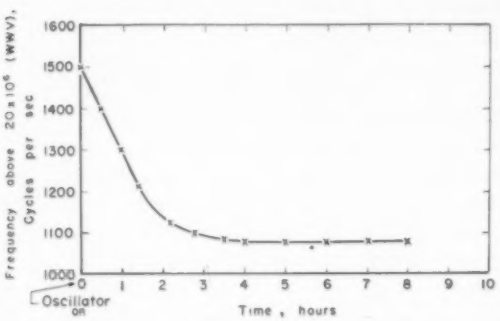

FIGURE 6. *Stability of crystal oscillator.*

In order to measure the distribution, another pair of small Helmholtz coils were mounted on the movable probe on either side of the sample, as shown in the photograph of figure 8. These Helmholtz coils were calibrated by changing the radio frequency applied to the probe by a small known amount that would shift the resonance pip off the marker line. The pip was then brought back into the original position by sending a small current through the Helmholtz coils. Then from $\Delta\omega = \gamma \Delta B$ (where γ is known to better than 1%) the Helmholtz coil constant was calculated. Ten determinations of the coil constant by this method showed a maximum deviation of 3 percent. The method used to measure the frequency change introduced an error mainly due to the uncertainty

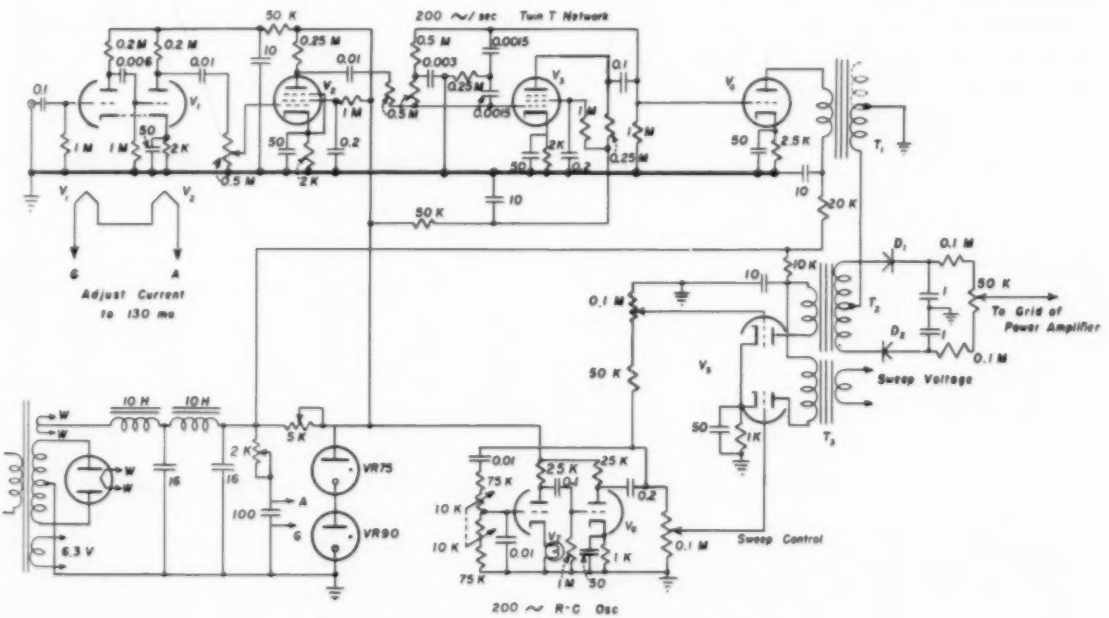

FIGURE 7. *Circuit details of magnet regulator.*

V_1, 12SC7; V_2, 12SJ7; V_3, 6SJ7; V_4, 6J5; V_5, 6SN7; V_6, 6SN7; V_7, 4-watt 120-volt lamp; $D_1 = D_2$, 1N34 crystal diodes; $T_1 = T_2$, thordarson T-20D77; T_3, universal output transformer; capacitances are in μf; K, thousands of ohms; M, megohms.

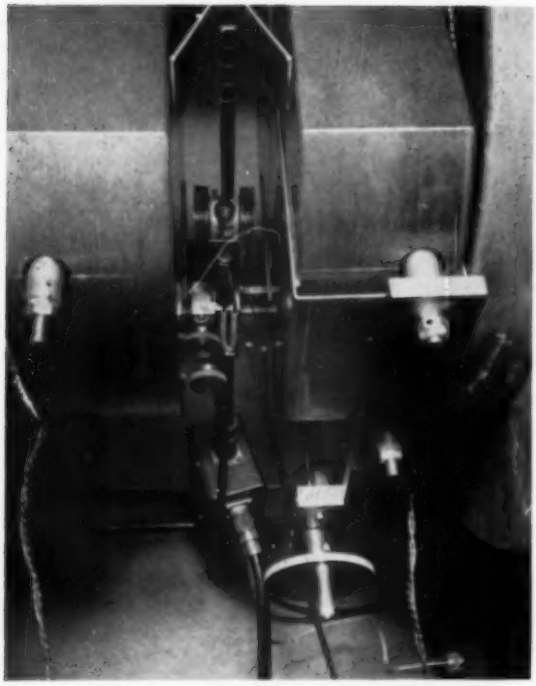

FIGURE 8. *Movable resonance probe.*

in reading a calibrated audio oscillator that was estimated at 2 percent. The coil constant for this method of calibration was then taken as [0.055 ± 5%] gauss/ma.

The gap was shimmed by using 2-mil nickel sheets fastened to a brass plate clamped to one of the pole faces. As thinner shims were not immediately available, the gap initially was shimmed on only one side. This gave rise to a slight gradient in the direction of the field, as may be seen by the field distribution curves shown in figure 9. Complete field plots were made on three different dates as indicated: before, during, and after the set of measurements were taken from which the gyromagnetic ratio was determined. In addition, frequent spot checks were made on the field distribution during the period when the absolute value of the field required for resonance was being obtained. The stability of the field distribution appeared very good, and no variation greater than that indicated in figure 9 was found. From the curves of figure 9, the average field over the region occupied by the bottom conductors of the force coil was found relative to the value where the nuclear sample was located during the absolute measurement of the field. The average field $\overline{B}$ was found to be lower than the field at the sample B_0 by 0.04 gauss. As the reproducibility of adjusting to the center of the resonance line is a little less than 0.02 gauss, the uncertainty in the calibration of the Helmholtz coils is negligible in comparison. Hence this field correction may be taken as (0.04 ±0.02) gauss.

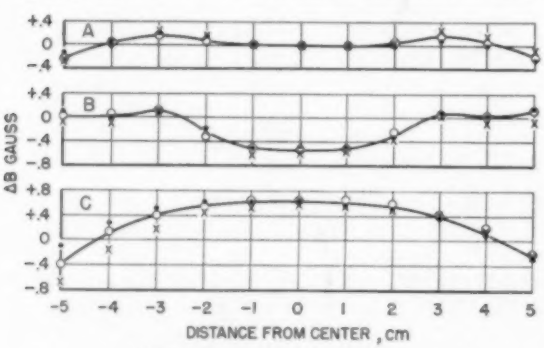

FIGURE 9. *Field distribution.*

A, at center of gap; B, +0.5 cm off gap center; C, −0.5 cm off gap center· ○, 10/21/48; ×, 11/16/48; ●, 3/4/49.

The deviation of the magnetic field from horizontal direction could contribute some error, but this was found to be less than 1 ppm. It was experimentally determined that a lack of perfect alinement of the plane of the rectangular coil in the gap, that is, a slight rotation about its point of support, would also have a negligible effect.

VI. Theory of the Magnetic Balance

The general method employed in the measurement of the magnetic field has already been described briefly. A period of about 30 min is required to make a determination. The full accuracy of the method cannot be realized unless the field is held constant during this period. It has been shown elsewhere in this paper how the effect of nuclear resonance absorption itself has been used to satisfy this condition to a high degree of perfection.

In principle, the method is based on the fact that an element of conductor of length dl cm carrying current i cgs emu perpendicular to a magnetic field of induction B gauss experiences a force dF dynes directed at right angles both to itself and to the field that is given by the following relation,

$$dF = iBdl. \tag{1}$$

As the force is measured in the vertical or y direction, the component of dl in the horizontal or x direction, dx, produces a force at the knife-edge of the balance. In order to arrive at the total force produced on a complete coil, it is necessary to integrate eq 1 over all its elements, as indicated below.

$$F=\int_{Coil} iB(x, y)dx. \tag{2}$$

The current, i, being everywhere the same in the circuit, the integration can be carried out numerically from the results of measurements on the width of the coil at various vertical or y positions, together with a measure of the field $B(x, y)$ at these vertical positions.

We may define the effective width of this coil when used as described with this particular magnet by the relationship

$$X=\frac{1}{\overline{B}}\int_{Coil} B(x, y)dx. \tag{3}$$

The value of X thus defined would be considerably affected by the stray field at the top wires of the coil; however, this field has been neutralized by the large Helmholtz coils described previously. The observed force F (dynes) in terms of $\overline{B}$, X, and I (amperes) in a coil of n turns is

$$F=\frac{nIX}{10}\overline{B}.$$

From this the value of the average field is

$$\overline{B}=\frac{10F}{nIX}. \tag{4}$$

VII. Construction of the Coil

A photograph of the completed coil is shown in figure 10. The nominal dimensions of the plate glass form are shown in figure 11. The coil has nine turns of wire that lie in grooves formed around the edge of the plate. The wires pass around the sides and bottom of the plate parallel to the edge of the glass and cross over to the next groove at the top. The horizontal stripes shown are silk ties that bind the wires and prevent accidental lateral displacement. The method of forming the grooves on the edges of the glass was similar to that devised by Moon [11]. The manner of supporting the form during lapping is shown in figure 12.

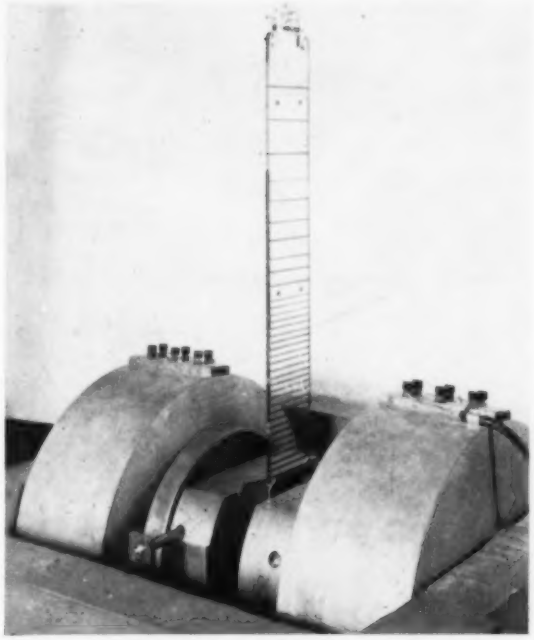

FIGURE 10. *Completed coil suspended in the magnet gap.*

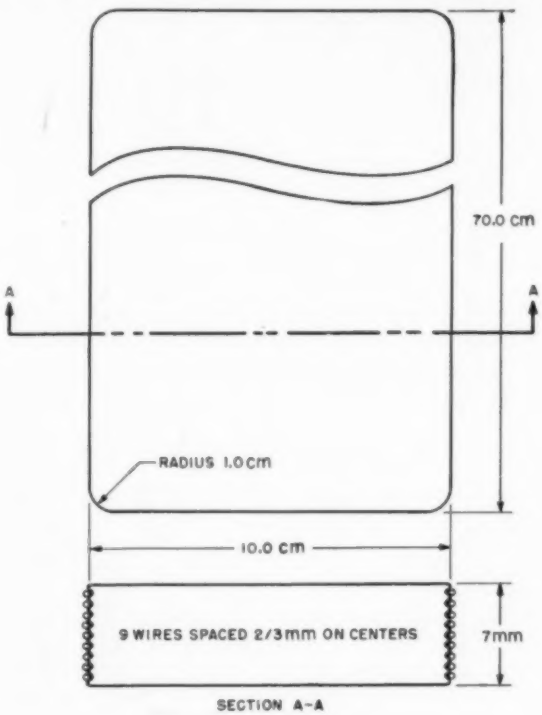

FIGURE 11. *Coil form.*

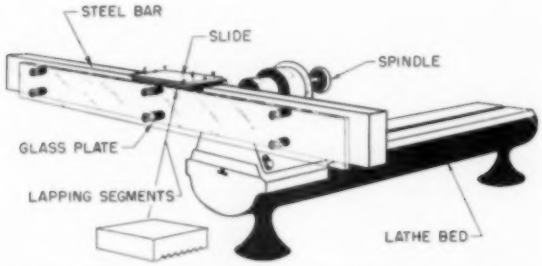

FIGURE 12. *Method of lapping grooves on edge of glass plate.*

The steel bar to which the plate is secured was annealed and ground parallel on the opposite faces. In addition to holding the glass, the edges of the bar were used to restrain the motion of the lapping tool to a straight line. The depth of lapping was controlled by adjusting the height of the lap relative to the edge of the bar. The assembly was rotated for alternate lapping on the two sides of the form. This procedure assured the same form of grooves on both sides. Grooves were worked around the corners and bottom by hand, using the flat side of the steel bar to keep the grooves in alinement. On completion, the over-all width of the coil form was practically as uniform as that of the bar.

It was convenient to place the wire on the form while the latter was securely fastened to the steel bar. Copper wire of the oxygen-free variety was drawn down through a number of dies from 1 mm to about 0.56 mm. The last drawing was carried out in a hallway in one straight piece and was wound directly onto the form without coming into contact with anything but the glass. A steady tension of 5 lb was held on the wire during winding. Current leads are brought out centrally at the top of the coil, and potential leads are fastened at the extreme ends of the winding near the edges of the plate.

VIII. Measurement of the Coil

Two measurements are necessary to get the distance between the central filaments of the wires: the over-all width of the coil and the mean diameter of the wire.

The coil was arranged for measurement in a temperature-controlled cabinet, as shown in figure 13. In this setup the width of each turn could be measured at various vertical positions. Measurements were made relative to Johannson gage blocks by means of a motor-driven micrometer devised by Moon [12]. This micrometer was provided with gear to bring it into position for each reading without having to enter the cabinet. Provisions were made for all essential adjustments of micrometer, coil, and end standard from the outside. Readings of the micrometer were estimated to 0.1 μ and would repeat to about 0.2 μ. The temperature of the end standard was ascertained from readings taken on an attached thermocouple, and that of the coil was gathered from thermometers plastered to it in several places. Most of the readings were taken at a nominal temperature of 25° C, but the coil was measured in several places at 29° and 33° C, making it possible to correct for the effect of temperature on the width.

The resistance of the winding was established at a known temperature. This was of use later when making corrections to the force on account of the expansion of the coil. The resistance of the coil was used as a measure of its temperature.

Results of measurements on the coil are shown in table 1, a. The result shown for each vertical position is the mean of the nine wires. Measure-

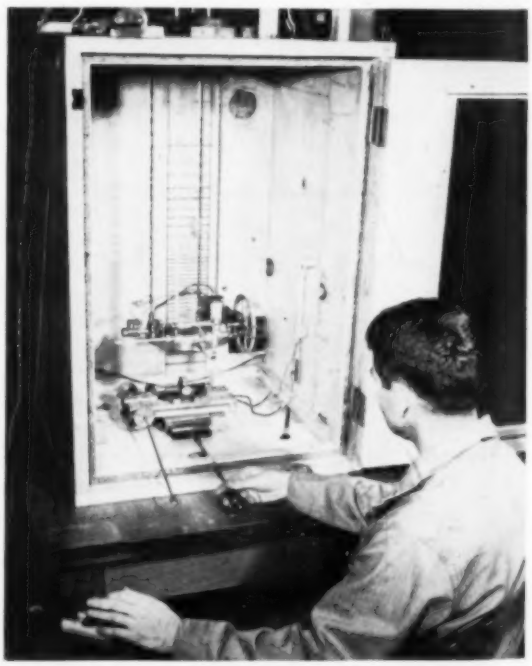

FIGURE 13. *Temperature-controlled cabinet for coil measurement.*

TABLE 1. *Coil measurements*

[Values given are the average of all 9 wires]

(a) OVER-ALL WIDTH OF RECTANGULAR COIL AT 25° C

Vertical position, y, relative to bottom wires	Width	Vertical position, y, relative to bottom wires	Width
cm	*mm*	*cm*	*mm*
0	80.5624	16.6	100.5781
1.0	100.2437	17.6	.5784
1.4	.5051	18.6	.5786
2.0	.7171	19.6	.5800
3.0	.6446	20.6	.5799
4.0	.6236	21.6	.5807
5.0	.5880	22.6	.5811
6.0	.5813	23.6	.5812
7.6	.5739	24.6	.5820
8.6	.5741	25.6	.5815
8.9	.5722	26.6	.5831
9.5	.5719	27.6	.5829
9.6	.5729	28.6	.5818
9.9	.5714	29.6	.5830
10.5	.5697	30.6	.5837
10.6	.5711	31.6	.5835
10.9	.5699	32.6	.5828
11.5	.5695	33.6	.5829
11.6	.5708	34.6	.5828
11.8	.5703	35.6	.5833
12.5	.5711	36.6	.5834
12.6	.5716	37.8	.5843
12.9	.5714	38.6	.5849
13.5	.5722	40.1	.5859
13.6	.5741	42.1	.5869
13.8	.5734	44.6	.5873
14.5	.5753	47.1	.5806
14.6	.5757	49.8	.5899
14.8	.5763	52.8	.5911
15.6	100.5757	56.3	.5906
		64.1	100.5869

(b) DIAMETER OF WIRE

[Measured in direction of plane of coil]

Wire No.	Vertical distance from bottom wires						
	7.6 cm	9.6 cm	10.6 cm	11.6 cm	12.6 cm	15.6 cm	Average
	mm	*mm*	*mm*	*mm*	*mm*	*mm*	*mm*
1R	0.5665	0.5667	0.5680	0.5680	0.5672	0.5675	0.5673
1L	.5669	.5669	.5671	.5664	.5664	.5662	.5667
2R	.5632	.5633	.5634	.5634	.5635	.5635	.5634
2L	.5682	.5684	.5683	.5683	.5682	.5679	.5682
3R	.5644	.5650	.5649	.5645	.5652	.5655	.5649
3L	.5632	.5632	.5631	.5623	.5622	.5619	.5627
4R	.5612	.5617	.5614	.5612	.5620	.5614	.5615
4L	.5613	.5613	.5612	.5612	.5612	.5612	.5612
5R	.5602	.5603	.5599	.5602	.5599	.5600	.5601
5L	.5595	.5600	.5595	.5601	.5601	.5600	.5599
6R	.5600	.5602	.5601	.5601	.5602	.5602	.5601
6L	.5600	.5602	.5601	.5600	.5601	.5600	.5601
7R	.5602	.5600	.5601	.5601	.5602	.5601	.5601
7L	.5602	.5602	.5602	.5602	.5602	.5602	.5602
8R	.5602	.5602	.5602	.5602	.5602	.5604	.5602
8L	.5612	.5615	.5613	.5615	.5614	.5617	.5614
9R	.5630	.5642	.5638	.5642	.5644	.5652	.5641
9L	.5604	.5602	.5603	.5602	.5603	.5602	.5603
Average	0.5622	0.5624	0.5624	0.5623	0.5624	0.5624	0.5624

ments in the range 0 to 7.6 cm were made with less accuracy than those above 7.6 cm. The field is so nearly uniform over this part of the coil that the error committed on this account is of no consequence. Between 7.6 cm and 15.6 cm, measurements were made with the greatest care. Beginning at 7.0 cm the silk ties were spaced 1.0 cm on centers. Entries in table 1, a, corresponding to more than one vertical distance between consecutive ties (9.5, 9.6, and 9.9 cm, for example), give an idea of the bulging of the wire.

The method of measuring the diameter of the wire was similar to that used on the over-all width of the coil. The wire was hung vertically from a rotatable head and was loaded with a weight equal to the winding tension. Measurements were made on the wire by comparison with a gage block of the same nominal size by means of a precision micrometer. The micrometer could be raised relative to the wire for measurements in different positions along the sample. An attempt to obtain the diameter of the wire parallel to the plane of the coil from measurements on samples taken from the ends of the windings resulted in an uncertainty of ± 0.0004 cm on account of lack of roundness in the wire. This uncertainty was removed later by measurements made on samples cut from both sides of each turn of the winding. It was found possible to mark the orientation of each sample before it was cut from its respective turn and to retain this marking during the diameter measurement. Results of these measurements are shown in table 1, b. As it turned out, the mean diameter of the wire parallel to the plane of the coil obtained in this way differed from the mean of all diameters obtained from the end samples by only 0.5 μ.

IX. The Distributed Field of the Electromagnet

The necessity of a knowledge of the normal component of the field over the region the coil occupies has been pointed out. This is not needed with much accuracy except over the lower part of the coil where the width changes rapidly. As previously described, the pole faces of the electromagnet were shimmed by trial with thin sheets of nickel to give essential uniformity over the bottom wires. The region over the bottom wires and up to a vertical distance of 7.0 cm was explored with a second movable proton resonance head, the first

head being used to hold the field constant at a fixed point. Above 7.0 cm the field was not sufficiently uniform to get a recognizable resonance pip. The region above 7.0 cm was mapped with a device consisting of a small coil rotated by the shaft of a synchronous motor at 1,800 rpm. The emf generated in the coil at the various vertical positions was commutated and measured on a potentiometer. Significant differences from the value at the bottom wires of the coil began at about 5.0 cm. The value of the field at the upper wires was about 3 gausses; this was neutralized to ± 0.02 gauss by means of Helmholtz coils. Indication of neutrality was by a delicately suspended magnet in the neighborhood of the wires. The values of the field at various vertical positions relative to the value B_r at some reference point within the magnet gap are shown in table 2.

TABLE 2. *Field $B(x, y)$ as a function of vertical distance*

[Values given for $B(x, y)/B_r$ have been averaged over x at the given value of y]

Vertical position, y, relative to bottom wires	Magnetic field $B(x, y)/B_r$	Vertical position, y, relative to bottom wires	Magnetic field $B(x, y)/B_r$
cm		*cm*	
0	1.0000	17.6	0.19
1.0	0.99990	18.6	.15
1.4	.99985	19.6	.13
2.0	.99980	20.6	.12
3.0	.9995	21.6	.10
4.0	.9991	22.6	.09
5.0	.9983	23.6	.07
6.0	.996	24.6	.06
7.6	.990	25.6	.06
8.6	.972	26.6	.05
8.9	.958		
		27.6	.04
9.5	.928	28.6	.04
9.6	.922	29.6	.03
9.9	.897	30.6	.03
10.5	.835	31.6	.03
10.6	.822	32.6	.02
10.9	.784	33.6	.02
11.5	.693	34.6	.02
11.6	.679	35.6	.02
11.8	.646	36.6	.01
12.5	.546		
		37.8	.01
12.6	.535	38.6	.01
12.9	.497	40.1	.01
13.5	.431	42.1	.01
13.6	.423	44.6	.005
13.8	.403	47.1	.005
14.5	.344	49.8	.005
14.6	.337	52.8	.004
14.8	.323	56.3	.002
15.6	.272	64.1	.001
16.6	.22		

X. Evaluation of the Factor X

The factor X has been defined as the effective width of the coil. In terms of the reference value B_r used in table 2, eq 3 may be rewritten $X=(B_r/\overline{B})\int[B(x, y)/B_r]dx$. The above integral is evaluated numerically, as illustrated in table 3, based on the data in tables 1 and 2. The reference point was so chosen that within the experimental accuracy $B_r=\overline{B}$. From $y=0$ to $y=7$ cm this could be determined with the resonance head; for the points beyond 7 cm, the reference point was obtained by locating the rotating coil at the normal position of the "force conductors" of the rectangular coil. It should be pointed out that the value of the field indicated in table 3 is the mean value taken over the interval Δy. As it affects the final result, the uncertainty in the evaluation of X can be properly divided into three parts having the following outer limits of error: width measurement 10 ppm, calibration of length standard 5 ppm, and field distribution 10 ppm.

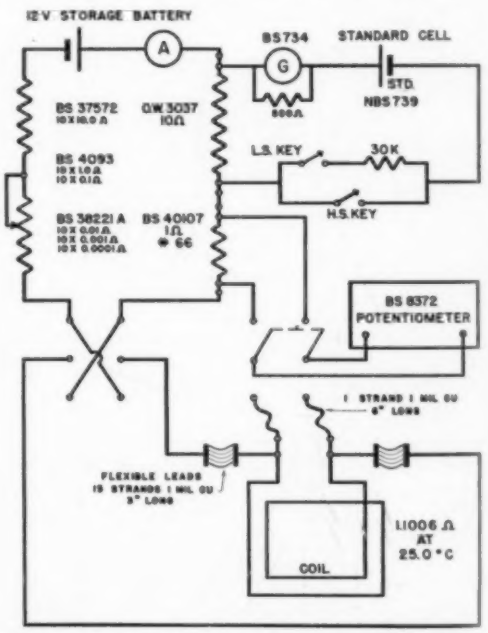

FIGURE 14. *Electrical connections of magnetic balance.*

TABLE 3. *Evaluation of the geometrical-factor X*

[Values given for $B(x,y)/B_r$ from table 2 have been averaged over the interval Δy. Width given is the over-all width minus the mean wire diameter]

y	Width	Δx	$\frac{B(x,y)}{B_r}$	$\frac{B(x,y)}{B_r}\Delta x$	y	Width	Δx	$\frac{B(x,y)}{B_r}$	$\frac{B(x,y)}{B_r}\Delta x$
cm	*cm*	*cm*			*cm*	*cm*	*cm*		
0	8.00000	+8.00000	1.00000	+8.00000	17.6	10.00160	+0.00003	0.20	+0.00001
1.0	9.96813	+1.96813	0.99995	+1.96803	18.6	10.00162	+.00002	.17	+.00000
1.4	9.99427	+0.02614	.99988	+0.02614	19.6	10.00176	+.00014	.14	+.00002
2.0	10.01547	+.02120	.99983	+.02120	20.6	10.00175	−.00001	.12	−.00000
3.0	10.00822	−.00725	.99965	−.00725	21.6	10.00183	+.00008	.11	+.00001
4.0	10.00612	−.00210	.9993	−.00210	22.6	10.00187	+.00004	.10	+.00000
5.0	10.00256	−.00356	.9987	−.00356	23.6	10.00188	+.00001	.08	+.00000
6.0	10.00189	−.00067	.9972	−.00067	24.6	10.00196	+.00008	.06	+.00000
7.6	10.00115	−.00074	.993	−.00073	25.6	10.00191	−.00005	.06	−.00000
8.6	10.00117	+.00002	.983	+.00002	26.6	10.00207	+.00016	.06	+.00001
8.9	10.00098	−.00019	.96	−.00018					
					27.6	10.00205	−.00002	.05	−.00000
					28.6	10.00194	−.00011	.04	−.00000
9.5	10.00095	−.00003	.94	−.00003	29.6	10.00206	+.00012	.04	+.00001
9.6	10.00105	+.00010	.93	+.00009	30.6	10.00213	+.00007	.03	+.00000
9.9	10.00090	−.00015	.91	−.00014	31.6	10.00211	−.00002	.03	−.00000
10.5	10.00073	−.00017	.87	−.00015	32.6	10.00204	−.00007	.03	−.00000
10.6	10.00087	+.00014	.83	+.00012	33.6	10.00205	+.00001	.02	+.00000
10.9	10.00075	−.00012	.81	−.00010	34.6	10.00204	−.00001	.02	−.00000
11.5	10.00071	−.00004	.74	−.00003	35.6	10.00209	+.00005	.02	+.00000
11.6	10.00084	+.00013	.69	+.00009	36.6	10.00210	+.00001	.02	+.00000
11.8	10.00079	−.00005	.66	−.00003					
12.5	10.00087	+.00008	.60	+.00005	37.8	10.00219	+.00009	.01	+.00000
					38.6	10.00225	+.00006	.01	+.00000
					40.1	10.00235	+.00010	.01	+.00000
12.6	10.00092	+.00005	.54	+.00003	42.1	10.00245	+.00010	.01	+.00000
12.9	10.00090	−.00002	.52	−.00001	44.6	10.00251	+.00006	.008	+.00000
13.5	10.00098	+.00008	.46	+.00004	47.1	10.00272	+.00021	.005	+.00000
13.6	10.00117	+.00019	.43	+.00008	49.8	10.00275	+.00003	.005	+.00000
13.8	10.00110	−.00007	.41	−.00003	52.8	10.00287	+.00012	.004	+.00000
14.5	10.00129	+.00019	.37	+.00007	56.3	10.00282	−.00005	.003	−.00000
14.6	10.00133	+.00004	.34	+.00001	64.1	10.00245	−.00037	.001	−.00000
14.8	10.00139	+.00006	.33	+.00002					
15.6	10.00133	−.00006	.29	−.00002	$\sum \frac{1}{B_r} B(x,y)\Delta x = 10.00108$				
16.6	10.00157	+.00024	.25	+.00006					

XI. Electrical Measurements

The electrical circuit of the magnetic balance is shown in figure 14. The current was held constant to about 1 ppm by manual adjustment of the series resistance to keep the potential drop produced in the 10-ohm standard equal to the emf of a standard cell, as indicated by galvanometer G.

The standard resistor was submerged in a thermostated and stirred oil bath. The standard cell was maintained at a constant temperature in another thermostated bath. On disconnecting the storage battery and standard cell and closing the galvanometer circuit, no thermal emf was found of any appreciable magnitude. The error in the value of the current on account of the standards was not more than 3 ppm.

The resistance of the coil while carrying current was ascertained by comparing the potential across it with that across a standard resistance of 1 ohm carrying the same current as shown in figure 14. In this way it was easy to find the resistance of the coil to 0.0001 ohm, allowing its temperature to be estimated to 0.1 deg C. The resistance of the coil at a known temperature was measured by means of a Mueller bridge at the time it was mounted in the temperature-controlled cabinet for the width measurement. This resistance was 1.1006 ohms at 25° C.

XII. Measurement of the Force

The force produced on the current-carrying coil was evaluated by comparison with the action of gravity upon a known mass that was placed upon the scalepan of the balance when the current was reversed. In case the comparison was not exact, a small correction was made to the mass in terms of the sensitivity of the balance, s, and the change in rest point of the balance, δ. Reversing the current in the coil has several advantages: it keeps the heating of the coil constant, thereby helping

to maintain the dead weight of the coil constant; it corrects for any lateral shift in the current; it corrects for attractive effects of the coil or other parts attached to the movable parts of the balance; and it doubles the observed force. Remembering the reversal of current and denoting the mass of the removable weight by m, and the acceleration of gravity by g, a working formula for the field $\overline{B}$ is given by

$$\overline{B}=\frac{5(m+s\delta)g}{nIX[1+a(t-25)]}, \tag{5}$$

where a is the coefficient of thermal expansion of the coil, and t is its temperature. In practice the current I has some fixed value according to the standards selected, and the magnetic field has some value consistent with the radio frequency applied to the proton probe to produce resonance; therefore, the mass, m, had to be adjusted by trial to a point where the correction, $s\delta$, was so small that the uncertainty in the sensitivity of the balance did not cause more than a tolerable error in the force. This mass, which is in the form of a cylinder, was then turned over to the Mass Section of the Bureau for standardization. A correction was made for the weight of displaced air to get the effective weight of the cylinder.

Turning points of the 2-kg Rueprecht balance were indicated by a spot of light reflected onto a glass scale from a mirror on the balance beam. The effective pointer length was 5.0 m. The dead load on the balance was 1,500 g. The change in weight on reversing the current was about 9.0 g. The sensitivity of the system was such that 1 mm on the scale corresponded to 1 part in 60,000 of the change in force. The turning points were estimated to 1/10 mm. The rest point, as estimated from averaging five turning points on one side and four on the other, would ordinarily be accurate to less than 1/10 mm; in this application there were fluctuations in the swings of the balance caused by varying air currents and building vibration, and perhaps slight variations in the average magnetic field that increase the uncertainty of a given rest point to several tenths of a millimeter. By taking the rest point about 10 times in a given run with the weight alternately off and on the scalepan, the fluctuations are averaged out giving the mean value of the difference in rest points, δ, accurate to about 5/10 mm.

XIII. Gyromagnetic Ratio of the Proton

The results of the measurements through January 7, 1949, are summarized in table 4. Many spot checks were made during these runs, which indicated that the field distribution was remaining remarkably constant. Subsequently, when the field was shimmed symmetrically with thinner shim stock, measurable variations in the distribution with time were noted. Therefore, in taking the data of table 5 with symmetrical shims, the field distribution was plotted immediately before and after the measurement of $\overline{B}$ with the balance. Likewise, a new mass constructed of platinum-iridium was used on the balance for these readings. These results, obtained about 5 months later, are practically identical with the earlier ones. Considering all the runs, the average deviation is approximately 10 ppm.

It will be noticed that the acceleration of gravity g appears in eq 5. The uncertainty [13] in this is taken as 5 ppm. The acceleration of gravity also arises in the absolute determination of the ampere [14]. Thus the current may be written

$$I=k\sqrt{g_1}, \tag{6}$$

where k is an experimental constant known to 10 ppm, to which must be added an error of 3 ppm arising in the comparison of the current used in this experiment with the standards, and g_1 is the value of the acceleration of gravity used in the measurement of the ampere. Substituting eq 6 into eq 5

$$\overline{B}=\frac{5(m+s\delta)g}{nkg_1^{1/2}X[1+a(t-25)]}. \tag{7}$$

Letting

$$h=g/g_1 \tag{8}$$

represent the ratio of the acceleration of gravity at the location of this experiment to that used in the determination of the ampere, eq 7 becomes

$$\overline{B}=\frac{5(m+s\delta)hg_1^{1/2}}{nkX[1+a(t-25)]}. \tag{9}$$

The advantage in this approach is that the quantity $hg_1^{1/2}$ is known to approximately 2.5 ppm, whereas the acceleration of gravity is known only to 5 ppm.

TABLE 4. *Summary of results—first series*

Acceleration of gravity at the balance g	980.081 cm/sec.^{2}
Geometrical factor of the coil (table 3)	10.00108 cm at 25° C.
Number of turns on coil n	9.
Expansion of the coil α	9.5×10^{-6}/deg C.
Sensitivity of the balance s	1.59 mg/cm.

Date	Temperature of coil	Mass	$s\delta$	Temperature correction	Corrected Mass	Current	$\overline{B}$	$(B_0-\overline{B})$	B_0	Deviation from average
	°C	mg	mg	mg	mg	amp	gausses	gausses	gausses	
Dec. 22, 1948	25.7	8779.49	−2.08	−0.06	8777.35	0.1017259	4697.58	+0.04	4697.62	0.06
Dec. 22, 1948	26.0	.49	−2.22	−.09	.29	259	.55	+.04	.59	.03
Dec. 23, 1948	26.0	.49	−2.34	−.09	.12	259	.46	+.04	.50	.06
Dec. 29, 1948	25.1	.49	−2.26	−.01	.22	259	.51	+.04	.55	.01
Dec. 30, 1948	25.0	.49	−2.16	.00	.33	259	.57	+.04	.61	.05
Dec. 31, 1948 *	24.5	8777.50	−0.51	+.04	8777.12	.1017259	.46	+.04	4697.50	.06
Jan. 3, 1949 *	24.1	.59	−.33	+.08	.34	259	.58	+.04	.62	.06
Jan. 7, 1949 *	25.5	.59	−.41	−.04	.14	259	.47	+.04	.51	.05
								Mean	4697.56	±0.05

* New brass mass used in measurements.

ν=measured value of resonance frequency=20,001,075 ±20 c/s.
γ_p=gyromagnetic ratio of proton$=2\pi\nu/B_0=2.67523\times10^4$ sec^{-1} gauss^{-1}.

TABLE 5. *Summary of results—second series*

In obtaining the data in this table, the following changes were made:
A platinum-irridium mass was used 8777.29 mg.
Symmetrical shims were used, i. e., the same on each pole face.
The field distribution was checked before and after each run.

Current—0.1017274 ampere

Date	Temperature of coil	$s\delta$	Temperature correction	Corrected mass	$\overline{B}$	$(B_0-\overline{B})$	B_0	Deviation from average
	°C	mg	mg	mg	gausses	gausses	gausses	
May 6, 1949	26.9	+0.30	−0.16	8777.43	4697.56	+0.02	4697.58	0.03
May 9, 1949	26.2	−.08	−.10	.11	.38	+.11	.49	.06
May 12, 1949	26.4	+.09	−.12	.26	.46	+.07	.53	.02
May 16, 1949	25.6	+.08	−.05	8777.32	.50	+.09	4697.59	.04
						Mean	4697.55	±0.04

ν=20,001,075 ±20 c/s.
γ_p=gyromagnetic ratio of proton$=2\pi\nu/B_0=2.67523\times10^4$ sec^{-1} gauss^{-1}.

The value of the acceleration of gravity g_l used in this experiment was 980.08 cm/sec^2, which was obtained along with h from a gravity survey made at this Bureau in 1948 by the Geological Survey. This is slightly different from the value given by Curtis [15].

The known contributing errors listed in the tabulation below were estimated conservatively. The square root of the sum of their squares results in an uncertainty of 22 ppm in the gyromagnetic ratio of the proton. The result can be stated as $\gamma_p=(2.67523\pm0.00006)\times10^4$ sec^{-1} gauss^{-1} uncorrected for the diamagnetic effect of the orbital electron. The stated error is thought to be several times the corresponding probable error. If the diamagnetic correction [16], which was not included in the preliminary result [17], is applied to the above value one obtains $\gamma_p=(2.67528\pm0.00006)\times10^4$ sec^{-1} gauss^{-1}.

The magnetic moment of the proton is known less accurately than the gyromagnetic ratio because of the uncertainty in the value of Planck's constant h. Using a value [18] of

$$h=(6.6234\pm0.0011)\times10^{-27}\text{ erg sec},$$

the magnetic moment of the proton is

$$\mu_p=(1.4100\pm0.0002)\times10^{-23}\text{ dyne cm/gauss}.$$

Contributing errors	Parts per million
Platinum-iridium mass m	1
Precision of balance used in this experiment $.8\,\delta$	9
Gravity $hg_1^{1/3}$	3
Experimental constant in measurement of the ampere in absolute units k	10
Comparison of current with standards	3
Width of coil	10
Length standard	5
Field distribution	10
Neutralization of stray field at upper wires	5
Adjustment of resonance pip to reference point on oscilloscope	4
Calibration of Helmholtz coils used for field distribution	4
Resonance frequency	1
Effect of ferric ions in sample	4

XIV. Comparison With Other Measurements

Gardner and Purcell [19] have just completed a measurement of the ratio of the precession frequency of the proton, $\omega=\gamma_p B_0$, to the cyclotron frequency, $\omega_e=eB_0/m$, of a free electron in the same magnetic field. After making the diamagnetic correction, they give for the ratio $\omega/\omega_e=(1.52100\pm0.00002)\times10^{-3}$. This ratio is the magnetic moment of the proton in Bohr magnetons and agrees very well with the value $\mu_p=(1.52106\pm0.00007)\times10^{-3}$ Bohr magneton obtained by Taub and Kusch [20]. These values of μ_p may be combined with the value of the gyromagnetic ratio of the proton to give a value of e/m. In this calculation it is preferable to use the value of Gardner and Purcell because of its greater accuracy and because the electron moment correction is not involved. This value of e/m becomes $e/m=\gamma_p.\omega_e/\omega=(1.75890\pm0.00005)\times10^{+7}$ emu gram^{-1}. This differs only slightly from the previously published value [21], which was obtained by combining our preliminary value of γ_p and the measurement of Taub and Kusch. Figure 15 shows the new value of e/m as compared with other experimental and recommended values summarized by DuMond and Cohen [18].

The value of the gyromagnetic ratio of the proton, and hence the above value of e/m, has recently received further confirmation since it has been used in determining the Faraday [22] in which excellent agreement with the iodine voltameter was obtained.

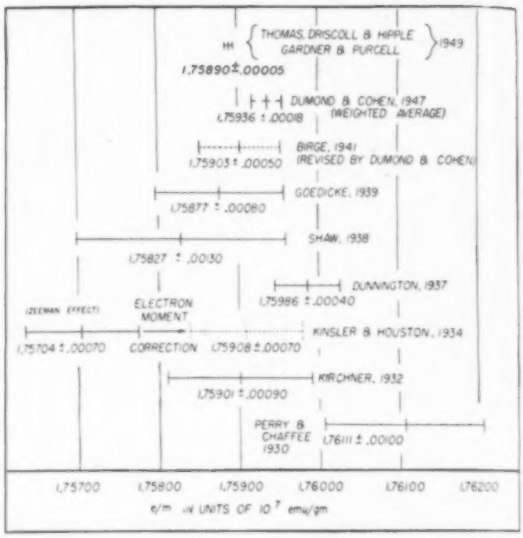

FIGURE 15. *Values for e/m as summarized by DuMond and Cohen compared with the measurements reported in this paper.*

The contributions of other staff members are gratefully acknowledged, and in particular the authors thank the following: Charles Moon, for advice on the construction and measurement of the coil; L. P. Slivka, for assistance in making many measurements on the coil; L. B. Macurdy, for the calibration of the masses; W. J. Hamer, for the calibration of standard cells; Anne Yung-Kwai, for the calibration of standard resistors; and I. H. Fullmer, for the calibration of gage blocks. Helpful suggestions were received from F. B. Silsbee, Chester Snow, and R. D. Huntoon.

XV. References

[1] I. I. Rabi, S. Millman, P. Kusch, and J. R. Zacharias, Phys. Rev. **55,** 526 (1939).
[2] F. Bloch, Phys. Rev. **70,** 460 (1946).
[3] E. M. Purcell, H. C. Torrey, and R. V. Pound, Phys. Rev. **69,** 37 (1946).
[4] N. Bloembergen, E. M. Purcell, and R. V. Pound, Phys. Rev. **73,** 679 (1948).
[5] L. M. Brown and E. M. Purcell, Phys. Rev. **75,** 1262 (1949).
[6] M. H. Pellat, J. phys. **6,** 175 (1887).

[7] A. Cotton and G. Dupouy, Congr. intern. d'Electricite 3 Sect. **2,** 208 (1932).
[8] F. A. Scott, Phys. Rev. **46,** 633 (1934).
[9] G. H. Briggs and A. F. A. Harper, J. Sci. Instruments **13,** 119 (1936).
[10] H. A. Thomas and R. D. Huntoon, Rev. Sci. Instruments **20,** 516 (1949).
[11] H. L. Curtis, C. Moon, and C. M. Sparks, J. Research NBS **21,** 375 (1938) RP1137.
[12] C. Moon, J. Research NBS **10,** 249 (1933) RP528.
[13] H. L. Dryden, J. Research NBS **29,** 303 (1942) RP1502.
[14] R. W. Curtis, R. L. Discoll, and C. L. Critchfield, J. Research NBS **28,** 133 (1942) RP1449.
[15] H. L. Curtis, J. Research **33,** NBS 235 (1944) RP1606.
[16] W. E. Lamb, Jr., Phys. Rev. **60,** 817 (1941). (The correction referred to on p. 581 is for the hydrogen atom. N. F. Ramsey, Phys. Rev. **77,** 567 (1950) has calculated the correction for the H_2 molecule to be 2.7×10^{-5}. If the frequency shift between H_2 and the Bureau sample were determined, the result reported might be changed slightly).
[17] H. A. Thomas, R. L. Driscoll, and J. A. Hipple, Phys. Rev. **75,** 902 (1949).
[18] J. W. M. DuMond and E. R. Cohen, Rev. Modern Phys. **20,** 82 (1948).
[19] J. H. Gardner and E. M. Purcell, Phys. Rev. **76,** 1262 (1949).
[20] H. Taub and P. Kusch, Phys. Rev. **75,** 1481 (1949); Kusch and Taub, **75,** 1477 (1949).
[21] H. A. Thomas, R. L. Driscoll, and J. A. Hipple, Phys. Rev. **75,** 992 (1949).
[22] J. A. Hipple, H. Sommer, and H. A. Thomas, Phys Rev. **76,** 1877 (1949).

WASHINGTON, September 29, 1949.

U. S. Department of Commerce
National Bureau of Standards

Research Paper RP2105
Volume 44, June 1950

Part of the Journal of Research of the National Bureau of Standards

Measurement of Sixty-Degree Specular Gloss

By Harry K. Hammond, III, and Isadore Nimeroff

Specular gloss is the attribute next to color that is most often used in the evaluation of the appearance of objects. For 10 years the American Society for Testing Materials has used a method of test for the 60° specular gloss of paint finishes based on research done at this Bureau. The ASTM method prescribes the illuminator and receiver apertures that are to be used. However, in order to determine the uncertainties involved in the calibration of gloss standards, the rate of change of gloss reading with change of aperture was investigated throughout the gloss scale. This was done by modifying an existing goniophotometer so that it became in effect a versatile glossmeter with provision for accurately controlling all of the known geometrical variables involved. Data obtained on the variation of gloss reading with aperture show that standards with widely different distributions of reflected light can be used to check the adjustment of glossmeters and the conformance of their apertures to ASTM specifications in the increasingly important medium- to high-gloss range. The problem of obtaining the diffuse correction, which involves source polarization and departure of the specimen from a perfect diffusor, has been investigated.

I. Introduction

The appearance of an object depends upon several factors; the illuminant, the reflection characteristics of the material, the surface texture, the illuminating and viewing geometry, and the observer. The color and glossiness of a specimen are determined by the spectral composition and geometrical distribution of the incident light and upon the transformations that take place upon reflection from the specimen. These two appearance attributes, color and gloss, are somewhat related. Color measurement may require correction for surface glossiness. Specular gloss measurement may require correction for diffuse reflectance.

The complete description of the light-reflecting properties of a specimen would require an infinite number of measurements of reflectance throughout a hemisphere for an infinite number of directions of illumination. Even an approach to such a set of data is uneconomical to obtain with present goniophotometric equipment. Usually one must be content to obtain one goniophotometric reflection curve for a single direction of illumination (see fig. 1). Furthermore, the question of how to interpret a goniophotometric curve still remains, for in contrast to spectrophotometric curves there has not yet been developed a satisfactory method for reducing the former to a simple meaningful numeric or set of numerics as has been done for the latter. Because of these circumstances, one must generally be content to measure the specular reflectance for one direction of illumination. Previous investigations have shown that the choice of direction as well as aperture for illumination and view is governed by the type of material involved. Hunter and Judd [1][1] found that 60° specular gloss correlated most satisfactorily with

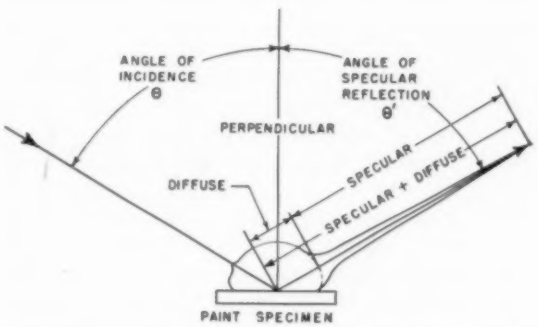

FIGURE 1. *Typical goniophotometric curve for a paint specimen, with defining terms.*

[1] Figures in brackets indicate the literature references at the end of this paper.

the surface appearance of paint finishes, and a method based on their investigations at this Bureau was tentatively adopted by ASTM in 1939. In order to simplify the discussions in this paper the problems treated are confined to 60° specular gloss, but the considerations involved apply to other specular angles as well.

Specular gloss could be measured without instrumental complication if there existed (1) an infinitesimal, high intensity, unpolarized light source; (2) perfect collimators; and (3) an infinitesimal but sensitive receiver. Then glossmeters could be readily duplicated. Practical sources, collimators, and receivers cause difficulty because imperfections in their construction combine with differences in reflected-light-flux distributions to give inconsistent gloss readings for various types of materials. If it were practical to make glossmeters with identical geometrical features, there would be no difficulty in comparing measurements made on different instruments. A more practical approach to the problem, however, lies in further standardizing gloss measurement by specifying tolerances for glossmeter geometry.

The original investigation, already referred to, on which the ASTM method is based, employed rectangular source and receiver apertures. This was done for two reasons. First, the type of lamp employed in the apparatus had a single, coiled filament producing a long narrow source, the cross section of which is rectangular; second, if the coiled lamp-filament were oriented with its axis perpendicular to the plane of measurement (see definition below) more light would be available because a larger aperture could be permitted in a plane perpendicular to the plane of measurement without appreciably affecting the gloss reading. Similarly, a proportionately larger receiver aperture in the plane perpendicular to the plane of measurement permits the receiver to gather light that would otherwise be lost because of change in direction on reflection from brush marks on brushed paint panels, when these are oriented, as they should be, with the marks parallel to the plane of measurement.

In order to determine the permissible geometrical tolerances, a "versatile" glossmeter has been developed. This instrument has provision for making the following adjustments:

1. The receiver aperture may be varied either parallel to or perpendicular to the plane of measurement.

2. The source aperture may be varied either parallel to or perpendicular to the plane of measurement.

3. The position of the image of the source may be varied with respect to the plane of the receiver entrance window.

4. The specular angle may be varied.

In addition to determining the permissible geometrical tolerances, there remains the problem of obtaining the diffuse correction. Measured values of diffuse correction do not agree exactly with those obtained by simple theory; however, the small discrepancy is accounted for by (1) The departure of the reflected light distribution of the specimen from that of the perfect diffusor; (2) The degree of polarization of the source; and (3) The reflectance of the surface.

II. Terms, Symbols, and Definitions

The purpose of glossimetry is to evaluate objectively some variable that may be used as an index of appearance ascribable to gloss. The most conveniently used variable involves some function of the geometrical distributions of the reflected light. For this reason it is advisable to define common reflectance terms as well as the more specialized concepts associated primarily with gloss measurement.

In addition to the definitions given below, there are two general concepts that should be discussed. The adjective "luminous" should be used whenever it is important that the defined term include weighting of the spectral energy distribution according to the luminosity function. A distinction must also be drawn between what may be called surface reflectance and body reflectance. Reflection of the latter type may be described as re-emission when the light penetrates the surface of the specimen and re-emerges at the incident face with a geometric distribution similar to that of a self-luminous source. The definitions of specular reflectance and diffuse reflectance given below involve the concepts of surface reflectance and body reflectance (re-emission), respectively.

The most important terms, definitions, and symbols used in this paper are given below.

Illuminance. Luminous flux incident per unit area of surface.

Luminous intensity (of reflected luminous flux in any direction). The solid-angular flux density.

Luminance. Luminous flux emitted per unit solid angle and per unit projected area.

Luminous (total) reflection. A general term for the process by which a part of the incident luminous flux leaves a specimen from the incident side.

Specular angle, θ'. The angle between the perpendicular to a plane surface and the reflected ray. This angle is numerically equal to the angle of incidence, θ, and lies in the same plane on the opposite side of the perpendicular; it is often designated $-\theta$ (refer to fig. 1).

Luminous specular reflection. The process by which incident luminous flux is reflected from a surface in an image-forming state.

Luminous diffuse reflection. The process by which incident luminous flux is reemitted (in a non-image-forming state).

Luminous specular reflectance. Ratio of luminous flux leaving a surface in an image-forming state to the incident luminous flux.

Luminous diffuse reflectance. Ratio of luminous flux reemitted at the illuminated surface of a nonself-luminous specimen to the incident luminous flux.

Luminous (total) reflectance. Ratio of luminous flux reflected by a specimen to the luminous flux incident on it. Diffuse reflectance plus specular reflectance equals total reflectance. It should be noted that the specular and diffuse reflectance components often cannot be separated for measurement.

Luminous directional reflectance. Ratio of luminous flux from the specimen when illuminated and viewed from specified directions to that from the perfectly reflecting, perfectly diffusing specimen, similarly illuminated and viewed.

Luminous fractional reflectance of a specimen. Ratio of luminous flux reflected within a specified solid angle to the luminous flux incident on the specimen.

Goniophotometer. An instrument used to obtain the geometric distribution of luminous flux.

Goniophotometric reflection curve. A plot of the geometric distribution of reflected luminous flux, for a specified distribution of incident flux, as a function of angle of view (see fig. 1).

Gloss. The function of luminous directional reflectance of a specimen responsible for its shiny or lustrous appearance.

Specular gloss, G_s. The ratio of the specularly reflected luminous flux, F_x, from a specimen surface for a specified angle of incidence, θ, to the specularly reflected luminous flux, F_s, from a standard surface for the same angle of incidence. Written symbolically:

$$G_s=(F_x/F_s)_{\theta,\theta'}, \qquad (1)$$

where θ' is the specular angle.

Specular glossmeter. An instrument for measuring specular gloss at a fixed specular angle.

Geometric conditions of illumination and view. Include the specular angle and the apertures of the source and receiver.

Source. A luminous body or area by which the specimen is illuminated.

Receiver. A photocell or an enclosure equipped with photocells responding to luminous flux from the specimen. The sensitive surface of the photocell or the opening to the enclosure is called the *receiver entrance window.*

Plane of measurement. The plane passing through the axes of incidence and view.

Aperture (of a source or receiver). The plane angle subtended by the source or receiver entrance window at the respective collimating lenses. With rectangular apertures the angles, α and β, may be used to describe the angular size of the aperture in the plane and perpendicular to the plane of measurement, respectively. In computing an aperture it is convenient to find the tangent of the half angle of the aperture. For example: the source aperture, α, in the plane of measurement is equal to $2\ \tan^{-1}(y/f)$, where y is the half dimension of the source in the plane of measurement, and f is the focal length of the collimating lens.

Fresnel reflector (nonmetallic). Specularly reflects a fraction, G_s, of luminous flux computed from the Fresnel equation [2],

$$G_s=\frac{E}{2}\left[\frac{\sin^2(i-r)}{\sin^2(i+r)}+\frac{\tan^2(i-r)}{\tan^2(i+r)}\right], \qquad (2)$$

where E is the illuminance, i is the angle of incidence, and r is the angle of refraction.

A more convenient form of this equation is obtained by expressing the angle of refraction in terms of the angle of incidence and the index of refraction, n, of the material. This is:

$$G_s=\frac{E}{2}\left\{\frac{\cos i-\sqrt{n^2-\sin^2 i}}{\cos i+\sqrt{n^2-\sin^2 i}}+\frac{n^2\cos i-\sqrt{n^2-\sin^2 i}}{n^2\cos i+\sqrt{n^2-\sin^2 i}}\right\}, \quad (3)$$

Perfect diffusor. Reflects light according to Lambert's Cosine Law, which states that the solid angular density of the luminous flux reflected from the surface in any direction varies as the cosine of the angle between that direction and the perpendicular to the surface.

Glossiness. The lustrous appearance of a surface ascribable to its gloss.

Lightness. That appearance attribute of a specimen which correlates with its luminous diffuse reflectance.

III. Glossmeters

Instruments for the measurement of specular gloss have been used for more than 30 years. In 1937, however, Hunter [3] described a photoelectric modification of the McNicholas goniophotometer, which is the earliest known photoelectric specular glossmeter. Since then glossmeters of this type and similar photoelectric types have been manufactured commercially.

1. Theoretical Glossmeter

The theoretical glossmeter consists of a source, source and receiver collimators, and a receiver (see fig. 2). If we had to deal only with an infinitesimal, unpolarized light source of high intensity, an infinitesimal receiver of high response, and perfect collimators, the problem of geometric tolerance specification would be eliminated. Such hypothetical glossmeter elements would have minimum aperatures and no lens aberrations and could be duplicated without causing error in the gloss readings. Measurement of specular gloss would then be completely reproducible from instrument to instrument if the specular angles were accurately determined.

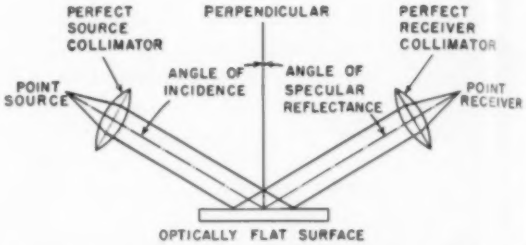

FIGURE 2. *Theoretical glossmeter, employing point source and point receiver.*

2. Practical Glossmeters

Most glossmeters in commercial use today employ an incandescent-filament lamp as a light source, a source lens to collimate the incident beam, a receiver lens to obtain at the receiver entrance window an image of the source reflected from a Fresnel reflector, and some type of photoelectric receiver [4], (see fig. 3). The source aperture is

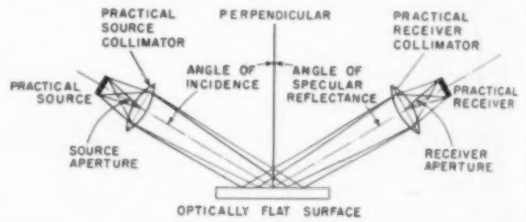

FIGURE 3. *Practical glossmeter, employing practical source and practical receiver.*

determined by the dimensions of the source and the focal length of the collimating lens. The receiver aperture is determined in a similar manner, using the dimensions of the receiver entrance window. Standard apertures may be specified, but errors of duplication cannot be avoided.

The collimating lenses used in commercial glossmeters are usually simple, uncorrected lenses, subject to such lens errors as astigmatism, spherical and chromatic aberration, and coma. Corrected lenses could be used, but the accuracy required in most gloss measurements can be obtained without this added expense. Because most commercial glossmeters are compactly made, the distances between elements and the apertures are physically small. This leads to errors in the setting of the specular angle, measurement of the source and receiver apertures, collimation of the incident beam, and positioning of the focussed im-

age of the source in the center of the receiver entrance window when reflected from a flat mirror surface.

3. The Versatile Glossmeter

In order to investigate the precision to which the many geometric variables of a glossmeter must be specified, an existing goniophotometer was modified to make a versatile glossmeter (see fig. 4). This glossmeter has provision for accurately controlling (1) the source and receiver apertures in both the α and β planes; (2) the angles of illumination and view; (3) the collimation; and (4) the position of the source image relative to the plane of the receiver aperture. Each of these variables can be changed individually to any desired degree of departure from the ASTM specifications.

Control of the source aperture is accomplished by employing a pair of condensing lenses to focus an image of the source on an adjustable metallic aperture. This aperture, serving as the new source of controllable size, is located in the focal plane of an achromatic collimating lens, the focal length of which is accurately known.

The specular angle is easily controlled since the source and receiver are located on the horizontal arms of a goniophotometer of which the angular scale may be set to within $\pm 0.1°$, and the specimen of which the gloss is to be measured is placed vertically on the turntable of the goniophotometer.

The receiver collimating lens also is an achromatic lens for which the focal length is accurately known. It is of such aperture and so positioned that there is no vignetting of rays that should reach the receiver. The receiver aperture is precisely located so that the image of the source is brought to focus at the plane of this aperture. Since there is no need to conserve space, this glossmeter was made large enough to allow for high accuracy of measurement of the apertures and the distances between elements.

IV. Glossmeter Variables

A surface lacking the smoothness of polished black glass will reflect some of the incident light in directions adjacent to that of specular reflection; consequently, some of the reflected light may fail to reach the instrument receiver, and a lower gloss reading may be obtained. It should

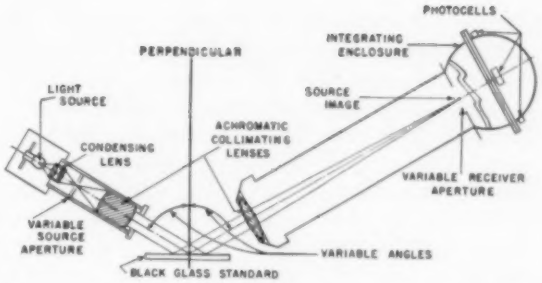

FIGURE 4. *NBS versatile glossmeter, employing variable source and receiver apertures, achromatic collimators, and variable angles of illumination and view.*

be pointed out that the specular reflectance, and consequently the gloss, of a nonmetallic specimen is a function of the index of refraction of the material of the specimen (see eq 3) as well as of the smoothness of the surface. Polished black glass of known index of refraction has been used to calibrate the upper end of the gloss scale. For low-gloss finishes, such as are used for camouflage by the Armed Services, the plane surface of a block of magnesium carbonate, which approximates the perfect diffuser, has been used as a standard at the lower end of the scale. This leaves the question of what material to use for intermediate standards. Horning and Morse [5] implied that in the medium- to low-gloss range average paint specimens have reflected light-flux distributions more like glazed ceramic tiles than like depolished black glass. From this standpoint tile should be preferable for use as gloss standards in the paint industry.

Recent cooperative work with the Sherwin-Williams Co. revealed, however, that better agreement in the measurement of high-gloss paints had been obtained on different glossmeters with the use of depolished black glass standards than with ceramic tile standards. In fact ceramic tile standards produced much larger instrument discrepancies for the same specimens. In order to analyze this situation, goniophotometric curves of fractional reflectance in the region of specular reflection were obtained for the paint specimen, a tile standard, and a sand-blasted depolished black glass standard having about the same 60° specular gloss (80 on the ASTM scale). These curves are shown in figure 5. For these measurements the goniophotometer source aperture was made 0.3° circular, and the receiver aperture was made 0.6°

883124—50——3

circular. A polished black glass standard was used, and the results are plotted on a fractional reflectance scale times 1,000, thus giving a value of 1,000 to the perfectly reflecting plane surface. From these curves it is seen that the light-flux distribution of the sand-blasted black glass standard is very similar to that of this particular high-gloss paint specimen, whereas the distribution of the tile standard is quite different. If a glossmeter having accurate ASTM apertures is used to determine the gloss of this paint specimen, the reading will be the same no matter which standard is used. On the other hand, if the receiver aperture were too large, very nearly the true gloss will be obtained with the glass standard, but a much lower reading will be obtained for this specimen if the tile standard is used for calibrating the instrument. The conclusion might be drawn at this point that instrumental aperture variation might be minimized by using the glass standard, and this would be true if all high-gloss specimens had flux distributions like the one illustrated here. However, as implied by Horning and Morse, many specimens are encountered with reflected light-flux distributions more like that of the tile standard, in which case nearly correct gloss readings would be obtained with this standard even though the receiver aperture were too large, whereas calibration with the glass standard would cause the instrument to give a reading higher than the correct value. Thus it is seen that if the reflected light-flux distributions of specimen and standard are nearly identical, the size of the apertures is not critical.

However, it is not practical to determine the distribution of each type of specimen, and it is even less practical to attempt to duplicate these distributions even approximately with durable materials that might be used as standards. The more practical approach to the problem is to make the glossmeter apertures as accurate as possible so that the instrument will give correct gloss readings no matter what the reflected light distribution of the specimen. Although glossmeter manufacturers may claim that the apertures are exactly correct, it would be desirable for the instrument operator to have a simple method to check their accuracy. This may be done by taking advantage of the facts pointed out above, namely that a glossmeter will read correctly two standards having radically different distributions of reflected light-flux only when apertures are correct.

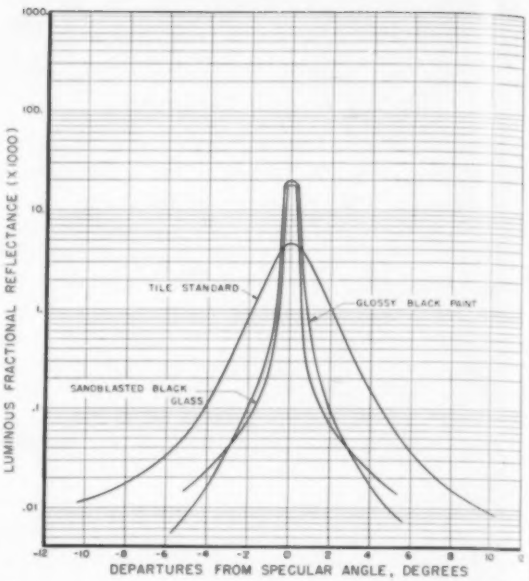

FIGURE 5. *Luminous fractional reflectance curves of high-gloss materials.*

Angle of illumination and view, 60°, source aperture, 0.3°, circular, receiver aperture 0.6°.

In the usual method of glossmeter operation, a polished glass surface is employed to make the initial calibration. The reading subsequently obtained for a tile standard should be the true value if the apertures are correct, too large if the receiver aperture is too large or too small if the aperture is too small, other adjustments being correct. It may be noted that the reproducible plane surfaces of different refractive index employed by Moore and Hunter [6] to avoid inaccuracies resulting from abrasions of a black glass standard do not serve to disclose errors arising from nonstandard apertures. In contrast to reflectance measurements where the apertures of the illuminating and viewing beams are relatively unimportant, the apertures employed in gloss measurement must be carefully specified and held with close tolerance if accurate glossimetry is to be accomplished. It should be stated here that in contrast to previous practice, it has been found not sufficient to specify the combined spreads of source and receiver aperture but each must be specified separately because

the ratio of source aperture to receiver aperture affects significantly the measured gloss value.

1. Receiver Aperture

To illustrate the magnitude of the effect of variation of the rectangular receiver aperture in the plane in which the specular angle is measured, designated α, and in the plane in the polar direction perpendicular to α, designated β, two series of measurement were made on plaques of different gloss. This was done for both depolished (sandblasted) black glass, and for glazed ceramic tiles. The results of these measurements are illustrated graphically in figures 6 and 7. These figures show the effect of variation in receiver aperture in the α and β planes, respectively, on the measured gloss values of tile and depolished black glass standards. It will be noted that the measured values for the tiles are a pronounced function of the receiver aperture. On the other hand, the measured values for the depolished black glass standards remain reasonably constant over the wide range of apertures employed. This is ascribable to the fact that high-gloss tile produces narrow-angle scattering near the specular angle, whereas depolished black glass produces wide-angle scattering.

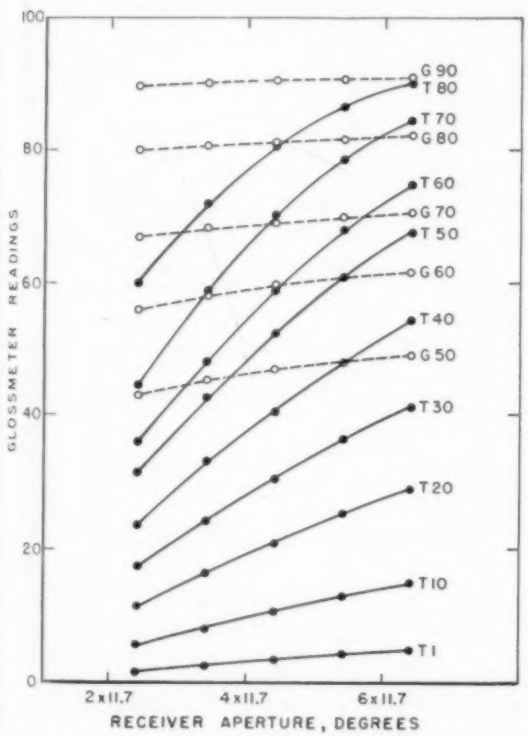

FIGURE 6. *Glossmeter readings obtained by varying the dimension of the receiver aperture in the α plane.*

The depolished black specimens are designated *G*, followed by the nominal gloss value; the glazed ceramic tile specimens are designated *T*, followed by the nominal gloss value.

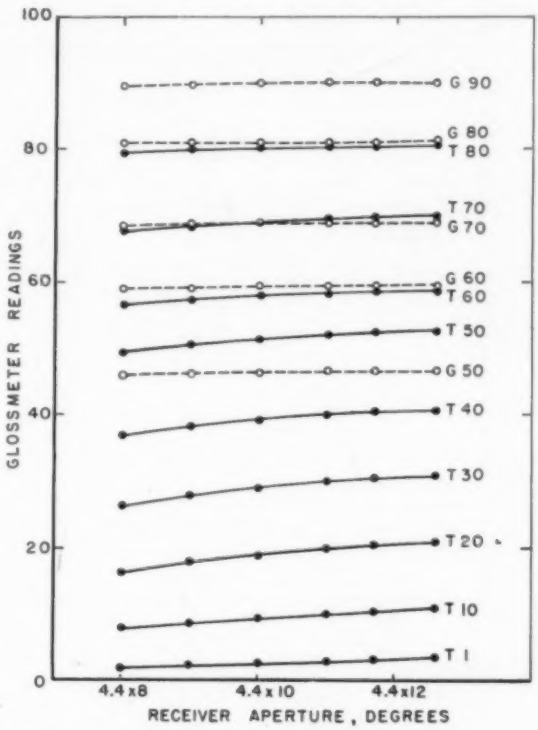

FIGURE 7. *Glossmeter readings obtained by varying the dimension of the receiver aperture in the β plane.*

The depolished black glass specimens are designated *G*, followed by the nominal gloss value; the glazed ceramic tile specimens are designated *T*, followed by the nominal gloss value.

2. Source Aperture

To determine the effect of source aperture variation on glossmeter readings and thus be able to determine permissible tolerances, data were obtained on the variation of measured gloss with source aperture with the receiver aperture held constant at the value prescribed in the ASTM method mentioned earlier. It was found that the variation of source aperture in the α plane affected the measured gloss of the plaques as shown in

figure 8; variation in this plane did not produce as pronounced measured gloss differences as for the receiver aperture variation. Variation in the β plane had a negligible effect on the measured gloss values, so the data are not shown here.

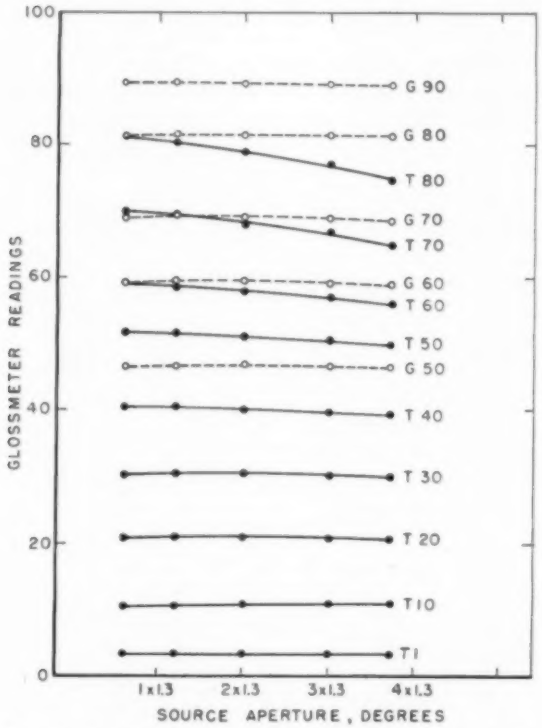

FIGURE 8. *Glossmeter readings obtained by varying the dimension of the source aperture in the α plane.*

The depolished black glass specimens are designated *G*, followed by the nominal gloss value; the glazed ceramic tile specimens are designated *T*, followed by the nominal gloss value.

3. Position of Source Image

Another question of practical importance is the effect of the position of the image of the source. A properly adjusted glossmeter will form an image of the source centered in the receiver entrance window when a flat polished surface is placed in the specimen position. Commercial glossmeters using simple lenses are difficult to adjust because chromatic abberration of the lenses causes light of different wavelengths to focus at different positions. If the red rays are brought to a sharp focus, the source image is surrounded by a blue haze. Conversely, if the blue rays are brought to a sharp focus, the image will be surrounded by a red haze. The effect of position of the source aperture with respect to the receiver entrance window was explored on the experimental glossmeter by placing spectacle-type lenses of low power between the specimen and receiver collimating lens. This procedure was used because the collimating lenses are not easily moved from their positions of optimum collimation. By using positive or negative lenses the image of the source was obtained before or behind the plane of the receiver entrance window. Figure 9 illustrates the effect produced on the measured gloss values. It shows that the greatest effect is produced on the glass values of the tile plaques, and that the effect on measured gloss values is not negligible for tile but is practically so for depolished glass. The data also show that there is no preferred direction of

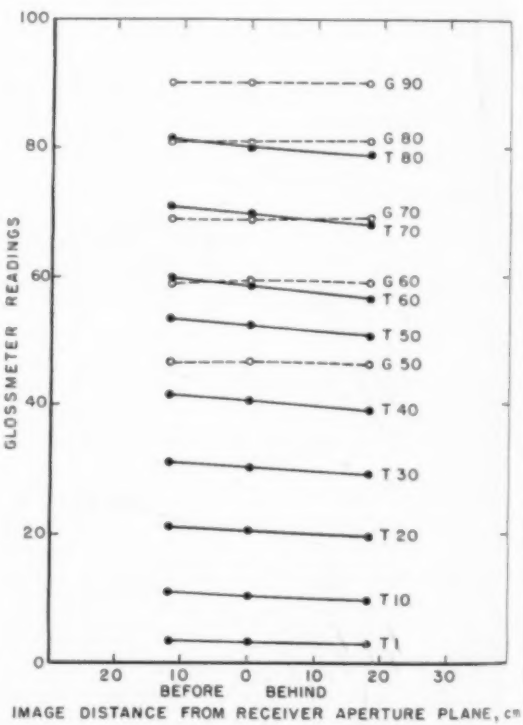

FIGURE 9. *Glossmeter readings obtained by varying the position of the focused image of the source relative to plane of the receiver aperture.*

The depolished black glass specimens are designated *G*, followed by the nominal gloss value; the glazed ceramic tile specimens are designated *T*, followed by the nominal gloss value. Focal length of receiver lens is 54.6 cm.

departure from the plane of the receiver entrance window.

4. Specular Angle

Glossmeters are usually adjusted so that the image of the source reflected from a plane reflector, such as that of polished opaque glass, falls on the center of the receiver entrance window. Suppose, however, that in making this adjustment the angle of incidence is disturbed and that it is found to be 59° or 61° instead of 60°. What effect will this error in the specular angle have on the gloss readings? It can be shown from the Fresnel equation (see definition of Fresnel reflector) that a departure of 1° in specular angle at 60° will cause a change of approximately 5 percent in the specularly reflected flux from a polished surface of refractive index 1.53. In the usual method of operation, the instrument is set to read correctly the value of the working standard, then the gloss of the test specimen is read relative to it. If the standard and specimen have nearly the same surface characteristics, no appreciable error will result.

Figure 10 shows the effect on the measured gloss of both tile and depolished glass standards with departure from the 60° specular angle. The illuminance was adjusted for each angle so that the instrument indicated the 60° specular gloss of the polished glass reference standard. It will be noted from the figure that for the range of angles investigated the measured gloss of the depolished glass plaques increases with increasing specular angle, but the measured gloss of the tile plaques decreases slightly. In making the adjustment for the standard, the illuminance for 59°, as an example, had to be increased. Then two factors are operating, (1) the increased illuminance and (2) the decreased directional reflectance due to Fresnel reflection. The effect on the depolished glass plaques is explainable by the assumption that the second factor acts more importantly than the first, since the surface is composed of many facets in the gross plane of the plaque. The effect on the tile plaques is explainable by the assumption that the second factor is operating less importantly than the first, since the higher index of refraction of this material causes a smaller relative increase in reflectance with increasing specular angle. Since the instrument is caused to give the same reading for the reference standard the depolished black glass plaques show slight increase in relative gloss, whereas the tile plaques show slight decrease in relative gloss with increasing angle of incidence.

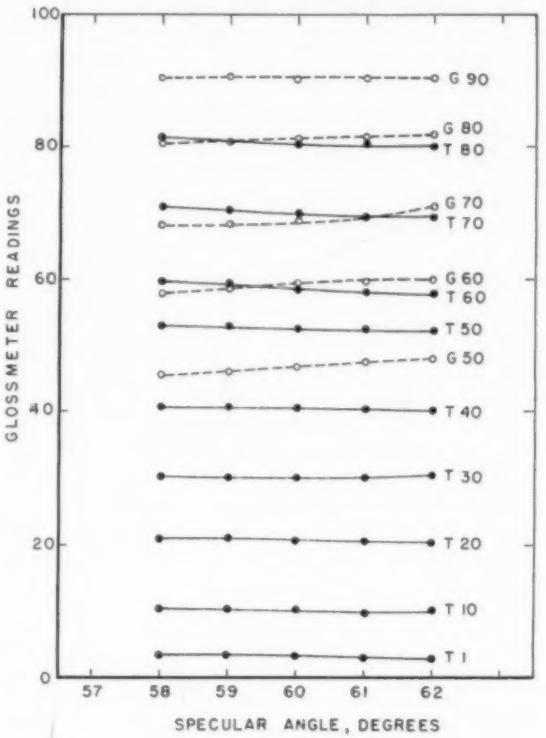

FIGURE 10. *Glossmeter readings obtained by varying the specular angle.*

The depolished black glass specimens are designated *G*, followed by the nominal gloss value; the glazed ceramic tile specimens are designated *T*, followed by the nominal gloss value.

V. Diffuse Correction

1. Simple Theory

We come now to the problem of diffuse correction. Figure 1 shows that the reflected light received by the glossmeter may be considered to be composed of two parts, the specular reflection or true gloss contributed by the surface of the specimen and the diffuse reflection contributed by the body of the specimen. Thus we see that the light-scattering property of the body of the specimen, or in a sense its body color, affects the measured gloss. In the case of high-gloss specimens, the diffuse component is a small fraction of the instrument reading, and many laboratories working with high-gloss materials do not correct or allow for it.

In the case of low-gloss specimens, however, this correction should be made especially when comparing specimens of different lightness.

(a) Hemisphere Method

Picture a perfectly reflecting, perfectly diffusing specimen which reflects no light specularly but which causes a "gloss" reading on the instrument because some of the diffusely reflected light reaches the receiver. What should be the magnitude of the correction to be substracted from the instrument reading to obtain the true gloss of the specimen? Lambert [7] showed that a perfectly diffusing specimen reflects light in such a manner that the luminous intensity in any direction is proportional to the cosine of the angle, ψ, between the perpendicular to the surface and the direction of reflection. He also showed that the perfect diffuser would appear equally bright in all directions, that is, that the luminance is constant.

Let us assume that the luminous flux reemitted by a perfect diffusor having luminance, B, and area, dA falls normally on the surface of a hemisphere of radius, R (see fig. 11). First we wish to compute the total flux, F, falling upon the entire hemisphere. The flux, dF, in a direction making an angle ψ with the perpendicular to the diffusor is evidently proportional to the projection of dA on a plane perpendicular to the direction ψ, or, $dA\cos\psi$, and to the solid angle, $d\Omega$, subtended at the diffusor. The proportionality constant is the luminance, B. Thus

$$dF=B\cos\psi dAd\Omega. \tag{4}$$

The solid angle,

$$d\Omega=2\pi R^2\sin\psi d\psi/R^2=2\pi\sin\psi d\psi,$$

where $d\Omega$ is now the hollow cone subtended at the specimen by the zone of width $Rd\psi$, whose semiangle is ψ. Therefore,

$$F=\pi BdA\int_0^{\pi/2}2\cos\psi\sin\psi d\psi=\pi BdA. \tag{5}$$

Now consider the flux, f, which falls on the receiver at an angle θ'.

From eq 4 above

$$df=B\cos\theta' dAd\omega.$$

The solid angle subtended by this receiver is

$$d\omega=\frac{R^2\alpha\beta}{R^2}=\alpha\beta,$$

where α is the aperture angle in the plane of measurement (the plane in which the specular angle θ' is measured), and β is the aperture angle in the plane perpendicular to the plane of measurement. The angles α and β are small and are measured in radians. Then

$$f=B\alpha\beta\cos\theta' dA. \tag{6}$$

Thus, of the reemitted luminous flux, the fraction, F_r, entering the receiver aperture is

$$F_r=\frac{f}{F}=\frac{\alpha\beta\cos\theta'}{\pi}. \tag{7}$$

For the ASTM receiver,

$$\alpha=4.4°,\ \beta=11.7°,\ \text{and}\ \theta'=60°.$$

Thus F_r is computed to be 0.0025. This means that the perfectly reflecting, perfectly diffusing specimen although in reality having no specular gloss would cause the instrument to read 2.5 if a perfect plane reflector were to read 1,000.

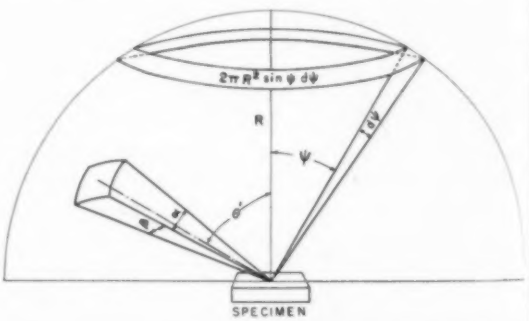

FIGURE 11. *Diffuse correction for the perfectly diffusing surface treated by the hemisphere method on the basis of simple theory.*

(b) Tangent Sphere Method

The magnitude of the diffuse correction may be obtained very simply by considering the illuminance E at any point on a sphere of diameter D tangent to the diffusor (see fig. 12). Let the

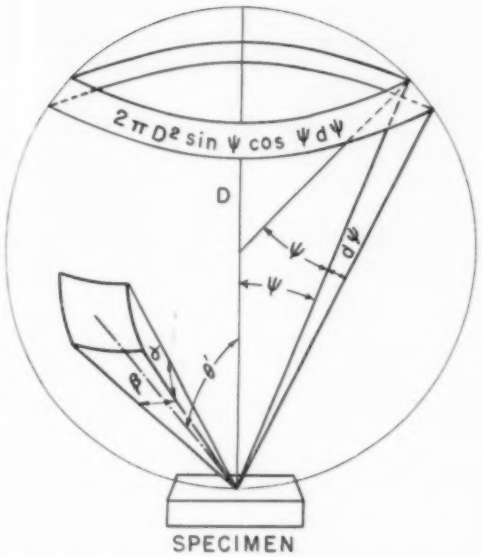

FIGURE 12. *Diffuse correction for the perfectly diffusing surface treated by the tangent sphere method on the basis of simple theory.*

luminous intensity in any direction perpendicular to the perfect diffusor of area dA be represented by $I_0 dA$ and the intensity in other directions by $I_\psi dA$. Then,

$$I_\psi dA = I_0 \cos \psi dA.$$

The illuminance, E_ψ, at any point on the sphere is the intensity in that direction multiplied by the cosine of the angle of incidence and divided by the square of the distance, $D^2\cos^2\psi$, from the perfect diffusor to that point on the sphere. Therefore,

$$E_\psi = \frac{I_\psi \cos \psi dA}{D^2 \cos^2 \psi} = \frac{I_0 dA}{D^2}. \quad (8)$$

Thus we see that the illuminance on the sphere is independent of the angle of view. Therefore the ratio, F_r, of the flux on a receiver to the total flux is simply the ratio of the area, a, of the receiver projected on the sphere to the area, A', of the whole sphere. But a, located at an angle θ' from the perpendicular to the diffusor, is $\alpha\beta D^2\cos\theta'$ and A' is πD^2. Therefore,

$$F_r = \frac{a}{A'} = \frac{\alpha\beta D^2 \cos \theta'}{\pi D^2} = \frac{\alpha\beta \cos \theta'}{\pi}. \quad (9)$$

This is the same as eq 7 obtained by integration of luminous flux over the hemisphere surface. It should be noted that the diffuse correction is the ratio of the area of the tangent sphere intercepted by α and β to the area of the whole sphere. It may be said, therefore, that the diffuse correction is numerically equal to the fraction of the tangent sphere intercepted by the solid angle formed by the instrument aperture.

2. Expansion of Theory

Practical surfaces, neither perfectly reflecting nor perfectly diffusing, will generally have smaller corrections than 2.5, but, except for black surfaces, the correction is appreciable and must be made in the low-gloss range in order to grade correctly low-gloss surfaces of different luminous reflectance. To determine the diffuse correction one must take into account the following: (a) reflectance of the specimen, (b) departure of practical surfaces from perfect diffusors, and (c) polarization of the source.

(a) Specimen Reflectance

With a goniophotometer or other glossmeter in which the illuminator can be rotated about the specimen in the plane of measurement, this correction is most easily evaluated by illuminating the specimen perpendicularly and viewing at an angle of 60°. When this is done the area illuminated is one-half of that previously illuminated, but the flux density is twice as great. If the surface is uniform, the diffuse correction is obtained directly except that a very small error is involved because the surface reflection is less for perpendicular than for 60° illumination. For a polished specimen having a refractive index of 1.53, the surface reflectance at 60° illumination is about 9 percent and at 0° is about 4 percent. This means that an additional 5 percent is added to the body illuminance, but since this flux is distributed over a hemisphere the increase in light entering the receiver is small. The fraction of the total light entering the receiver was previously computed to be 0.0025. Since the surface-reflected light is now decreased by 5 percent, the body-reflected light is increased by the same fraction, so that the diffuse correction for 60°, −60° condition as measured under 0°, −60° conditions is high by 5 percent of the magnitude. This means that for a speci-

men having a measured diffuse correction of 0.0021 the true diffuse correction would be 0.0020 or, on the usual specular gloss scale, the discrepancy would be 0.1 gloss unit. This discrepancy in the diffuse correction is proportional to the gloss, and is zero for a perfectly diffusing surface. In practice this discrepancy is so small that correction for it is unnecessary. If, on the other hand, 60° illumination and perpendicular viewing are used, the instrument reading will have to be halved to obtain the diffuse correction, because the projected area for perpendicular view is twice that for 60° view.

(b) Practical Diffusors

On the master instrument, figure 4, at this Bureau it was found that magnesium oxide, which is often thought of as the practical approach to the perfectly reflecting, if not perfectly diffusing surface, has a diffuse correction of 2.1. This value was obtained numerous times and though not vastly different from 2.5 certainly gives a larger discrepancy than could be accounted for by experimental error. Previous investigation of the diffusing properties of the surfaces of magnesium oxide by McNicholas [8] and Preston [9] revealed that it is not a perfect diffusor. This was confirmed by us for magnesium oxide; and similar data were obtained for two other materials. Figure 13 illustrates graphically the results of this investigation.

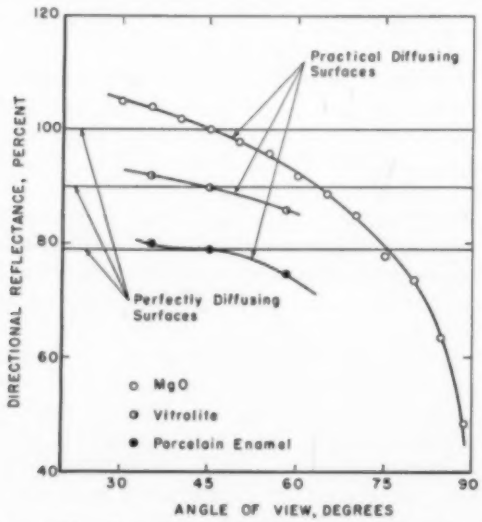

FIGURE 13. *Departure of practical surfaces from the concept of the perfect diffusor.*

It will be recalled that the reflectance of magnesium oxide prepared in a prescribed manner [10] is assigned a value of 1.00 when illuminated at 45° and viewed perpendicularly. For 0°, 60° conditions the directional reflectance of these oxide specimens was found to be only 92.5 percent of the value assigned for 0°, 45° illuminating and viewing conditions. This accounts for nearly half the discrepancy found between the computed and the measured values for the diffuse correction.

(c) Source Polarization

It will be recalled that the Fresnel reflectance of a surface is a function of the degree of polarization of the incident light as well as the angle of incidence and the index of refraction of the surface. The degree of polarization of the source was measured by rotating a polaroid filter in the emitted beam and recording the maximum and minimum transmittances. The difference of the readings was divided by the sum to obtain polarization. The data obtained show that this source (a C–6 filament) is polarized 5 percent along the axis of the coil, or perpendicular to the plane of measurement. Filament polarizations of 15 to 20 percent for straight filaments were reported by Worthing [11]. Because the 60° angle is almost the polarizing angle for glass, approximately 5 percent less incident flux is required to obtain the same reflected flux from a polished glass surface than if the source were unpolarized. Although the polarization is destroyed by a low-gloss surface, partial polarization of the incident light causes a greater fraction to be reflected from the polished surface of the high-gloss standard. Consequently, the reduced incident light on the specimen reduces the computed value of the diffuse component by 5 percent of its magnitude.

These three sources of error, (1) surface reflectance, (2) departure from perfect diffusor, and (3) polarization of the source, taken together account for the discrepancy between the computed and the measured values of the diffuse correction.

VI. Gloss Scale and Standards

Any assembly of apparatus such as a glossmeter requires calibrating and the adoption of a scale on which measurements will be based. The theoretical specular gloss standard is the perfect mirror that is assigned a value of 1,000. The practical

primary standard is a piece of polished black glass whose specular reflectance is computed from Fresnel's equation when the index of refraction of the glass is known. Black glass is used for this purpose, because all of the light flux not specularly reflected is absorbed by the body of the material and the problems associated with diffuse correction are eliminated.

In order to provide means for checking the adjustment of glossmeters and to assist in more accurate measurement of 60° specular gloss, this Bureau has investigated the suitability of various materials for use as standards, and has recently assembled sets of standards for issue. Each set consists of two white Vitrolite gloss plaques having nominal gloss values 1 and 90, and eight glazed ceramic plaques having nominal gloss values 10, 20, 30, 40, 50, 60, 70, and 80. The plaques are approximately 4¼ in. square. Figure 14 is a photograph of the plaques together with the box in which the set of ten standards is furnished. Although the plaques are not intended to be used as standards of distinctness-of-image gloss, the photograph in figure 15 has been taken to indicate approximately the gloss steps involved, since for these plaques 60° specular gloss steps agree in order with distinctness-of-image gloss steps estimates.

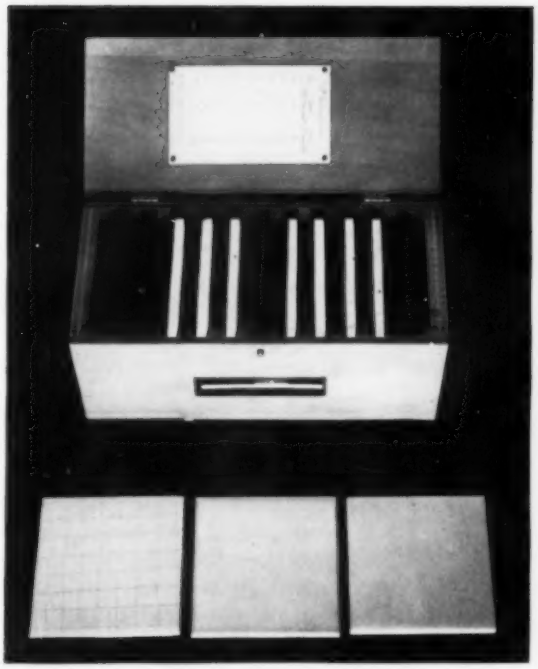

FIGURE 14. *Set of NBS gloss standards, with box in which they are issued.*

VII. Summary and Recommendations

Although photoelectric measurements of specular gloss at a particular angle are convenient for the evaluation of surface appearance, such measurements do not completely evaluate the gloss characteristics, much less the over-all appearance of the surface. In general, the specular gloss of high-gloss surfaces can best be differentiated by observation at small angles from the perpendicular, whereas matte surfaces can best be differentiated at large angles from the perpendicular.

Problems inherent in practical glossmeters have been empirically treated here. After permissible discrepancies in gloss values have been decided upon, the tolerances for the geometric variables for 60° specular gloss can be obtained from the curves in figures 5 to 9. If a deviation of ± 1 gloss unit is specified, then the tolerances can be readily ascertained. On the basis of the data obtained by the authors on the versatile glossmeter and a permis-

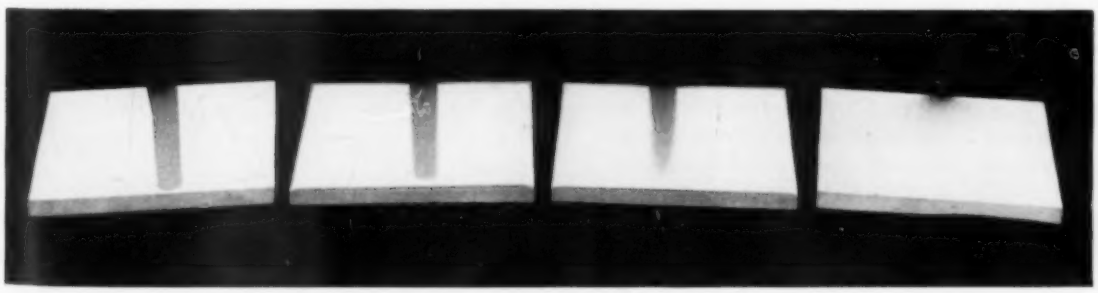

FIGURE 15. *Photographic representation of specular gloss standards.*

The standards are arranged in order of decreasing specular gloss from left to right, as shown by the more readily photographed gradation of the distinctness of reflected images. For these standards distinctness-of-reflected-image gloss correlates with specular gloss.

883124—50——4

sible deviation of ±1 gloss unit, the recommendations shown in table 1 are made.

TABLE 1. *Recommended tolerances for practical 60° glossmeters*

Variable	Recommended tolerance
Receiver aperture:	
In plane of measurement	±0.1°.
Perpendicular to plane of measurement.	±0.2°.
Source aperture in plane of measurement.	±0.2°.
Position of source image [1]	±5% of the focal length of receiver lens.
Specular angle	±0.3° from the specified specular angle.

[1] For uncorrected lenses, source image should be focussed for the circle of least confusion.

In view of the fact that these discrepancies are cumulative, it is recommended that manufacturers and users of practical glossmeters be careful that the geometric variables be held well within the recommended tolerances; for if all the variables happen to contribute errors in the same direction though they are just within the recommended tolerances, the reading may be in error by as much as 5 gloss units.

The authors express their appreciation to D. B. Judd for invaluable suggestions and advice during preparation of this paper and also to E. M. Hagaman for his ingenuity and assistance in the construction of the versatile glossmeter.

VIII. References

[1] R. S. Hunter and D. B. Judd, ASTM Bulletin No. 97, 11 (March 1939).

[2] A. Fresnel, Calcul des teintes que polarization developpe dans lames cristallisees, Ann. chim. phys. **17,** 194, 312 (1821).

[3] R. S. Hunter, Methods of determining gloss, J. Research NBS **18,** 19 (1937).

[4] ASTM tentative method of test for 60° specular gloss of paint finishes, ASTM designation D523, Book of ASTM Standards, Part II (1949).

[5] S. C. Horning and M. P. Morse, The measurement of the gloss of paint panels, Official Digest (Fed. Paint and Varnish Products Clubs) **266,** 153 (1947).

[6] D. G. Moore and R. S. Hunter, Use of liquid surfaces as standards of specular gloss, J. Am. Ceramic Soc. **24,** 167 (1941).

[7] J. H. Lambert, Photometria sive de mensura et gradibus luminis, colorum et umbrae, p. 324, Augsburg (1760).

[8] H. J. McNicholas, Absolute methods in reflectometry, BS J. Research **1,** 29 (1928) RP3.

[9] J. S. Preston, The reflection factor of magnesium oxide, Trans. Opt. Soc. (London) **31,** 15 (1929).

[10] NBS Letter Circular LC547, Preparation and colorimetric properties of magnesium-oxide reflectance standard (1939).

[11] A. G. Worthing, Deviation from Lambert's law, and polarization of light emitted by incandescent tungsten, tantalum, and molybdenum, and changes in the optical constants of tungsten with temperature, J. Opt. Soc. Am. **13,** 635 (1926).

WASHINGTON, February 13, 1950.

U. S. Department of Commerce
National Bureau of Standards

Research Paper RP2106
Volume 44, June 1950

Part of the Journal of Research of the National Bureau of Standards

Rate of Shrinkage of Tendon Collagen: Further Effects of Tannage and Liquid Environment on the Activation Constants of Shrinkage

By C. E. Weir and J. Carter

Further studies of the rate of shrinkage of tendon collagen are reported. Metallic tannages decreased heat and entropy of activation. Three organic tannages yield evidence of cross-linking by increasing heat of activation. Effects of aqueous solutions of salts of alkali and alkaline earth metals and organic materials are studied. The results—decreased heat and entropy with increasing concentration of alkali salts and a similar behavior with organic solutes over a portion of the concentration range—are interpreted as due to interaction of solutes at hydrogen bonds. Solutions of alkaline earth salts increase heat and entropy of activation. A mechanism of shrinkage designed to explain the results of these studies is proposed. Applications of the experimental method are discussed.

I. Introduction

This investigation represents a continuation of studies of the effects of tannage and environment on the rate of shrinkage of tendon collagen and on the heat, entropy, and free energy of activation of the shrinkage process. It was shown that shrinkage of collagen could be treated as a rate process [1],[1] and that tanning or treatment with sodium chloride, sulfuric acid, and sodium hydroxide generally decreases the heat and entropy of activation. Chrome tanning, however, was shown to cause a marked increase in all activation constants. As a result of the foregoing studies, it was concluded that the various tannages and ionic media investigated interacted principally at salt bonds, possibly causing rupture of these bonds. Chrome tanning was assumed to form cross linkages or to reinforce existing cross linkages.

This report contains further data on the effect of tannage and shows that increased activation constants result from tannages such as quinone and glyoxal, which might be expected to form cross linkages. The effect of environment is studied in greater detail with aqueous solutions of organic solutes and additional inorganic salts being investigated. It is shown that, inasmuch as organic solutes also decrease the activation constants, this decrease may not be attributed specifically to salt-bond interactions of the solute. The behavior of tendon collagen in aqueous solutions is indicative of an extremely complex system, and, in general, no interpretation of the data obtained with solutions is offered.

[1] Figures in brackets indicate the literature references at the end of this paper.

II. Method of Measurement and Treatment of Results

The experimental details of the measurements, as well as the method of analysis of the data, have been described previously [1] and will be treated only briefly here.

Measurements of rate of shrinkage of kangaroo-tail tendon were made at approximately four different temperatures spaced 2 deg to 3 deg C apart, each temperature of measurement being maintained to within ± 0.1 deg C by means of a temperature-controlled water bath. The data consisting of length and time measurements were interpolated to obtain the time of half shrinkage designated as $t_{1/2}$ and defined as the time at which the length of

tendon, l, is one-half of the sum of the initial length, l_0, and the final length, l_∞.

Experimental values of $t_{1/2}$, in seconds, and the reciprocal of the absolute temperature, $1/T$, are introduced into the equation,

$$\log \frac{0.693h}{kTt_{1/2}} = \frac{-\Delta H}{2.303R} \times \frac{1}{T} + \frac{\Delta S}{2.303R}. \quad (1)$$

In eq 1, h is Planck's constant; k, Boltzmann's constant; ΔH, the heat of activation; ΔS, the entropy of activation; and R, the gas constant. This equation is a result of the theory of absolute reaction rates [2] and the utilization of $t_{1/2}$ in place of the reaction-velocity constant. A discussion of this substitution has been given previously [1]. A plot of the left term as ordinate and $1/T$ as abscissa yields a line having a slope proportional to ΔH and an intercept proportional to ΔS. Values of ΔH and ΔS are calculated from the data by the method of least squares and are used in conjunction with the well-known relationship,

$$\Delta F = \Delta H - T\Delta S, \quad (2)$$

to determine ΔF, the free energy of activation. Since ΔF varies with temperature, the temperature for which the calculation was made is denoted by a subscript.

Since ΔF is directly related to the rate of shrinkage, the value of ΔF_{60} may be taken as a measure of the temperature range in which shrinkage occurs at an experimentally measurable rate. It should be noted that a value of ΔF of the order of 25 kcal corresponds to a shrinkage half-time of the order of 1 minute. For purposes of comparison, there are tabulated values of the shrinkage temperature, T_s, obtained directly from the experimental data and defined as the temperature at which half-shrinkage occurs in 1 minute.

From the effect of treatment and environment on the heat of activation, ΔH, calculated from the theory of absolute reaction rates—or the energy of activation E in the Arrhenius expression [2], which is approximately the same numerically—conclusions have been drawn concerning the structure of collagen, the mechanism of tanning, and the mechanism of shrinkage. Some conclusions have similarly been drawn from variations in values of ΔF_{60}. In order to arrive at such conclusions as to the effect of treatment, it has been necessary to assume that the size of the unit taking part in the shrinkage process is unaffected by treatment.

Three general types of results have been obtained in these experiments, namely: ΔH and ΔS decrease while ΔF_{60} increases (inorganic tannages); ΔH, ΔS, and ΔF_{60} increase (deaminization and postulated organic cross-linking tannages); no simple correlation exists between ΔH, ΔS, and ΔF_{60} (variation of environment with organic and inorganic solutes and chemical modifications excluding deaminization). The data are divided into these three general categories, although for purposes of comparison the separation is not adhered to rigorously in some instances.

A more detailed exposition of the mechanism of shrinkage as related to the activation process is given in section IV.

III. Results and Discussion

1. Tannage With Inorganic Materials

Tendons were tanned with several inorganic materials in addition to those previously described [1]. Tannage was effected by immersing the tendons in solutions of the inorganic salts and adjusting the pH of the solutions with acid or alkali to the optimum value. After a 24-hour immersion tendons were removed, washed thoroughly, and stored in distilled water at pH6. The results of tests on these specimens are given in table 1.

By comparison of the values of ΔH, ΔS, and ΔF_{60} for the tanned specimens with those for untreated tendon, which were obtained previously [1] and are included for reference, it is seen that ΔH and ΔS values are lowered whereas ΔF_{60} values are, in general, increased on tannage. Consideration of the standard deviations of the measurements indicates that most changes are too small to be considered significant, except insofar as ΔF_{60} values of copper and mercury tannages are concerned. Since ΔF_{60} is a measure of the "shrinkage temperature" [1], it is seen that most shrinkage temperatures were increased as a result of the tannages.

It will be noted that little correlation exists between the values of ΔF_{60} and the ash content, considered to be a measure of the amount of combined material. Ash content of mercury tannage was not obtained, but wet digestion and precipitation with H_2S showed qualitatively that a small amount of mercury was present.

TABLE 1. *Effect of tannage with inorganic tanning materials*

Tannage	Tanning material	Ash (dry basis)	ΔH	ΔS	ΔF_{25}
		Percent	*kcal/mole*	*cal/mole deg*	*kcal/mole*
Tungsten	Sodium tungstate [3]	30.9	110	253	25.5
Molybdenum	Sodium molybdate [3]	15.0	119	284	24.7
Phosphate	Calgon [3]	1.1	129	311	25.5
Copper	Ammoniacal copper sulfate	3.1	141	340	28.0
Mercury	Mercuric chloride	.....	120	276	28.7
Untreated tendon [1]	.....	.....	141	349	24.7
Standard deviation of value obtained on untreated tendon [1].	.....	.....	15	43	0.6

As far as can be ascertained, the effects of copper and mercury are being reported for the first time. Both materials appear to tan if elevation of the shrinkage temperature is considered a criterion of tannage. Copper interacts with collagen rapidly and readily in solutions containing both cuprammonia ion and undissolved cupric hydroxide. Mercury reacts from solutions of mercuric chloride having a pH close to the precipitation point. Extensive studies of these reactions have not been made, but hide squares have been subjected to the treatments. Copper appears to produce good "leathering," but mercury treatment appears to resemble "tawing." Both reactions appear to be somewhat reversible.

There is no indication from the results of tannage with inorganic materials that any metallic tannage investigated resembles chrome tannage, which produces an elevation of 80 percent or more in the heat, entropy, and free energy of activation.

2. Cross-Linking Tannages and Treatments

In a previous investigation [1] it was concluded that chrome tanning either formed cross-linkages between neighboring polypeptide chains or reinforced existing linkages. This conclusion was based on the fact that chrome tanning caused an increase in ΔH, which was not found with any other tannage then studied. Three other tannages have been observed to cause an increase in ΔH, namely, quinone, glyoxal, and cyclohexane disulfonyl chloride, as well as treatment designed to deaminize the parent collagen. The results of tests on specimens subjected to these treatments are given in table 2, and graphs representing a portion of these data are shown in figure 1.

Tannages with cyclohexane sulfoynyl chlorides were made in a two-phase system consisting of a solution of the sulfonyl chloride in cyclohexanone and an aqueous solution of sodium bicarbonate. Tannage required several weeks, being considered satisfactory when specimens immersed in water at room temperature showed no indication of putrefaction in 1 week.

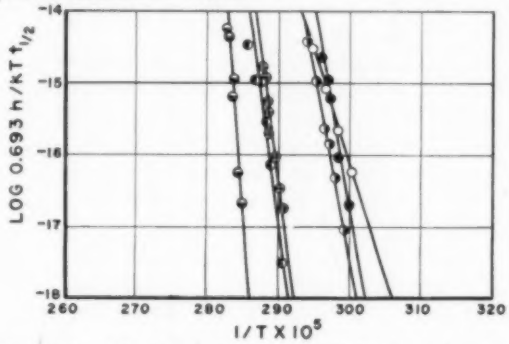

FIGURE 1. *Effect of postulated cross-linking agents on rate of shrinkage.*

○, Cyclohexane monosulfonyl chloride tanned; ◑, cyclohexane disulfonyl chloride tanned; ⊕, glyoxal tanned; ◐, quinone tanned; ●, deaminized 72 hours, pH 6.4; ◒, deaminized 72 hours, chrome tanned.

TABLE 2. *Effect of cross-linking treatments*

Treatment	ΔH	ΔS	ΔF_{25}
	kcal/mole	*cal/mole deg*	*kcal/mole*
Tanned with cyclohexane monosulfonyl chloride [4]	145	361	24.9
Tanned with cyclohexane disulfonyl chloride [4]	217	573	26.4
Tanned with glyoxal at pH 5.2	288	760	34.6
Tanned with quinone at pH 4.0	271	710	35.9
Deaminized 24 hours at 0° C, tested at pH 5.5, set A	185	477	26.3
Deaminized 72 hours at 0° C:			
Tested at pH 6.4, set A	230	613	25.7
Tested at pH 4.3, set A	191	493	26.5
Deaminized 72 hours at 0° C and chrome-tanned (1.1% Cr_2O_3), set A	456	1,225	48.4
Deaminized 48 hours at 0° C, set B	256	701	22.7
Deaminized 48 hours at 0° C and glyoxal-tanned at pH 5.2, set B	313	877	20.8
Deaminized 48 hours at 0° C and quinone-tanned at pH 5.0, set B	300	827	24.5
Tanned with chromium [1] (1.02% Cr_2O_3)	390	1,041	44.1

Tannage with glyoxal was carried out in a 5-percent aqueous solution of glyoxal at pH 5.2 for 24 hours.

Tannage with quinone was conducted in a saturated aqueous solution of quinhydrone at pH 4.0 for 24 hours.

Deaminization was carried out according to the procedure of Highberger [5]. Deaminized tendons were chrome-tanned by the two-bath process described previously [1]. Deaminization was performed in two separate experiments, the first of which was designed to ascertain the effect of deaminization on chrome tanning. Results from measurements on this sample are designated as set A. The second experiment was designed to determine the effect of deaminization on glyoxal and quinone tannage, and results of this experiment are designated as set B.

The results shown in table 2 show that tannage with the monosulfonyl chloride yields normal values of ΔH, ΔS, and ΔF_{80}. However, if tannage is carried out with the disulfonyl chloride, it is observed that ΔH, ΔS, and ΔF are increased significantly. The cyclohexane monosulfonyl chloride tannage has been investigated by Patterson [4] who concluded that the sulfonyl chloride reacts with amino groups present in the collagen, the reaction proceeding with liberation of HCl as follows:

$$R'-SO_2Cl+H_2N-R\rightarrow R'-SO_2HN-R+HCl, \quad (3)$$

where R′ represents a cyclohexane group and R a peptide chain. Similarly, a disulfonyl chloride may be expected to link two amino groups as follows:

$$R-NH_2+ClSO_2-R'-SO_2Cl+H_2N-R\rightarrow 2HCl+R-NHSO_2R'\ SO_2HN-R. \quad (4)$$

Since collagen contains amino groups in excess of those involved in peptide linkages [6], reaction 4 might be expected to proceed between pairs of amino groups in the required spatial configuration. This reaction might form an external bridge along the peptide chain or a cross-linkage between peptide chains. The fact that an increased value of ΔH results from this tannage supports eq 4, since such linkages would presumably be broken in the activation process and therefore larger ΔH values would be required. The compound formed in eq 3 would not result in increased ΔH values, as the linkage formed would not be expected to be critical from the point of view of activation.

It has been found [1] that tannage with formaldehyde did not increase ΔH, which was taken to indicate that cross-linking did not occur in this tannage [7]. However, it might be expected that a dialdehyde would cross-link two free amino groups, and tests made with glyoxal-tanned specimens show large increases of ΔH consistent with this view. The same result was obtained with quinone tannage as shown in table 2. It will be noted that glyoxal and quinone produced approximately twice as great an *increase* in ΔH as the disulfonyl chloride. Inasmuch as the extent of the reactions is not known, no conclusions may be drawn from this result. The proposed reactions involved between collagen and aldehydes and quinone have been outlined in detail [3] and will not be discussed here.

It is noted that the results obtained from the two deaminization experiments—sets A and B—agree as regards effect of deaminization on ΔH and ΔS, but not on ΔF_{80}. The reason for this discrepancy is not known but may be attributed to differences in treatment subsequent to deaminization. At the conclusion of deaminization and thorough washing in *cold* water, the specimens acquire a golden yellow color. If tested immediately, it is found that the warm water required for shrinkage causes an apparent elevation of the temperature required for shrinkage and simultaneously a deepening of the color of the specimens. If deaminized specimens stand in water at room temperature, the color likewise deepens to a reddish brown. Set A was tested several weeks after deaminization, whereas set B was tested within a few days after preparation. The difference in time of standing may be the cause of the discrepancy in ΔF_{80} values. The significant increase in ΔH values found on deaminization may be interpreted to mean that the interaction of nitrous acid with collagen produces some degree of cross-linking between peptide chains.

Stubbings and Theis [8] have found that the ϵ-amino group of lysine in collagen is destroyed rapidly during deaminization, but that the arginine residue is attacked slowly. The ϵ-amino group of lysine has little influence on chrome tanning, as shown by the 250 kcal/mole *increase* in ΔH caused by 1.1 percent of Cr_2O_3 in the deaminized specimens. This value agrees with

the *increase* of 240 kcal/mole in ΔH caused by 1.0 percent of Cr_2O_3 in untreated specimens [1]. These results imply that the ϵ-amino group of lysine is not primarily involved in chrome tanning.

Glyoxal and quinone tannages cause increase in ΔH values of deaminized specimens. This increase is consistent with postulated cross-linking due to the tannages. However, the *increase* in ΔH observed on tanning deaminized specimens is less than half that obtained on tanning untreated specimens. This finding probably indicates that the ϵ-amino group of lysine is involved in the reactions with glyoxal and quinone, but that reaction also occurs at other groups—possibly at the arginine residue not removed in deaminization. It appears that cross-linking caused by glyoxal and quinone takes place, partly at least, between the ϵ-amino groups of lysine as expected.

3. Chemical Modifications

In order to ascertain the effect of certain treatments on the collagen molecule, tests were made on chemically modified collagen. It must be emphasized that the results of such tests are not liable to strict interpretation because of the complexity of collagen and the lack of detailed information on specific changes caused in the molecule. The following treatments were investigated.

(a) Dry Heat

A sample of air-dried tendon collagen was heated for 48 hours at 50° C, for 72 hours at 100° C, for 72 hours at 120° C, and for 72 hours at 150° C. At the conclusion of the heating period at each temperature a specimen of suitable size was removed, soaked in water for 72 hours, and tested. It is to be noted that a single sample was carried through the heating cycle so that the specimen, removed at 150° C, had been subjected to temperatures of 50°, 100°, and 120° C for the periods specified.

(b) Esterification

Esterification of free carboxyl groups was attempted by the method described by Fraenkel-Conrat and Olcott [9] using methyl alcohol. The reaction was carried out for 4 days at room temperature. A portion of the specimens was washed free of acid in a salt solution, while the remainder was subjected to the action of concentrated ammonium hydroxide for 24 hours, washed, and tested.

(c) Methyl Magnesium Iodide

Vacuum-dried tendons were subjected to the action of methyl magnesium iodide at 30° C for 1 week. Possible reaction products were hydrolyzed in a pickle solution at 0° C, and the tendons were washed free of acid and salt, and tested.

The results of tests of specimens subjected to the foregoing treatments are given in table 3.

TABLE 3. *Effect of chemical modifications*

Treatments	ΔH	ΔS	ΔF_{80}
	kcal/mole	*cal/mole deg*	*kcal/mole*
Heated at 50° C for 48 hr	165	422	24.9
Heated at 50° C for 48 hr and at 100° C for 72 hr	136	340	23.1
Heated at 50° C for 48 hr, at 100° C for 72 hr, and at 120° C for 72 hr	88	204	20.1
Heated at 50° C for 48 hr, at 100° C for 72 hr, at 120° C for 72 hr, and at 150° C for 72 hr	(a)	(a)	(a)
Methyl magnesium iodide	148	375	23.7
Esterified with methyl alcohol, washed	(a)	(a)	(a)
Esterified with methyl alcohol – subsequent ammonia treatment	160	427	17.5

[a] No measurements possible.

It is observed that dry heat appears to deteriorate collagen since ΔH, ΔS, and ΔF_{80} values appear to decrease monotonically. Results obtained on specimens heated at 50° and 100° C, however, are not significantly different from those obtained on untreated material. After heating at 120° C, a drastic, significant lowering is found, whereas specimens subjected to heating at 150° C shrank and disintegrated on soaking so that no measurements could be made. Kanagy [10] has shown that carbon dioxide and water are liberated from leather heated in dry air and oxygen and concludes that oxidation may be occurring at temperatures as low as 80° C. This oxidation may be the cause of the rapid decrease in cohesive forces shown by the figures of table 3.

Treatment with methyl magnesium iodide produced no visible reaction, and the results obtained are normal. Since the Grignard reagent is a severe dehydrating agent, it would appear likely that the results obtained on dry heating are due to the effect of heating and not merely to loss of water.

Esterification produced a product that appeared unstable in water, and no measurements were made

on these specimens. Following esterification, specimens were washed in a salt solution for several weeks until the pH of the solution showed no decrease on standing in contact with the specimens for 24 hours. However, on replacing the salt solution with water, extreme swelling occurred, and it was not possible to perform measurements on the specimens. The cause of this swelling is not known, but previous studies have also shown swelling as a consequence of esterification [11].

Specimens subjected to treatment with a solution of concentrated ammonia after esterification, in expectation of replacing the ester groups with amide groups, appeared to be stable in water, but yielded low ΔF_{60} values.

4. Effect of Changing Test Medium

(a) Special Considerations of Data on Effect of Test Medium

Results obtained on tanned tendons appear much easier to interpret than data concerning the effect of variation of the test medium. In tanning tests, the data for tanned tendons are compared with those for untanned specimens tested under the same conditions of environment. When the medium is changed, comparison of results with those of a standard environment (i. e., water, pH 6 to 7, 60° C) may lead to conclusions that are erroneous, because the chemical potential of the test medium is changed by addition of solute. The chemical potentials of both solvent and solute may be involved in the activation process in an unknown manner. Eyring and Stearn [12] and Neurath et al. [13] discuss this point in detail. It appears, therefore, that it is of questionable value to attempt the interpretation of the data obtained with aqueous solutions.

(b) Neutral Salts of Alkali Earth Metals

Previous experiments [1] on the effect of sodium chloride solutions yielded results that were interpreted as the result of solute ions interacting at ionic linkages in the collagen. In order to ascertain the effect of other salts, measurements were made using aqueous solutions of a variety of neutral salts of various concentrations. The results obtained for salts of alkali metals are given in table 4.

The similarity of the general nature of the results obtained with sodium nitrate and potassium chloride solutions to those previously reported for sodium chloride is to be noted. Sodium sulfate solutions produce somewhat different effects, while lithium chloride and sodium thiocyanate solutions produce drastic lowering of T_s values.

TABLE 4. *Effect of solutions of salts of alkali metals*

Solute	Concentration	pH	ΔH	ΔS	ΔF_{60}	T_s
	Mole/liter H_2O		*kcal/mole*	*cal/mole deg*	*kcal/mole*	*° C*
$NaNO_3$	0.02	6.8	152	384	23.7	63
Do	.5	6.3	125	311	20.9	55
Do	3.0	5.5	97	233	19.6	50
Do	7.0	.....	110	260	23.0	61
Do	(a)	6.4	90	200	23.8	64
Na_2SO_4	0.10	.....	130	322	22.7	61
Do	.25	.....	116	278	23.6	63
Do	.5	.....	96	214	24.7	68
Do	1.0	.....	106	232	28.4	79
NaSCN	0.1	5.5	133	332	22.8	61
Do	.5	6.0	136	356	17.7	49
Do	1.0	.....	123	327	14.0	40
KCl	0.1	6.4	114	274	23.2	61
Do	.5	6.3	124	307	22.1	59
Do	1.0	6.1	103	241	23.1	61
Do	3.8	5.7	101	225	26.4	71
LiCl	1.0	6.5	135	349	19.1	52
Do	2.5	.....	132	347	16.4	45
Do	3.5	6.4	128	335	16.6	46
Do	5.0	6.8	121	335	9.6	27

[a] Saturated at 20° C.

C. Neutral Salts of Alkaline Earth Metals

The drastic action of alkaline earth chlorides is well known [14], and it is of interest to ascertain the effect of solutions of such salts on the activation process. Studies were confined to the chlorides of barium, calcium, and magnesium, and the sulfate of magnesium. The latter is of particular interest since it is widely used as a filler in sole leathers. The results of these tests are shown in table 5.

The similarity of the results obtained with the chloride solutions is marked as is the difference between the effects of chloride and sulfate of magnesium. The divergence of the data obtained with solutions of magnesium chloride and magnesium sulfate is shown graphically in figure 2.

It was not possible to pursue investigations of solutions of alkaline earth chlorides to higher concentrations, as shrinkage occurs at or below room temperature in such solutions. Some of the results reported necessitated measurements below the ambient temperature. However, to resolve the

question of a minimum shrinkage temperature with these salts, observations were made in every instance on saturated solutions of the chlorides. It was found that shrinkage occurred very slowly at discrete regions of the specimens below 20° C in all saturated solutions, which shows that there is no minimum on these curves corresponding to the minimum shrinkage temperature observed for solutions of the alkali chlorides.

TABLE 5. *Effect of solutions of salts of alkaline earth metals*

Solute	Concentration	pH	ΔH	ΔS	ΔF_{30}	T_s
	Mole/liter H_2O		*kcal/mole*	*cal/mole deg*	*kcal/mole*	*° C*
$BaCl_2$	0.10	6.1	137	347	21.8	59
Do	.25	6.1	215	594	17.0	52
Do	.50	6.1	206	578	13.5	46
Do	1.00	5.9	175	494	10.3	38
$CaCl_2$	.10	6.6	136	347	20.9	56
Do	.25	6.6	160	424	18.7	52
Do	.50	6.2	140	372	16.2	46
Do	.75	6.0	230	667	7.7	40
$MgCl_2$	.02	6.1	110	263	22.8	61
Do	.10	6.1	132	334	20.9	57
Do	.25	6.0	139	356	20.3	55
Do	1.00	.....	191	540	11.4	42
Do	1.40	.....	210	601	10.3	41
$MgSO_4$	.10	.....	164	434	22.4	60
Do	.50	.....	122	297	22.8	61
Do	1.00	.....	134	326	25.3	67
Do	1.70	.....	121	274	30.2	81
Do	2.20	.....	139	317	33.9	91
Do	(a)	.....	119	257	33.4	92

a Saturated at 20° C.

(d) Solutions of Organic Solutes

The previous conclusion that salts interacted principally at salt-bonds was tested by subjecting specimens to test media of aqueous solutions of organic materials. Such experiments were also expected to yield information on the role of water in the shrinkage process. The complete results of these tests are given in table 6 and for ethyl alcohol and dioxane in figure 3.

The results given in table 6 show that, except for glycerine, the organic solutes, in general, behave in a similar manner to the alkali chlorides in dilute solutions. In more concentrated solutions, however, all quantities increase significantly. If ionic linkages exist in collagen, and are involved in the shrinkage process, it would be expected that ΔH should increase by virtue of the lowering of the dielectric constant in these solutions and the increased cohesive energy of the collagen

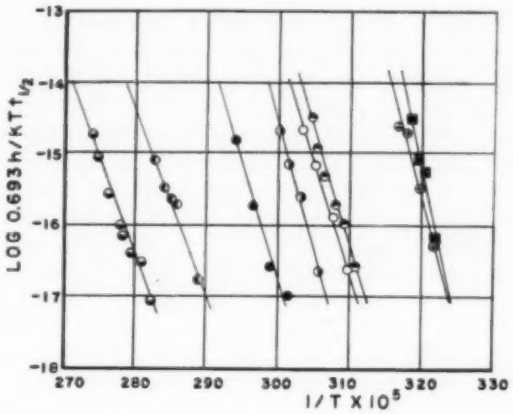

FIGURE 2. *Effect of magnesium chloride and magnesium sulfate solutions on rate of shrinkage.*

◑, $MgSO_4$, 0.1-M solution; ●, $MgSO_4$, 1-M solution; ◐, $MgSO_4$, 1.70-M solution; ◒, $MgSO_4$, saturated solution; ○, $MgCl_2$ 0.1-M solution; ◓, $MgCl_2$, 0.25-M solution; ⊗, $MgCl_2$, 1-M solution; ■, $MgCl_2$ 1.4-M solution.

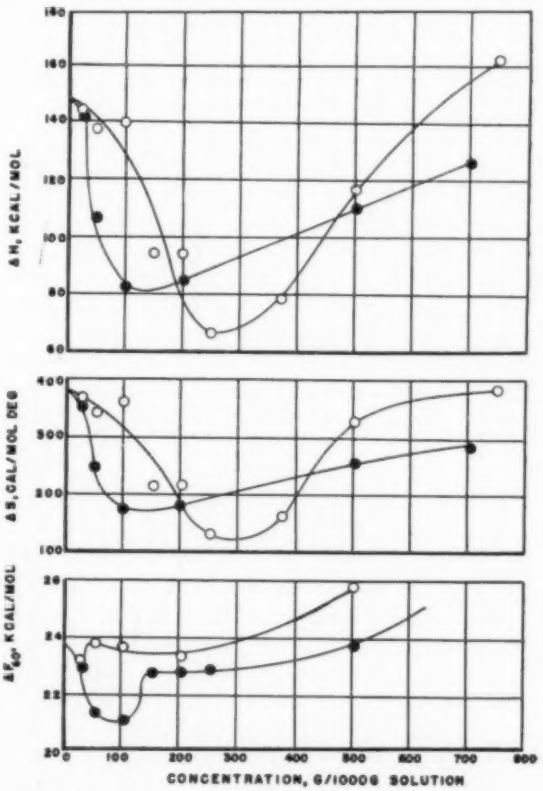

FIGURE 3. *Heat, entropy, and free energy of activation in aqueous solutions of alcohol and dioxane.*

●, Alcohol solutions; ○, dioxane solutions.

molecule. The reverse effect was observed, and it appears that ionic linkages are probably not involved in the shrinkage process, and furthermore that effects produced by solutions of alkali salts are probably not the result of interactions of ions at such linkages. The alternative explanation of this effect [1] that the results obtained are due to interactions of the various solutes at hydrogen bonds existing in the collagen is, therefore, proposed as more in accord with the experimental facts.

TABLE 6. *Effect of aqueous solutions of organic materials*

Solute	Concentration	ΔH	ΔS	ΔF_{80}	T_s
	g/1,000 g solution	*kcal/mole*	*cal/mole deg*	*kcal/mole*	*° C*
Dioxane	25	145	367	23.2	62
Do	50	136	343	21.4	59
Do	100	141	360	21.1	57
Do	150	95.1	217	22.8	60
Do	200	94.4	215	22.8	60
Do	250	66.5	131	22.9	60
Do	370	78.7	165	23.8	64
Do	500	137	328	27.5	74
Do	750	162	384	34.7	87
Ethyl alcohol (95%)	25	144	364	23.0	61
Do	50	107	249	23.9	64
Do	100	83	178	23.7	62
Do	200	85	184	23.4	63
Do	500	110	256	25.8	71
Do	700	127	287	30.9	[a] 86
Glycerine	25	122	295	23.9	64
Do	100	129	315	23.7	62
Do	170	137	342	22.7	61
Do	250	189	510	19.6	54
Do	500	225	622	18.2	53
Do	921	56	96	24.3	70
Glucose	25	152	383	24.5	64
Do	50	120	290	23.9	64
Do	100	122	298	23.1	61
Do	200	147	374	22.1	58
Do	400	144	370	21.3	56
Do	700	151	388	21.8	59

[a] This value obtained by extrapolation of experimental data.

The results obtained with glycerine differ from those obtained with the other organic solutes. Values of ΔF_{80} show that a decrease in shrinkage temperature takes place in concentrated glycerine solutions such as are used in testing shrinkage temperature [13]. This result suggests that the use of glycerine for such measurements is not desirable. It would seem that when shrinkage temperatures exceeding 100° C are to be measured, the use of water under pressure should yield more reliable results. Results obtained in solutions containing 97.9 percent of glycerine were not obtained under the same experimental conditions as other results and are, therefore, not to be compared with the other data. It was observed that this concentrated glycerine solution penetrated tendon collagen slowly, and the results shown were obtained on specimens soaked in glycerine for 30 days. The low heat of activation obtained, together with the observed swelling in glycerine, indicate a deterioration of collagen by glycerine. This finding emphasizes the fact that all results reported must be considered as "short term" effects only.

IV. Mechanism of Shrinkage of Collagen

Many qualitative descriptions of the mechanism of shrinkage of collagen have been published [16, 17]. Theories that have been proposed are in substantial agreement, differing only in minor aspects. As a result of the present studies, a qualitative mechanism has been evolved that is in general agreement with those previously reported. However, details of the shrinkage process, which have not been considered in any previous report, are vital in this mechanism and will be discussed at length. The proposed process is as follows:

Collagen may be pictured as containing regions of varying degrees of order. The structure of the highly ordered regions of parent collagen has been studied extensively by means of X-ray diffraction [18, 19]. Results of such studies are interpreted to indicate a grid-like network of polypeptide chains cross-linked by hydrogen bonds and separated by a distance of 4.4 A. Neighboring grids are separated approximately 11 A by side chains, which link the grids to each other.

A general picture of the shrinkage process may be described as follows: It might be expected that over some elevated temperature range *dry* collagen would become amorphous [20], but decomposition occurs before these temperatures are attained [21]. However, upon immersing collagen in an aqueous medium, water penetrates between the grids of chains, increasing the spacing irregularly from 11 A to at least 17 A [18]. If this system is heated, the increase in kinetic energy due to the combined thermal agitation of the polypeptide chains *and the imbibed water* becomes sufficient at some elevated temperature

to rupture the stabilizing, cross-linking bonds. The unsupported chains then spontaneously undergo disorientation to a folded configuration of higher entropy. In the folded configuration, the chains occupy a greater volume [22] and exhibit no evidence of long-range periodicity [19]. The swollen, thermally contracted collagen is rubber-like and probably contains few, if any, cross-linkages between peptide chains. The term "cross-linkage," as used here, refers to any lateral bonding through primary or secondary valence forces.

The foregoing picture is well known and generally accepted. However, this mechanism does not account either for the inhomogeneous nature of the shrinkage process reported in a previous paper [1], and which has been shown to occur even in submicroscopic fibrils [23], or for the time dependence of the phenomenon. In order to explain this behavior, the following detailed mechanism of the shrinkage process is proposed:

Inasmuch as variations in chain spacing, spatial orientation, and chemical structure probably exist in pure collagen, it is not likely that all cross linkages possess equal energies, or even that extremely small, arbitrary regions contain equal numbers of such linkages. A small region containing few linkages of low energy is considered to represent a site favorable for initiation of shrinkage, i. e., a "shrinkage nucleus."

Consider a region containing such a nucleus. The nucleus is assumed to contain a large number of peptide chains and their accompanying cross-linkages. Due to kinetic energy of thermal agitation and thermal bombardment by water molecules, any particular cross linkage may be broken and a degree of freedom thereby imparted to two chains even at a low temperature. Upon loss of the linkage, the sites of the former bond are assumed to be saturated with water molecules made available by motion of the chains and held by secondary chemical forces. Barring further developments, the water molecules attached to the chains may be ejected by agitation of the partially free chains, and recombination of the original bond may thus occur after a suitable interval. Shrinkage of a pair of chains freed in this manner is not likely to occur because of the rigidity conferred by neighboring chains that are still cross-linked. As the temperature is raised, more energy is available for bond rupture, and the number of bonds broken per unit time becomes larger. The chains freed by the ruptures move about, combine with water, subsequently recombine, etc.

It is assumed that when some large minimum number of bonds in this nucleus are open at the same instant, the structure is so weakened that there exists a very high probability that the nucleus will proceed to a more stable configuration (the shrunken state) by chain folding. For this process it is believed cooperation between many chains is required, therefore many chains shrink simultaneously. The configuration in which the requisite number of bonds are open is considered to be the activated complex [1].

These shrinkage nuclei may occur at random locations throughout the collagen, and shrinkage initiated in such nuclei may possibly occur at any time. However, it is obvious the process is both temperature and time dependent—a rate process—although the probability of such occurrence at low temperature becomes prohibitively small. The nodules of initiation of shrinkage previously described [1] are ascribed to shrinkage occurring at these shrinkage nuclei.

Following the formation of a single shrunken nucleus, intact bonds existing between chains in the immediate vicinity are most probably subjected to higher forces imposed by loss of reinforcing bonds that existed in the shrunken nucleus and the distortion caused by this material. The shrunken nucleus may be expected to grow, therefore, both laterally and longitudinally at the expense of the chains in these directions.

In the lateral directions the nucleus is expected to grow rapidly, as smaller numbers of chains in these directions may collapse as a unit. This rapid lateral growth is believed to result in the gelatinous rings previously described [1]. Longitudinal growth will take place more slowly, because the intact lateral structure in these directions will necessitate cooperation between more chains, and therefore simultaneous shrinkage of a large number of chains. The processes occurring in the regions longitudinally adjacent to the shrunken nucleus are, therefore, pictured as very similar to those occurring in the "shrinkage nucleus" itself, and shrinkage will take place only after a large number of bonds are open simultaneously.

Longitudinal shrinkage probably occurs at a somewhat higher rate than initiation of shrinkage,

as bonds in the longitudinally adjacent regions are probably subjected to larger forces arising from the deformation and freedom of motion of chains in the shrunken nucleus. The longitudinal growth, however, will probably exhibit essentially the same time and temperature dependence as the formation of the shrunken nuclei. This assumption is justified by linearity of rate data over the temperature range studied, although an exception has been noted [1] in the case of highly swollen tendons in which large numbers of bonds are probably broken before testing, or in which smaller units may shrink because of the swollen condition of the collagen.

The energy absorbed by the shrinkage nucleus and the corresponding longitudinally adjacent region in the transformation from the condition in which the cross linkages are intact to that configuration in which the requisite minimum number for shrinkage are broken, is the heat of activation, ΔH. For the reasons given previously, it is believed that ΔH is essentially the same for both the initiation and propagation of shrinkage. The values of ΔH obtained in these studies are probably an average of two very large, nearly identical values corresponding to the initiation and the propagation of shrinkage.

The shrunken collagen in the wet condition will be rubber-like, as available cross-linking sites are combined with water molecules. On partial or complete drying, cross linkages will be reformed between active sites of adjacent folded chains. The dry, or partially dry, shrunken collagen, therefore, will be rigid despite the folded configuration of the chains.

The bonds that cross-link the peptide chains of parent collagen and which are involved in the foregoing mechanism have not been identified. The nature of these bonds does not affect the proposed process. From these studies it is concluded that the *only* bonds involved in the process are the hydrogen bonds existing between laterally adjacent peptide linkages. This conclusion has not been reached by virtue of direct evidence of the participation of hydrogen bonds, but by considerations and data pointing to the nonparticipation of salt bonds. The reasons for rejecting the concept that salt bonds are involved in shrinkage are as follows:

The number of such linkages is probably small because of the spatial requirements involved. Hydrogen bonds may be estimated to possibly outnumber salt bonds by a factor of seven.

Salt bonds existing in an aqueous medium of the type used in shrinkage measurements are expected to be labile.

Deaminization of collagen does not produce the effect expected if salt bonds are involved in shrinkage.

Similarity of results obtained with various solutions containing inorganic and organic solutes shows common effects of these two types of solute. The results obtained with solutions of organic solutes are the reverse of what might be expected if salt bonds were involved, and therefore it appears that results with electrolytic solutions are also to be ascribed to effects of solute on hydrogen bonds.

The foregoing description is believed to describe successfully the data and observations obtained in these studies.

V. Practical Application

The results of the investigations described in this and in a preceding report [1] appear to have definite practical applications. The method of evaluation of the effect of tannage yields quantitative data of a more fundamental nature than the measurement of shrinkage temperature alone. It has been indicated that organic tanning materials may produce effects comparable to those produced by chrome, and it is not inconceivable that by proper choice of pH, concentration, etc., these materials might produce acceptable substitutes for chromium in tanning.

A second application lies in the investigation of the effects of salts and solutes in general on collagen. The results shown here indicate that magnesium sulfate might be a good preservative for hide, possibly better than sodium chloride. In order to evaluate the effect of solutes, further studies on specimens immersed for extended periods of time would be required. However, the present investigation shows that such studies would be advisable with magnesium sulfate but useless with lithium chloride, etc. This method appears to offer excellent possibilities as a "screening" test.

The entropy and heat values obtained on specimens tested in aqueous solutions may be of practical significance, but, in view of present

knowledge, it appears unwise to interpret these values.

VI. References

[1] C. E. Weir, J. Research NBS **42,** 17 (1949) RP1947.

[2] S. Glasstone, K. Laidler, and H. Eyring, The theory of rate processes (McGraw Hill Book Co., Inc., New York, N. Y., 1941).

[3] J. McLaughlin and E. R. Theis, The chemistry of leather manufacture (Reinhold Publishing Corp., New York, N. Y., 1945).

[4] G. H. Patterson, Report to the 44th Annual Meeting of the American Leather Chemists Assn., Bretton Woods, N. H., June 1948.

[5] J. H. Highberger and C. E. Retsch, J. Am. Leather Chem. Assoc. **34,** 131 (1939).

[6] J. R. Kanagy, Chemistry of collagen, NBS Circular C458 (1947).

[7] J. H. Highberger, J. Am. Leather Chem. Assoc. **42,** 493 (1947).

[8] R. L. Stubbings and E. R. Theis, Report to the 44th Annual Meeting of the American Leather Chemists Assoc., Bretton Woods, N. H., June 1948.

[9] Fraenkel-Conrat and H. S. Olcott, J. Biol. Chem. **161,** 259 (1945).

[10] J. R. Kanagy, J. Am. Leather Chem. Assoc. **36,** 609 (1941).

[11] J. H. Bowes and R. H. Kenten, Biochem. J. **44,** 142 (1949).

[12] H. Eyring and A. B. Stearn, Chem. Rev. **24,** 253 (1939).

[13] H. Neurath, J. P. Greenstein, F. W. Putnam, and J. O. Erickson, Chem. Rev. **34,** 157 (1944).

[14] E. R. Theis and R. G. Steinhardt, Jr., J. Am. Leather Chem. Assoc. **37,** 433 (1942).

[15] Federal Specification for Leather and Leather Products KK–L–311. U. S. Government Printing Office, Washington 25, D. C.

[16] W. E. Braybrooks, D. McCandlish, and W. R. Atkin, J. Intern. Soc. Leather Trades Chem. **23,** 135 (1939).

[17] A. Kuntzel, Stiasny Festschrift (Edward Roether, Darmstadt, Germany, 1937).

[18] W. A. Astbury, J. Intern. Soc. Leather Trades Chem. **24,** 69 (1940).

[19] R. S. Bear, J. Am. Chem. Soc. **66,** 1297 (1944).

[20] R. G. Mitton, J. Intern. Soc. Leather Trades Chem. **29,** 169 (1945).

[21] J. R. Kanagy, J. Am. Leather Chem. Assoc. **35,** 632 (1940).

[22] C. E. Weir, J. Am. Leather Chem. Assoc. **47,** 108 (March 1949).

[23] G. C. Nutting and R. Borasky, J. Am. Leather Chem. Assoc. **43,** 96 (1948).

Washington, October 10, 1949.

U. S. Department of Commerce
National Bureau of Standards

Research Paper RP2107
Volume 44, June 1950

Part of the Journal of Research of the National Bureau of Standards

Molecular Microwave Spectra Tables[1]

By Paul Kisliuk[2] and Charles H. Townes[2]

This paper presents a group of tables that give the frequencies, assignment of quantum numbers, and intensities of over 700 microwave absorption lines. The best available values of other pertinent molecular data, such as moments of inertia, dipole moments, quadrupole coupling constants, and rotation-vibration constants are also included. The frequencies are listed once for each molecule and again in consecutive ascending order of frequency. References are given for all data included. Frequencies listed to the nearest megacycle were generally measured with a cavity wave meter and may be in error by as much as 10 megacycles, whereas those given to a fraction of a megacycle are generally known to an accuracy of about 0.1 megacycle.

A short discussion of microwave spectra and important formulas is given. For easy calculation of hyperfine structure Casimir's function is tabulated up to $J=10$ and $I=9/2$.

Introduction

These tables were undertaken because of the interest and encouragement of a number of workers in microwave spectroscopy. Beside encouragement, our colleagues have provided a considerable amount of unpublished information so that the tables could be as complete and up-to-date as possible. However, the considerable activity in microwave spectroscopy makes obsolescence of the present tables inevitable, and it is expected that they will be revised and republished from time to time. Suggestions or additions for future editions of these tables will be gladly received, either by the authors or the Microwave Standards Section, National Bureau of Standards, Washington, D. C. A supplement to bring these tables up to date will soon be issued. It is especially hoped that information obtained on microwave spectral lines that is not otherwise published will be received so that it may be included in the tables and thus made available.

Only molecular lines of frequency greater than 1,000 megacycles have been listed. This excludes nuclear resonances found by molecular beam techniques rather than the usual microwave absorption measurements, as well as the lines of atomic hydrogen and cesium that fall in the microwave region. All lines reported in the literature or otherwise available prior to February 1949 have been listed. In addition to those actually observed and listed, a large number of other lines may readily be predicted from the information provided.

The primary information is presented in an alphabetic listing of the molecules by isotopic species, which is subdivided according to the transition, except for the hyperfine components, which are presented in order of frequency. With the listing of each molecule, all available molecular constants are given that are needed in interpreting the spectra. These include moments of inertia, dipole moments, quadrupole coupling constants, and rotation-vibration constants. In addition to the observed frequency and the transition assigned to each line, we have included a calculated value for the intensity and references to the latest sources of data from each laboratory that has measured the line. The most precise reported values of the frequencies were used, or the average if there seemed no reason for preference. Frequencies listed to the nearest megacycle were generally measured with a cavity wavemeter and are subject to an error of 10 or more megacycles, whereas those given to a fraction of a megacycle are generally known to an accuracy of about 0.1 megacycle.

Another listing of all the lines in order of frequency is included, with sufficient information to locate the line in the first table and a classification

[1] Work supported jointly by the Signal Corps, the Office of Naval Research, and the National Bureau of Standards.
[2] Physics Department, Columbia University.

of the line as strong, medium, or weak. We have arbitrarily taken lines of maximum absorption coefficient less than 5×10^{-7}cm^{-1} as weak, those from 5×10^{-7} to 10^{-5}cm^{-1} as medium, and those greater than 10^{-5}cm^{-1} as strong.

The general characteristics of the microwave spectra of most molecules may be explained on the basis of a rigid rotator model. Molecules are conveniently divided into three classes; linear molecules, symmetric tops, and asymmetric tops [26].[3] For linear molecules the frequency of pure rotational lines is given to a good approximation by: [26]

$$\nu_{J\to J+1}=2(J+1)B_v-4D_v\{(J+1)^3-(J+1)l^2\}\ \text{sec}^{-1}$$

$$\text{and}\ B_v=\frac{h}{8\pi^2}\left\langle\frac{1}{I}\right\rangle_{Av.}=B_e-\sum_i\alpha_i\left(v_i+\frac{d_i}{2}\right)$$

where J is the total angular momentum quantum number,
l is the angular momentum quantum number along the figure axis (zero for the ground vibrational state),
D_v is the centrifugal distortion coefficient in sec^{-1},
B_v is the average reciprocal moment of the molecule in sec^{-1},
B_e is the reciprocal moment in sec^{-1} if the nuclei were in the equilibrium position,
α_i is a coefficient of the change in reciprocal moment per quantum of excitation of the i^{th} vibrational state, and v_i and d_i are the corresponding quantum number and degree of degeneracy.

In addition there is a splitting term for the degenerate vibrational states [53]. To a somewhat rougher approximation the frequencies for both linear molecules and symmetric tops is given by $\nu=2B(J+1)$, where B is a slowly varying function of the quantum numbers. The case of the asymmetric top is complex, and is discussed in reference [9, 29] and earlier papers quoted therein.

In the event that one or more of the nuclei has a quadrupole moment different from zero, the resulting coupling to the molecular electric field splits the energy levels into a hyperfine structure which depends on the various possible orientations of the nuclear spin. The interaction between nuclear magnetic moments and molecular magnetic fields is usually much smaller, and has thus far been observed only as a small correction in the ammonia spectrum. The quadrupole interaction for the case of a single nucleus in a linear or symmetric top molecule is given by references [5, 7a, and 58a]. The energies are given by

$$E_Q=(eQq)\left\{\frac{3K^2}{J(J+1)}-1\right\}\left[\frac{\frac{3}{4}C(C+1)-I(I+1)J(J+1)}{2(2J+3)(2J-1)I(2I-1)}\right],$$

where

$C=F(F+1)-I(I+1)-J(J+1)$,
$F=J+1, J+I-1\ \ldots\ |J-I|$,
eQq=quadrupole coupling constant.
K=projection of J on molecular symmetry axis.

A tabulation of the function in square brackets for $J=0$ to 10 is given in table 3. The somewhat more complex situation when two nuclei have quadrupole coupling is discussed in reference [51].

The maximum absorption of a spectral line is independent of pressure and may be written [58]

$$\alpha_{max.}=\frac{8\pi^2Nf|\mu_{ij}|^2\nu^2}{3ckT\Delta\nu},$$

where N is the number of molecules per cubic centimeter,
f is the fraction of the molecules in the lower state of the transition,
ν is the frequency of the line,
c is the velocity of light,
k is Boltzmann's constant,
T is the absolute temperature,
$\Delta\nu$ is the half width of the line at half maximum,
μ_{ij} is the electric dipole matrix element.

The vibrational frequencies and the classical approximation for the sum of rotational states necessary to calculate f, as well as expressions for the dipole matrix elements for the various types of molecules may be found in Herzberg [26], or Wu [61], who also discuss more accurate formulae for the energy levels. The corresponding information for asymmetric molecules is tabulated in the papers of King, Hainer, and Cross [9, 29]. Since the hyperfine splitting is small compared to the

[3] Figures in brackets indicate the literature references at the end of this paper.

line frequency, a total absorption coefficient may be calculated ignoring the nuclear interaction, the result being then divided among the hyperfine components. Relative intensities of the hyperfine components can be obtained from tables of relative intensities of the analogous fine structure components [8, 60].

Thus the only quantity not as yet evaluated on the right-hand side of the formula above is $\Delta\nu$ the half width of the line at half maximum intensity. Although it surely depends on the dipole moment, among other things, no good theoretical evaluation is possible at present.* It has in a few cases been measured experimentally, however, and in these cases the formula for the intensity given above has been satisfactorily confirmed [53]. At low pressures $p/\Delta\nu$ is constant for a given transition, and for the cases where $\Delta\nu$ has not been measured, we have assumed the reasonable value of $\Delta\nu=25$ mc for 1 mm of mercury. It is this approximation that limits the accuracy of most of the intensities listed in these tables rather than the basic assumptions of the theory or the use of the classical sum of states, except in certain cases where the dipole moments have not been accurately measured. Errors as large as a factor of two or more would not be at all surprising in the cases where the half-widths have not been measured, but we consider that intensities with errors of even this magnitude may be useful, and may be easily corrected when better half-widths become available. The relative intensities for the various isotopes, hyperfine components, and excited states of a single molecule are considerably more reliable.

After substituting the accepted values for the universal constants and putting $e^{-h\nu/kT}\cong 1$, we find for the assumed temperature of 300° K and $\Delta\nu=25$mc, the intensities of pure rotational spectra become:

For linear molecules

$$\gamma_{max.}=2.19\times10^{-18}\mu^2\nu^3\text{cm}^{-1}.$$

For symmetric top molecules

$$\gamma_{max.}=4.83\times10^{-22}\sqrt{A}\mu^2\nu^3\left\{1-\frac{K^2}{(J+1)^2}\right\}\text{ cm}^{-1},$$

where

μ is in Debye units (10^{-18} esu/cm),

ν is the frequency in megacycles,

A is the reciprocal moment of inertia in megacycles $=10^{-6}h/8^2\pi I_A$,

J is the quantum number of total angular momentum,

K is the quantum number of the component of the angular momentum along the figure axis.

In some molecules, nuclear spin and molecular symmetry considerations influence intensities. The only common case involves three identical nuclei of spin ½ off the molecular axis as in CH_3Cl or AsF_3. In such molecules, the intensity of each line involving a value of K that is a multiple of three (including zero) is enhanced with respect to other lines by a factor of two.

Throughout the table we have given reciprocal moments of inertia, B and A, quadrupole couplings, (eqQ), doubling constants, q, and the α's and D_v's in megacycles per second. The dipole moment, μ, is always in Debye units, and is taken from "Tables of Electric Dipole Moments" by L. G. Wesson, published by Massachusetts Institute of Technology Laboratory for Insulation Research, unless otherwise stated.

The cases of ammonia and O_2, and probably some of the spectra not yet analyzed are in one way or another exceptions to the cursory treatment above, and are, where possible, discussed individually.

Symbols Used in Tables

A, Largest reciprocal moment of inertia for asymmetric molecules, or unique reciprocal moment of inertia for symmetric top molecules, in megacycles.

α_i, Change in reciprocal moment of inertia per quantum of excitation of the i^{th} vibrational state, in megacycles.

B Intermediate moment of inertia for asymmetric top molecules, or nonunique reciprocal moment of inertia for symmetric top molecules, in megacycles.

B_0, Average B for ground vibrational state, in megacycles.

C, Smallest reciprocal moment of inertia for asymmetric top molecules, in megacycles.

D, Centrifugal distortion coefficient in megacycles.

$\Delta\nu$, Half-width of line in megacycles at half maximum (line width parameter) with gas pressure 1 mm of mercury.

*A considerable amount of work has been published on this problem since this introduction was written.

eqQ, Quadrupole coupling constant, in megacycles.

F, Total angular momentum quantum number.

F_i, F of initial or lower energy state.

F_{ii}, Vector sum of J and spin of nucleus with larger quadrupole coupling, in cases where two nuclei have appreciable quadrupole coupling. Subscript i indicates initial or lower energy state.

F_f, F of final or higher energy state.

F_{if}, Same as F_{ii}, but for final or higher energy state.

γ, Maximum absorption coefficient in cm^{-1}, or "intensity."

I, Nuclear spin (in units $h/2\pi$).

J, Total orbital angular momentum quantum number.

K, Projection of J on molecular symmetry axis.

M, Medium intensity ($5\times10^{-7}-10^{-5}cm^{-1}$).

μ, Dipole moment in Debye Units (10^{-18} esu).

q, l-type doubling constant in megacycles.

S, Strong Intensity. ($>10^{-5}cm^{-1}$).

v_i, Quantum number of the i^{th} normal vibration.

W, Weak Intensity. ($<5\times10^{-7}cm^{-1}$).

TABLE 1

Molecules Listed Alphabetically by Chemical Symbol

AsF_3 (*Arsenic trifluoride*).

The value of A was calculated from the estimates of internuclear angles and distances given by reference [13], and the intensities of the lines for which the transitions have not been assigned were calculated by comparing the observed relative intensities with those of the identified lines. The fraction of molecules in the ground vibrational state was assumed to be 0.9.

$\mu=2.65$
$B=5,883.0$
$A=3900.$
$(eqQ)_{As}=-235$
} Reference [13].

AsF_3
$J=1-2,\ K=0$

F_i	F_f	*Frequency*	*Intensity*	*Reference*
1/2	3/2	23,458.6	3.1×10^{-7}	[13]
5/2	5/2	23,463.0	3.4×10^{-7}	
1/2	1/2	23,517.0	3.1×10^{-7}	
5/2	7/2	23,522.4	2.3×10^{-6}	
3/2	5/2			
3/2	3/2	23,564.6	3.9×10^{-7}	

$J=1-2,\ K=1$

3/2	5/2	23,472.6	5.8×10^{-7}
3/2	3/2	23,494.2	3.0×10^{-7}
5/2	5/2	23,501.6	2.4×10^{-7}
5/2	7/2	23,532.1	1.1×10^{-6}
1/2	1/2	23,575.3	2.3×10^{-7}

} [13]

unidentified (probably excited states]

23,512.9	1.5×10^{-7}
23,543.2	3×10^{-7}
23,553.0	5×10^{-7}

} [13]

BH_3CO (*Borine carbonyl*).

Vibrational frequencies of BH_3CO have not been analyzed. The excited vibrational levels for which B and μ are given here are hence arbitrarily labeled with subscripts 1 and 2. For calculation of intensities, the fraction of molecules in the ground vibrational state was assumed to be 0.9.

$\mu=1.79$ [49d]
$\mu_{v_{2=1}}=1.77$ [49d]
$A\cong122,000$ [22]

	$B^{10}H_3CO$	$B^{11}H_3CO$	
$B_0=$	8979.4	8657.2	[22, 49d]
$B_{v_{1=1}}=$	9002.7		[49d]
$B_{v_{2=1}}=$	8985.8		[49d]
$D_J=$	0.177		[49d]
$(eq\ Q)_B=$	+3.30	+1.55	[22]

$B^{10}H_3C^{12}O^{16}$	F_i	F_f	*Frequency*	*Intensity*	
$J=0-1$			17,961.2	7.8×10^{-7}	[49d]
$J=1-2,\ K=0$					
	3	2	35,919.02	3.0×10^{-7}	
	3	3			
	2	1			
	3	4	35,919.53	4.2×10^{-6}	
	4	5			
	2	2			
	4	3	35,919.86	5.9×10^{-7}	
	4	4			
	2	3	35,920.14	1.1×10^{-6}	
$J=1-2,\ K=1$					
	2	1	35,917.62	4.1×10^{-7}	
	4	5			
	2	2	35,917.88	2.0×10^{-6}	
	4	4	35,918.20	4.5×10^{-7}	
	3	3			
	3	4	35,918.50	1.3×10^{-6}	[22]
$B^{11}H_3C^{12}O^{16}$					
$J=1-2,\ K=0$					
	1/2	3/2	34,628.62	2.1×10^{-6}	
	3/2	5/2			
	5/2	7/2	34,628.90	4.8×10^{-6}	
	3/2	3/2			
	5/2	5/2	34,629.32	4.8×10^{-6}	
$J=1-2,\ K=1$					
	1/2	1/2	34,627.24	1.5×10^{-6}	
	5/2	7/2	34,627.50	7.3×10^{-6}	
	5/2	5/2			
	3/2	3/2	34,627.73	3.6×10^{-6}	
	3/2	5/2	34,627.89	3.8×10^{-6}	

BrCN (*Cyanogen bromide*).

The half-width reported in [53] has been used in calculating the intensity.

$\mu = 2.94$

$\Delta\nu = 21. \pm 3.$ [53]

	$Br^{79}C^{12}N^{14}$	$Br^{81}C^{12}N^{14}$	$Br^{79}C^{13}N^{14}$	$Br^{81}C^{13}N^{14}$	
$B_0 =$	4120. 190	4096. 760	4073. 355	4049. 606	[53, 42]
$(eqQ)_{Br} =$	686. 2	573. 2			
$^{a}(eqQ)_{N} =$	−3. 83				
$\alpha_1 =$	11. 36	11. 23			
$\alpha_2 =$	−11. 49	−11. 49			
$q =$	3. 91	3. 845			

$Br^{79}C^{12}N^{14}$

$J = 9$–10, $v = 0$		82, 405	4.0×10^{-3}	[41]

F_i	F_f	*Frequency*	*Intensity*		
$J = 2$–3, $v = 0$					
3/2	3/2	24, 583. 00	4.3×10^{-6}	[53]	
5/2	5/2	24, 633. 71	5.6×10^{-6}		
5/2	7/2	24, 713. 05	6.5×10^{-5}		
7/2	9/2				
1/2	3/2	24, 755. 22	2.9×10^{-5}		
3/2	5/2				
7/2	7/2	24, 884. 57	4.3×10^{-6}		
$J = 2$–3, $v_1 = 1$					
5/2	7/2	24, 645. 82	4.0×10^{-6}	[53]	
7/2	9/2				
1/2	3/2	24, 687. 11	1.8×10^{-6}		
3/2	5/2				
$J = 2$–3, $v_1 = 1$					
l_1 1/2	3/2	24, 760. 76	7.5×10^{-6}	[53]	
7/2	9/2				
l_2 1/2	3/2	24, 784. 02	7.5×10^{-6}		
7/2	9/2				
l_1 3/2	5/2	24, 803. 00	6.9×10^{-6}		
5/2	7/2				
l_2 3/2	5/2	24, 826. 70	6.9×10^{-6}		
5/2	7/2				
l_1 7/2	7/2	24, 890. 0	7.3×10^{-7}		
l_2 7/2	7/2	25, 006. 0	7.3×10^{-7}		
$J = 2$–3, $v_2 = 2$					
$l = 2$ 3/2	3/2	24, 860. 6	6.5×10^{-7}	[30]	
3/2	5/2				
$l = 2$ 5/2	3/2	24, 981. 5	9.8×10^{-7}		
5/2	5/2				
5/2	7/2				
$J = 3$–4, $v = 0$					
5/2	5/2	32, 804. 56	5.8×10^{-6}	[42]	
7/2	9/2	32, 956. 68	1.5×10^{-4}		
9/2	11/2				
3/2	5/2	32, 976. 40	8.6×10^{-5}		
5/2	7/2				
$J = 8$–9, $v = 0$		74, 165	2.9×10^{-3}	[41]	

$Br^{79}C^{13}N^{14}$

$J = 3$–4, $v = 0$				
7/2	9/2	32, 581. 73	1.7×10^{-6}	[42]
9/2	11/2			
3/2	5/2	32, 601. 46	9.2×10^{-7}	
5/2	7/2			

$Br^{81}C^{12}N^{14}$

$J = 2$–3, $v = 0$				
3/2	3/2	24, 465. 33	4.2×10^{-6}	[53]
5/2	5/2	24, 507. 38	5.4×10^{-6}	
5/2	7/2	24, 573. 86	6.3×10^{-5}	
7/2	9/2			
1/2	3/2	24, 608. 92	2.7×10^{-5}	
3/2	5/2			
7/2	7/2	24, 717. 19	4.2×10^{-6}	
$J = 2$–3, $v_1 = 1$				
5/2	7/2	24, 506. 75	3.9×10^{-6}	[53]
7/2	9/2			
1/2	3/2	24, 541. 18	1.7×10^{-6}	
3/2	5/2			
$J = 2$–3, $v_2 = 1$				
l_1 1/2	3/2	24, 622. 93	7.7×10^{-6}	[53]
7/2	9/2			
l_2 1/2	3/2	24, 645. 82	7.7×10^{-6}	
7/2	9/2			
l_1 3/2	5/2	24, 658. 89	6.8×10^{-6}	
5/2	7/2			
l_2 3/2	5/2	24, 682. 13	6.8×10^{-6}	
5/2	7/2			
$J = 3$–4, $v = 0$				
5/2	5/2	32, 643. 13	5.6×10^{-6}	[42]
7/2	7/2	32, 720. 28	7.4×10^{-6}	
7/2	9/2	32, 770. 13	1.4×10^{-4}	
9/2	11/2			
3/2	5/2	32, 786. 65	8.2×10^{-5}	
5/2	7/2			
9/2	9/2	32, 913. 24	5.7×10^{-6}	
$J = 8$–9, $v = 0$		73, 742	2.8×10^{-3}	[41]
$J = 9$–10, $v = 0$		81, 936	3.8×10^{-3}	

$Br^{81}C^{13}N^{14}$—Continued

$J=3$–4, $v=0$	F_i	F_f	*Frequency*	*Intensity*	
	7/2	9/2	32, 392. 59	1.5×10^{-6}	[42]
	9/2	11/2			
	3/2	5/2	32, 409. 06	9.2×10^{-7}	
	5/2	7/2			

CF_3CH_3. Since the dipole moment and vibrational frequencies of this molecule are not available, it is impossible to calculate the intensity. However, observed intensities are estimated in [5], and these are given. The weaker line is probably due to an excited vibrational state.

$B_0=5185$ [17]
$\mu=2.33$ [39b]

CF_3CH_3

	Frequency	*Intensity*	
$J=1$–2, $K=0,1$	20, 679. 9	5×10^{-7}	[39a]
	20, 710. 6	1×10^{-6}	[17, 39a]
	20, 742. 32	2×10^{-6}	[17, 39a]
$J=2-3$	31, 020. 7		[39a]
	31, 066. 8		
	31, 114. 4		

$CHClF_2$. The spectrum of this asymmetric top molecule has not been analyzed. The assignment of weak, medium, or strong is that of the reference and does not correspond necessarily to the convention adopted in this table.

$\mu=1.29$

Frequency	*Intensity*	
22, 217	W	[11]
22, 247	W	
22, 305	M	
22, 353	W	
22, 386	W	
22, 410	S	
22, 436	W	
22, 462	W	
22, 481	M	
22, 545	W	
22, 553	W	
23, 308	S	
23, 644	W	
23, 680	W	
23, 733	S	
23, 803	W	
23, 826		
23, 845	S	

CH_2Br_2 (*Methylene bromide*)

$\mu\cong1.6$

Frequency	
25, 056	[57]

CH_2CF_2 (*Unsymmetrical difluoroethylene*)

$\mu=1.366$
$A_0=11,002$
$B_0=10,428.5$
$C_0=5,345.6$ [37a]

$C^{12}H_2C^{12}F_2$

Transition	*Frequency*	*Observed intensity*	
	21, 482	M	[37a] (excited vibrational state)
	21, 549	W	
	21, 573	W	
	21, 689	M	
8_3-8_4	21, 734	M	
	22, 236	M	
	22, 281	S	
	22, 383	M	
	22, 391	M	
	22, 660	W	
	22, 752	S	
	23, 181	M	
	23, 206	W	
	23, 214	M	
	23, 220	M	
	23, 234	W	
	23, 323	M	
	23, 361	M	
7_2-7_3	23, 433	S	
	23, 649	M	
	23, 770	M	
	23, 812	M	
	23, 986	M	
	24, 021	M	
	24, 150	W	
	24, 294	M	
	24, 323	S	
	24, 352	M	
	24, 357	W	
	24, 450	S	
	24, 545	M	
	24, 579	W	
	24, 602	W	
	24, 639	M	
	24, 734	M	
6_1-6_2	24, 770	S	
	24, 806	W	
	24, 808	W	
6_2-6_3	25, 248	M	
	25, 350	S	
	25, 450	M	
	25, 516	S	
5_0-5_1	25, 729	S	
	25, 741	M	
	26, 118	S	
	26, 163	M	
$4_{-1}-4_0$	26, 328	S	
	26, 337	M	
1_0-2_{-1}	26, 410	W	
1_0-2_{-1}	26, 466	M	

Transition	Frequency	Observed intensity	
	26, 634	S	
$3_{-2}-3_{-1}$	26, 649	M	
	26, 723	W	
	26, 832	M	
	26, 865	S	
$3_{-3}-3_{0}$	26, 880	M	
$1_{-1}-2_{-2}$	26, 992	S	
$4_{-2}-4_{1}$	27, 014	S	
	27, 112	M	
	27, 216	M	
$5_{-1}-5_{2}$	27, 297	S	
	27, 412	M	
	27, 681	S	
$6_{0}-6_{3}$	27, 818	S	
	27, 972	S	[37a]
	28, 174	S	
	28, 314	W	
	28, 339	M	
	28, 412	S	
	28, 439	M	
	28, 458	M	
	28, 551	W	
	28, 575	W	
	28, 615	W	
$7_{1}-7_{4}$	28, 689	W	
	28, 852		
	28, 858		
	28, 954	S	
$1_{1}-2_{0}$	36, 632	M	

CH_2Cl_2 (*Methylene chloride*).

Turner [57] has given the relative intensities listed for this asymmetric top molecule. This author has also made transition assignments but they have been questioned by Gwinn [23a], and are not listed here. Frequencies given are a plausible compromise between those of reference [57] and [11].

$\mu = 1.6$

Frequency		Observed relative intensity
23, 476	[11]	
24, 440	[57]	4
24, 471	[57]	7
24, 577	[57, 11]	4
24, 627	[57]	4
24, 631	[57]	4
24, 636	[57, 11]	4
24, 842	[57, 11]	2
24, 916	[57]	2
24, 967	[57]	2
24, 970	[57]	4
24, 976	[57]	6
24, 996	[11]	
25, 018	[57]	2
25, 038	[57]	6
25, 046	[57]	6
25, 047	[57]	2
25, 053	[57, 11]	2
25, 073	[57, 11]	7
25, 099	[57, 11]	2
25, 123	[57, 11]	8
25, 221	[11]	
25, 269	[57, 11]	7
25, 280	[57]	6
25, 710	[57]	7
25, 745	[57]	2
25, 748	[57]	6
25, 751	[57]	2
25, 848	[57]	10
26, 007	[57]	7
26, 295	[57]	9

CH_3Br (*Methyl bromide*) $\mu = 1.79$ $A \simeq 150{,}000$

	CH_3Br^{79}	CH_3Br^{81}	
Br_0	9568.4	9532	Reference [23, 38a].
$(eqQ)_{Br}$	577.3	482.4	

$C^{12}H_3Br^{79}$

F_i	F_f	Frequency	Intensity	
$J=0-1$, $K=0$				
3/2	1/2	18, 922.41	4.8×10^{-7}	[38a]
3/2	3/2	19, 252.13	9.7×10^{-7}	[38a]
3/2	5/2	19, 107.97	1.5×10^{-6}	[38a]
$J=1-2$, $K=0$				
3/2	3/2	38, 157.30	2.5×10^{-6}	[23]
3/2	5/2	38, 260.10	1.4×10^{-5}	[23]
5/2	7/2	38, 260.10	1.4×10^{-5}	[23]
1/2	1/2	38, 272.40	1.9×10^{-6}	[23]
5/2	5/2	38, 404.49	2.1×10^{-6}	[23]
1/2	3/2	38, 417.09	1.9×10^{-6}	[23]
$J=1-2$, $K=1$				
1/2	1/2	38, 128.40	1.4×10^{-6}	[23]
1/2	3/2	38, 200.52	1.4×10^{-6}	[23]
5/2	7/2	38, 237.14	7.0×10^{-6}	[23]
5/2	5/2	38, 309.45	1.6×10^{-6}	[23]
3/2	3/2	38, 330.25	1.9×10^{-6}	[23]
3/2	5/2	38, 381.70	3.5×10^{-6}	[23]

$C^{12}H_3Br^{81}$

F_i	F_f	Frequency	Intensity	
$J=0-1$, $K=0$				
3/2	1/2	18, 943.77	4.7×10^{-7}	[38a]
3/2	3/2	19, 160.82	9.5×10^{-7}	[38a]
3/2	5/2	19, 040.32	1.4×10^{-6}	[38a]
$J=1-2$, $K=0$				
3/2	3/2	38, 030.77	2.4×10^{-6}	[23]
3/2	5/2	38, 116.65	1.4×10^{-5}	[23]
5/2	7/2	38, 116.65	1.4×10^{-5}	[23]
1/2	1/2	38, 126.97	1.9×10^{-6}	[23]
5/2	5/2	38, 237.14	2.1×10^{-6}	[23]
1/2	3/2	38, 247.77	1.9×10^{-6}	[23]
$J=1-2$, $K=1$				
1/2	1/2	38, 006.47	1.4×10^{-6}	[23]
1/2	3/2	38, 066.72	1.4×10^{-6}	[23]
5/2	7/2	38, 097.45	6.7×10^{-6}	[23]
5/2	5/2	38, 157.70	1.5×10^{-6}	[23]
3/2	3/2	38, 175.08	1.8×10^{-6}	[23]
3/2	5/2	38, 218.21	3.5×10^{-6}	[23]

CH_3CCH (*Methyl acetylene*).

This molecule, while probably a symmetric top, has ten distinct vibrational frequencies, two or three of which are low enough to be appreciably excited at room temperature, the lowest ($\nu_{10}=336\ cm^{-1}$) to several quanta of vibrational energy. In addition, centrifugal distortion will separate levels of equal J but different K. The transitions have not been assigned, but we include the observed relative intensities.

$\mu=.75$
$B\cong 8{,}408$ [35]

CH_3CCH

$J=2$–3	*Frequency*	*Relative intensity*	
	51, 260	50	[35]
	51, 264	80	
	51, 266	100	
	51, 296	10	
	51, 313	10	
	51, 314	10	
	51, 318	5	
	51, 319	5	
	51, 334	15	
	51, 363	30	
	51, 410	30	
	51, 416	30	
	51, 418	15	
	51, 419	15	
	51, 464	15	

CH_3Cl (*Methyl chloride*).

$\mu=1.86$
$A\cong 150{,}000$

$C^{12}H_3Cl^{35}$	$C^{12}H_3Cl^{37}$
$B_0=13{,}292.89$ [23]	13, 088. 19 [23]
$(eqQ)=-75.33$ [23,27b]	−58. 5 [23, 27b]

$C^{13}H_3Cl^{35}$	$C^{13}H_3Cl^{37}$
$B_0=12{,}796.2$ [11]	12, 590. 0 [11]

$C^{12}H_3Cl^{35}$	F_i	F_f	*Frequency*	*Intensity*	
$J=0-1,\ K=0$					
	3/2	3/2	26, 570. 77	4.4×10^{-6}	[23]
	3/2	5/2	26, 589. 49	6.6×10^{-6}	
	3/2	1/2	26, 604. 57	2.2×10^{-6}	
$C^{12}H_3Cl^{37}$					
$J=0-1,\ K=0$					
	3/2	3/2	26, 164. 57	1.4×10^{-6}	[23]
	3/2	5/2	26, 179. 30	2.1×10^{-6}	
	3/2	1/2	26, 191. 13	7.1×10^{-7}	

$C^{13}H_3Cl^{35}$					
$J=0-1,\ K=0$					
	3/2	3/2	25, 577. 2	4.5×10^{-6}	[11]
	3/2	5/2	25, 596. 0	6.7×10^{-6}	
	3/2	1/2	25, 611. 2	2.2×10^{-6}	
$C^{13}H_3Cl^{37}$					
$J=0-1,\ K=0$					
	3/2	3/2	25, 195. 2	1.4×10^{-9}	[11]
	3/2	5/2	26, 183. 0	2.1×10^{-9}	
	3/2	1/2	25, 167. 4	6.9×10^{-10}	

CH_3CN (*Methyl cyanide*).

$\mu\cong 3.4$
$(eqQ)_N=-4.67$
$A\cong 150{,}000$
$B_0=9198.45$ [28]

	F_i	F_f	K	*Frequency*	*Intensity*	
$J=0$–1	1	1	0	18, 400 − 1. 40	4.7×10^{-6}	[36]
	1	2	0	18, 400	7.8×10^{-6}	
	1	0	0	18, 400 + 2. 10	1.6×10^{-6}	
$J=1$–2	1	2	1	36, 793. 64	3.1×10^{-5}	[28]
	0	1	0	36, 794. 26	2.8×10^{-5}	
	2	2	1			
	2	3	1	36, 794. 88	5.7×10^{-5}	
	1	2	0	36, 795. 38	1.2×10^{-4}	
	2	3	0			
	0	1	1	36, 796. 27	1.4×10^{-5}	
	1	1	0	36, 797. 52	1.4×10^{-5}	

Excited vibrational states		
	36. 870. 94	[27]
	36, 903. 40	
	36, 942. 15	

CH_2F (*Methyl fluoride*)

$\mu=1.81$
$A\cong 150{,}000$
$\Delta\nu=20$. Reference [19]

$C^{12}H_2F$	$C^{13}H_2F$
$B_0=25{,}535.85$	24, 862. 37

$C^{12}H_2F$	*Frequency*	*Intensity*	
$J=0$–1, $K=0$	51, 071. 69	1.4×10^{-4}	[23, 19, and private communication.]

$C^{13}H_2F$			
$J=0$–1, $K=0$	49, 724. 73	1.5×10^{-6}	[19]

CH_3I (*Methyl iodide*).

$\mu=1.5$
$A\cong 150{,}000$
$(eqQ)_I=-1934$

$B_0=$	$C^{12}H_3I$	$C^{13}H_3I$	
	7501.250	7119.040	[23]

$C^{13}H_3I$

F_i	F_f	Frequency	Intensity
$J=1-2$, $K=0$			
3/2	5/2	29, 598. 95	9.2×10^{-7}
7/2	7/2	29, 673. 95	1.4×10^{-6}
7/2	5/2	29, 773. 95	2.3×10^{-7}
3/2	3/2	29, 872. 52	1.4×10^{-6}
7/2	9/2	30, 046. 99	5.0×10^{-6}
5/2	7/2	30, 079. 72	2.6×10^{-6}
3/2	1/2	30, 121. 32	1.0×10^{-6}
5/2	5/2	30, 179. 71	2.6×10^{-6}
5/2	3/2	30, 453. 46	6.3×10^{-7}
$J=1-2$, $K=1$			
5/2	7/2	29, 735. 71	2.5×10^{-6}
5/2	5/2	29, 782. 71	1.8×10^{-6}
5/2	3/2	29, 923. 50	1.8×10^{-6}
7/2	7/2	29, 939. 87	1.4×10^{-6}
7/2	5/2	29, 986. 84	2.4×10^{-7}
3/2	5/2	30, 075. 08	9.5×10^{-7}
7/2	9/2	30, 123. 64	5.1×10^{-6}
3/2	3/2	30, 215. 95	1.4×10^{-6}

[23]

$C^{13}H_3I$

$J=1-2$, $K=0$	
3/2 5/2	28, 069. 99 1.0×10^{-8}
7/2 7/2	28, 145. 01 1.5×10^{-8}
3/2 3/2	28, 343. 64 1.5×10^{-8}
7/2 9/2	28, 518. 14 5.5×10^{-8}
5/2 7/2	28, 550. 86 2.9×10^{-8}
5/2 5/2	28, 650. 91 2.9×10^{-8}
$J=1-2$, $K=1$	
5/2 7/2	28, 206. 90 2.8×10^{-8}
5/2 5/2	28, 253. 84 2.0×10^{-8}
7/2 7/2	28, 411. 19 1.5×10^{-8}
7/2 9/2	28, 594. 74 5.6×10^{-8}
3/2 3/2	28, 687. 21 1.5×10^{-8}

[23]

CH_3NC (*Methyl isocyanide*).

$(eqQ)_N<0.5$, $A\simeq$ 150, 000

$B_0=$	$C^{12}H_3NC^{12}$	$C^{13}H_3NC^{13}$
	10, 052. 79	9, 695. 802

[28]

$C^{12}H_3N^{14}C^{12}$

	Frequency
$J=0-1$, $K=0$	20, 160
$J=1-2$, $K=1$	40, 210. 27
$J=1-2$, $K=0$	40, 211. 16
Excited vibrational states	40, 313. 37
	40, 364. 07
	40, 366. 55
	40, 424. 49
$C^{13}H_3N^{14}C^{13}$	
$J=1-2$, $K=1$	38, 782. 21
$J=1-2$, $K=0$	38, 783. 21

[36]

[28]

CH_3NCS (*Methyl Isothiocyanate*). All of the transitions of this slightly asymmetric rotor are approximately degenerate except those for which $\tau=1-J$ and $2-J$. Excited vibrational states are labeled D, E, and J in conformity with [19].

$\mu=3.18$

	CH_3NCS^{32}	CH_3NCS^{34}	
$\frac{1}{2}(B+C)=$	2526.2	2461.7	[1a]

Transition		Frequency	Observed relative intensity
$C^{12}H_3N^{14}C^{12}S^{32}$			
$J=3-4$		20. 020	<1
	$3_{-2}-4_{-3}$	20, 140	10
	Deg. line	20, 216	100
		20, 230	<1
	Deg. line, E	20, 241	7
	Deg. line, D	20, 350	20
		20, 413	<1
	Deg. line, J	20, 443	40
$J=4-5$		24, 824	1
		24, 971	1
		25, 077	1
		25, 100	<1
		25, 161	<1
	$4_{-3}-5_{-4}$	25, 195	10
	Deg. line	25, 269	100
	Deg. line, E	25, 306	7
	$4_{-2}-5_{-3}$	25, 333	10
		25, 390	<1
		25, 409	1
	Deg. line, D	25, 442	25
	Deg. line, J	25, 550	40
	$4_{-2}-5_{-3}$, J	25, 653	<1
$C^{13}H_3N^{14}C^{12}S^{32}$			
$J=4-5$	Deg. line	24, 143	<1
$C^{12}H_3N^{14}C^{13}S^{32}$			
$J=4-5$	Deg. line	25, 002	<1
$C^{12}H_3N^{14}C^{12}S^{33}$			
$J=4-5$	Deg. line	24, 930	<1
$C^{12}H_3N^{14}C^{12}S^{34}$			
$J=3-4$	Deg. line	19, 700	5
	Deg. line, J	19, 929	1
$4-5$	Deg. line	24, 609	5
	Deg. line, J	24, 910	2
$5-6$	Deg. line	29, 700	

[1a]

[23]

CH_3NH_2 (*Methylamine*).

$\mu=1.2$

$1/2(B+C)\cong22{,}700$ [18]

Frequency
21, 712
21, 935
22, 258
22, 535
22, 590
22, 595
22, 612
22, 732
22, 740
22, 977
23, 115
23, 205

[28]

	Frequency	
	23, 295	
	23, 300	
	23, 305	
	23, 335	
	23, 404	[25]
	23, 425	
	23, 430	
	23, 446	
	23, 510	
	23, 680	
	24, 015	
	24, 078	
	24, 320	
	24, 528	
	24, 890	
	24, 896	
	25, 000	
	25, 065	
	25, 200	
	25, 470	
$J=0$–1	45, 324. 24	[18]
	45, 324. 94	

CH_2NO_2 (*Nitromethane*).

$\mu \cong 3.1$

Frequency	*Observed relative intensity*	
20, 385	75	
23, 250	115	
23, 021		
23, 467		
23, 483		
23, 706		
24, 017		[11, 15]
24, 428		
24, 448		
24, 599		
25, 400	118	
25, 412	60	

CH_3OH. This asymmetric top molecule has been investigated by five different laboratories. The listed lines represent a reasonable compromise between their somewhat conflicting results. The lines for which a single J is listed are probably due to a hindered internal rotation and are discussed in reference [6].

$\mu \cong 1.66$

J	*Frequency*	
	20, 910	[14, 25]
	20, 971	[14, 25]
	21, 350	[25]
	21, 550	[14, 25]
	22, 305	[25]
	23, 121. 2	[14, 25, 33]
	23, 346. 8	[14, 25]
	23, 425	[14, 25, 33]
	23, 854. 4	[14, 25, 33]
	24, 911	[33]
	24, 926	[33]
3	24, 928. 70	[14, 33, 6]
4	24, 933. 47	[6]
2	24, 934. 38	[14, 25, 6]
5	24, 959. 08	[14, 25, 33, 6]
6	25, 018. 14	[14, 25, 33, 6]
	25, 053	[33]
7	25, 124. 88	[14, 25, 33, 6]
8	25, 294. 41	[14, 25, 33, 6]
	25, 381	[33]
9	25, 541. 43	[14, 25, 33, 6]
	25, 797	[14, 33]
10	25, 878. 18	[14, 33, 6]
	26, 120	[33]
	26, 310	[14, 33]
	26, 562	[14]
	47, 840	[18]
	48, 010	[18]
	48, 357	[18]
	48, 363	[18]
	48, 396	[18]
	48, 404	[18]
	48, 700	[18]

CH_3OD

	Frequency	
$J=0$–1	47, 052	[18]
	47, 266	
	47, 346	

CH_3SCN (*Methyl thiocyanate*). Only the strongest lines of this slightly asymmetric molecule have been measured.

$\mu = 3.16$

$\frac{1}{2}(B+C) = 2877.$ [1a]

$C^{12}H_3S^{32}C^{12}N^{14}$	*Frequency*	
$J=3$–4	22, 680	[1a]
$J=4$–5	28, 380	

C_2H_3Cl (*Vinyl chloride*)

$\mu = 1.44$

	$C_2H_3Cl^{35}$	$C_2H_3Cl^{37}$	
	$A_0 = 56, 100$	56, 070	
	$B_0 = 6030.5$	5903. 7	
	$C_0 = 5445.2$	5341. 3	[20a]
$eQ(\partial^2 V/\partial a^2)_{Cl} =$	-57.4		
$eQ(\partial^2 V/\partial b^2)_{Cl} =$	26. 2		

	Transition	*Frequency*	
$C_2^{12}H_3Cl^{35}$	1_{01}–2_{02}	22, 946. 9	
	1_{10}–2_{11}	23, 538. 9	[20a]
	1_{11}–2_{12}	22, 369. 6	
$C_2^{12}H_3Cl^{37}$	1_{01}–2_{02}	22, 485. 9	
	1_{10}–2_{11}	23, 055. 0	[20a]
	1_{11}–2_{12}	21, 930. 2	

C_2H_4O (*Ethylene oxide*). This asymmetric top has been investigated in two laboratories. Frequencies given are those of reference [10] and [10a] which appear to be the more precise. The lines $C_2D_4O^{16}$ were observed with enriched material, not with the intensities listed for the deuterium natural abundance of 0.02 percent.

$\mu = 1.88$

	C_2H_4O	C_2D_4O	
A_0	25, 471	20, 389	
B_0	22, 110	15, 449	[10, 10a]
C_0	14, 091	11, 538	

	Transition	Frequency	Intensity	
$C^{12}H_4O^{16}$	$3_1 - 3_3$	23, 134	3.9×10^{-6}	[10, 39]
	$3_{-1}-3_1$	23, 610	4.1×10^{-6}	[20, 39]
	$4_0 - 4_2$	24, 834. 3	1.2×10^{-5}	[10, 39]
	$2_{-2}-2_0$	24, 924. 4	3.9×10^{-6}	[10, 39]
	$5_1 - 5_3$	29, 688	1.2×10^{-5}	[10]
	$4_2 - 4_4$	34, 150	1.3×10^{-5}	[10a]
	$2_{-1}-2_1$	34, 158	3.0×10^{-6}	[10a]
	$6_0 - 6_2$	36, 791	3.4×10^{-5}	[10]
	$7_1 - 7_3$	37, 329	2.5×10^{-5}	[10]
	$5_{-1}-5_1$	37, 781	1.7×10^{-5}	[10]
	$6_2 - 6_4$	38, 702	3.4×10^{-5}	[10]
	$0_0 - 1_0$	39, 582	8.3×10^{-6}	[10]
	$3_0 - 3_2$	39, 677	1.2×10^{-5}	[10]
	$4_{-2}-4_0$	41, 581	1.9×10^{-5}	[10a]
	$8_2 - 8_4$	43, 398	6.6×10^{-5}	[10a]
$C^{12}D_4O^{16}$	$4_{-2}-4_0$	21, 964	7.4×10^{-21}	[10a]
	$3_{-3}-3_1$	24, 055	3.4×10^{-21}	
	$5_{-1}-5_1$	24, 668	1.1×10^{-20}	
	$2_{-1}-2_1$	26, 365	2.4×10^{-21}	
	$6_{-2}-6_0$	28, 495	1.8×10^{-20}	
	$3_1 - 3_1$	29, 080	5.0×10^{-21}	
	$0_0 - 1_0$	31, 943	5.1×10^{-21}	
	$3_{-2}-3_0$	33, 285	6.4×10^{-21}	
	$8_{-2}-8_0$	35, 068	3.7×10^{-20}	
	$3_0 - 3_2$	35, 341	7.4×10^{-21}	
	$5_1 - 5_3$	39, 592	1.8×10^{-20}	

ClCN (*Cyanogen chloride*)

$\mu = 2.66$ [53]

$\Delta\nu = 25$ [53]

$Cl^{35}C^{12}N^{14}$

F_{1i}	F_i	F_{1f}	F_f	Frequency	Intensity	
$J=1$–2, $v=0$						
1/2		3/2		23, 862. 57	9.3×10^{-6}	[53]
5/2	3/2	5/2	5/2	23, 863. 5	3.6×10^{-7}	
5/2	7/2	5/2	5/2	23, 863. 8	3.6×10^{-7}	
5/2	3/2	5/2	3/2	23, 864. 0	1.9×10^{-6}	
5/2	7/2	5/2	7/2	23, 864. 2	4.1×10^{-6}	
5/2	5/2	5/2	5/2	23, 864. 5	2.6×10^{-6}	
5/2	5/2	5/2	7/2	23, 864. 9	3.6×10^{-7}	
5/2	5/2	3/2	3/2	23, 865. 1	3.5×10^{-7}	
5/2	5/2	3/2	1/2			
5/2	3/2	3/2	3/2	23, 878. 6	5.5×10^{-7}	
5/2	3/2	3/2	5/2			
5/2	7/2	3/2	5/2	23, 878. 9	5.0×10^{-7}	
5/2	5/2	3/2	3/2	23, 879. 7	6.2×10^{-8}	
5/2	5/2	3/2	5/2			
1/2		1/2		23, 883. 30	9.2×10^{-6}	
5/2	7/2	7/2	7/2	23, 884. 2	7.7×10^{-6}	
3/2	3/2	5/2	5/2			
3/2	3/2	5/2	3/2	23, 884. 8	1.2×10^{-6}	
3/2	5/2	5/2	5/2	23, 884. 9	1.5×10^{-5}	
5/2	5/2	7/2	7/2			
5/2	7/2	7/2	9/2	23, 885. 16	2.9×10^{-5}	
5/2	3/2	7/2	5/2			
3/2	5/2	5/2	7/2	23, 885. 3	1.1×10^{-5}	
3/2	1/2	5/2	3/2	23, 886. 0	4.0×10^{-6}	
5/2	5/2	7/2	5/2	23, 886. 2	1.2×10^{-6}	
5/2	5/2	7/2	1/2			
3/2	3/2	3/2	3/2	23, 899. 59	3.9×10^{-6}	
3/2	3/2	3/2	5/2			
3/2	5/2	3/2	3/2	23, 900. 20	9.6×10^{-6}	
3/2	5/2	3/2	5/2			
3/2	1/2	3/2	1/2	23, 900. 7	2.1×10^{-6}	
3/2	1/2	3/2	3/2			
3/2		1/2		23, 920. 91	1.9×10^{-6}	
$J=1$–2, $v_2=1$						
3/2		5/2	1_1	23, 917. 9	4.5×10^{-6}	
3/2		3/2	1_1	23, 925. 5	1.8×10^{-6}	
5/2		5/2	1_1	23, 928. 7	1.4×10^{-6}	
5/2		7/2	1_1	23, 938. 6	8.2×10^{-6}	
1/2		3/2	1_1	23, 944. 4	1.7×10^{-6}	
3/2		5/2	1_2	23, 948. 2	4.5×10^{-6}	
1/2		1/2	1_1	23, 954. 5	3.5×10^{-6}	
3/2		3/2	1_2			
5/2		5/2	1_2	23, 958. 4	1.8×10^{-6}	
5/2		7/2	1_2	23, 968. 6	8.2×10^{-6}	
1/2		3/2	1_2	23, 974. 4	1.7×10^{-6}	
1/2		1/2	1_2	23, 984. 6	1.7×10^{-6}	

	$Cl^{35}C^{12}N^{14}$	$Cl^{37}C^{12}N^{14}$	$Cl^{35}C^{13}N^{14}$	$Cl^{37}C^{13}N^{14}$	
$B_0=$	5970. 821	5847. 252	5939. 795	5814. 710	[42, 53]
$(eqQ)_{Cl}=$	−83. 4	−65. 3			
$(eqQ)_N=$	−3. 63				

$J=2-3$, $v=0$

F_i	F_f	Frequency	Intensity	
7/2	7/2	35, 805. 09	1.4×10^{-5}	[42]
1/2	3/2	35, 820. 65	1.0×10^{-4}	[42]
3/2	5/2			[42]
5/2	7/2	35, 825. 95	2.3×10^{-4}	[42]
7/2	9/2			[42]
5/2	5/2	35, 835. 74	2.0×10^{-5}	[42]

$Cl^{35}C^{13}N^{14}$

$J=1-2$, $v=0$

5/2	7/2	7/2	9/2	23, 760. 98	3×10^{-7}	[53]

$J=2-3$, v=0

7/2	7/2	35, 618. 81	1.5×10^{-7}	[42]
1/2	3/2	35, 634. 85	1.1×10^{-6}	[42]
3/2	5/2			[42]
5/2	7/2	35, 639. 78	2.4×10^{-6}	[42]
7/2	9/2			[42]
5/2	5/2	35, 649. 56	2.1×10^{-7}	[42]

$Cl^{37}C^{13}N^{14}$

$J=1-2$, $v=0$

1/2	3/2	3/2	5/2	23, 372. 72	1.5×10^{-6}	[53]
1/2		1/2		23, 389. 00	3.0×10^{-6}	[53]
3/2	3/2	5/2	5/2	23, 389. 61	2.1×10^{-6}	[53]
5/2	7/2	7/2	9/2	23, 390. 53	9.4×10^{-6}	[53]
5/2	3/2	7/2	5/2			[53]
3/2	5/2	3/2	5/2	23, 402. 47	1.3×10^{-6}	[53]

$J=2-3$, $v=0$

7/2	7/2	35, 067. 99	4.4×10^{-6}	[42]
1/2	3/2	35, 080. 39	3.1×10^{-5}	[42]
3/2	5/2			[42]
5/2	7/2	35, 084. 15	7.2×10^{-5}	[42]
7/2	9/2			[42]
5/2	5/2	35, 091. 97	6.2×10^{-6}	[42]

$Cl^{37}C^{13}N^{14}$

$J=1-2$, $v=0$

5/2	7/2	7/2	9/2	23, 260. 3	1×10^{-7}	[53]

$J=2-3$, $v=0$

7/2	9/2	34, 889. 05	4.5×10^{-7}	[42]

HCF_3 (*Fluoroform*). In the absence of other information, A was calculated using the $C-F$ distance estimated by the authors, assuming tetrahedral angles. It was also assumed that 0.9 of the molecules were in the ground vibrational state.

$\Delta\nu=18$
$\mu=1.59$
$B_0=10,348.74$
$A=5,600$ } [19]

$HC^{12}F_3$

$J=1-2$, $K=0,1,2$	Frequency	Intensity	
	41, 394. 95	2.2×10^{-5}	[19]

HCN (*Hydrocyanic acid*). This line is really a triplet, and the calculated intensity is for the sum of all three hyperfine components.

$\mu=2.8$
$B_0=44,336$
$(eqQ)_N=-4.7$
$\Delta\nu=25.$ } [41]

$HC^{13}N^{14}$ $J=0-1$	88, 671	1.1×10^{-2}	[41]

H_2CO (*Formaldehyde*)

$\mu=2.3$
$A_0=364,500$
$B_0=51,720$
$C_0=45,338$ } [49a]

	Transition	Frequency	
$H_2C^{13}O^{16}$	$3_{-1}-3_{-2}$	28, 974. 85	[49a]
	$4_{-2}-4_{-3}$	48, 284. 60	[49a]
	$5_{-3}-5_{-4}$	72, 409. 35	[49a]
	$0_0\ -1_{-1}$	72, 838. 14	[49a]

H_2O (*Water*). The water line has been investigated at higher pressures by several workers not quoted herein. The intensity of the HDO lines follows the procedure adopted throughout this table of using natural abundancies where possible, the abundance of D being taken as 0.02 percent.

	H_2O	Reference	HDO	
$\mu=1.94$		[20]	1. 84	[49b, 48]
$\Delta\nu=7$		[2, 55]	6. 5	[49b]

	Transition	Frequency	Intensity	
H_2O^{16}	$5_{-1}-6_{-5}$	22, 235. 22	9.6×10^{-6}	[20, 24, 55]
HDO^{16}	$2_{-1}-2_{-2}$	10, 278. 99	8.6×10^{-9}	[49b]
	$4_{-3}-3_{-1}$	20, 460. 40	1.3×10^{-8}	[44, 49b]
	$5_0\ -5_1$	22, 307. 67	1.0×10^{-8}	[24, 48]
	$3_0\ -3_1$	50, 236. 90	1.1×10^{-7}	[49b]

HNCS (*Isothiocyanic acid*).

$\frac{1}{2}(B+C)=$	$HN^{14}C^{12}S^{32}$ 5866. 0	$DN^{14}C^{12}S^{32}$ 5474. 3	$HN^{14}C^{13}S^{32}$ 5847. 3	$DN^{14}C^{13}S^{32}$ 5459. 8	$HN^{14}C^{12}S^{34}$ 5728. 8	[1]

$J=1-2$

	Frequency	
$HN^{14}C^{12}S^{32}$	23, 464	[1]
$DN^{14}C^{12}S^{32}$	21, 897	[1]
$HN^{14}C^{13}S^{32}$	23, 389	[1]
$DN^{14}C^{13}S^{32}$	21, 839	[1]
$HN^{14}C^{12}S^{34}$	22, 915	[1]

ICl. The half widths, dipole moment and intensities are discussed in reference [54].

$\mu = 0.65$	[54]
$B_e = 3422.300$	
$(eqQ)_{Cl^{35}} = -82.5$	
$(eqQ)_I = -2930.0$	[54]
$= 16.060$	
$\Delta\nu_{3-4} = 5.5$	
$\Delta\nu_{0-1} = 3.15$	[59]

ICl^{35}

				Frequency	Intensity	
$J=0$–1, $F_1=5/2$–$7/2$				6, 980	1.1×10^{-6}	[59]
$J=3$–4, $v=0$						
F_{1i}	F_i	F_{1f}	F_f			
3/2	2	5/2	3	27, 194. 75	9.1×10^{-7}	
3/2	1	5/2	2	27, 202. 64	5.0×10^{-7}	
3/2	3	5/2	4	27, 204. 99	1.5×10^{-6}	
5/2	3	7/2	4	27, 217. 51	1.4×10^{-6}	
5/2	2	7/2	3	27, 221. 02	1.0×10^{-6}	
5/2	4	7/2	5	27, 225. 32	2.0×10^{-6}	
5/2	1	7/2	2	27, 228. 34	7.3×10^{-7}	
1/2	1	3/2	2	27, 242. 59	3.9×10^{-7}	
1/2	2	3/2	3	27, 254. 90	1.1×10^{-6}	
7/2, 9/2		9/2		27, 283. 66		
7/2, 9/2		9/2		27, 286. 25		
7/2, 9/2		9/2		27, 292. 63		
7/2, 9/2		9/2		27, 295. 05		
7/2, 9/2	5	11/2	6	27, 333. 85	2.8×10^{-6}	[54]
11/2	5	13/2	6	27, 336. 68	6.8×10^{-6}	
11/2	6	13/2	7			
11/2	4	13/2	5	27, 337. 38	6.8×10^{-6}	
11/2	7	13/2	8			
9/2	3	11/2	4	27, 346. 31	1.9×10^{-6}	
9/2	4	11/2	5	27, 554. 71	2.3×10^{-6}	
9/2	6	11/2	7	27, 356. 58	3.4×10^{-6}	
9/2	5	11/2	6	27, 357. 73	2.8×10^{-6}	
$v=1$						
11/2		13/2		27, 208. 54	2.2×10^{-6}	
ICl^{37}						
$J=0$–1 5/2		7/2		6, 684	3.1×10^{-7}	
$J=3$–4 11/2		13/2		26, 181. 6	4.4×10^{-6}	

ICN (*Cyanogen iodide*).

$\mu = 3.71$	
$Bo = 3225.527$ for $IC^{12}N$	[53]
3177. 035 for $IC^{13}N$	[42]
$(eqQ)_N = 3.80$	
$(eqQ)_I = -2420.$	
$\Delta\nu = 20.$	[53]
$\alpha_1 = 9.33$	
$\alpha_2 = -9.50$	
$q = 2.69$	

$IC^{12}N^{14}$

	F_i	F_f	Frequency	Intensity	
$J=3$–4, $v=0$					
	11/2	11/2	25, 393. 87	7.1×10^{-6}	
	3/2	5/2	25, 711. 50	2.0×10^{-5}	
	5/2	7/2	25, 728. 77	2.9×10^{-5}	
	1/2	3/2	25, 752. 65	1.4×10^{-5}	
	7/2	9/2	25, 783. 50	4.2×10^{-5}	
	9/2	9/2	25, 789. 85	1.1×10^{-5}	[53]
	11/2	13/2	25, 823. 08	7.5×10^{-5}	
	9/2	11/2	25, 837. 64	5.7×10^{-5}	
	7/2	7/2	25, 954. 36	1.2×10^{-5}	
	3/2	3/2	25, 969. 58	6.9×10^{-6}	
	5/2	5/2	25, 991. 92	1.0×10^{-5}	
$v_1=1$					
	11/2	13/2	25, 748. 18	7.0×10^{-6}	[53]
	9/2	11/2	25, 763. 23	5.3×10^{-6}	
$v_2=1$					
	1_1 5/2	7/2	25, 802. 92	3.8×10^{-6}	
	1_1 3/2	5/2	25, 815. 34	3.8×10^{-6}	
	1_1 7/2	9/2	25, 829. 31	7.8×10^{-6}	
	1_2 7/2	9/2	25, 850. 78	7.8×10^{-6}	
	1_1 9/2	11/2	25, 872. 24	1.1×10^{-5}	[53]
	1_2 9/2	11/2	25, 893. 73	1.1×10^{-5}	
	1_1 11/2	13/2	25, 906. 28	1.4×10^{-5}	
	1_2 11/2	13/2	25, 927. 66	1.4×10^{-5}	
$v_2=2$					
$l=2$					
	11/2	13/2 1_2	26, 046. 32	3.5×10^{-6} P	[30]
$J=4$–5, $v=0$					
	13/2	13/2	31, 848. 77	8.5×10^{-6}	
	11/2	11/2	32, 200. 58	1.5×10^{-5}	
	5/2	7/2	32, 203. 57	5.7×10^{-5}	
	7/2	9/2	32, 215. 56	7.3×10^{-5}	
	3/2	5/2	32, 226. 85	4.4×10^{-5}	[42]
	9/2	11/2	32, 248. 52	9.3×10^{-5}	
	13/2	15/2	32, 268. 33	1.5×10^{-4}	
	11/2	13/2	32, 278. 55	1.2×10^{-4}	
	9/2	9/2	32, 386. 29	1.8×10^{-5}	
$J=11$–12, $v=0$					
			77, 413.	7.7×10^{-3}	[41]
$J=12$–13, $v=0$					
			83, 864.	9.7×10^{-3}	[41]

$IC^{13}N^{14}$

$J=4$–5, $v=0$				
5/2	7/2	31, 718. 28	5.5×10^{-7}	
7/2	9/2	31, 730. 50	7.2×10^{-7}	
3/2	5/2	31, 741. 50	4.3×10^{-7}	[42]
9/2	11/2	31, 763. 34	9.1×10^{-7}	
13/2	15/2	31, 783. 31	1.4×10^{-6}	
11/2	13/2	31, 793. 46	1.1×10^{-6}	

NH_3 (*Ammonia*). The ammonia spectrum is unusual in being produced primarily by inversion or vibration rather than rotation of the molecule. It has considerably greater intensity than other micro-wave spectra of the same frequency, with the result that it is the first known and most widely studied microwave spectrum. The dependence of inversion frequency on the rotational quantum numbers J and K of the molecule produces a "fine" structure with frequencies given by the formula [45]

$$\nu = 23{,}785.75 - 151.450(J^2+J-K^2) + 59.892K^2 + 0.49569(J^2+J-K^2)^2 - 0.37674K^2(J^2+J-K^2) + 0.06554K^4.$$

This formula applies with an accuracy of about 2 mc for small J and K up to about $J=12$ except when $K=3$, for which deviations are somewhat larger [45, 34]. The expression [40]

$$\nu = 23{,}787 - 151.3\ J(J+1) + 211.0\ K^2 + 0.5503\ J^2(J+1)^2 - 1.531\ J(J+1) + 1.055\ K^4,$$

applies with an accuracy of about 30 mc up to $J=16$. Each one of the lines listed for $N^{14}H_3$ may be expected to show hyperfine structure due to the N^{14} quadrupole coupling [7a, 58a]. Additional small frequency shifts of this hyperfine structure due to the N^{14} nuclear magnetic coupling have been detected [40, 24a, 27a]. The resulting symmetric patterns of two weak lines on each side of the lines listed have been studied up to $J=9$ [40], but the weak lines are not listed in this table. The frequency difference between these lines and the strong component that is listed are given by

$$\delta\nu = \pm\left\{\frac{3}{4}eqQ\left[1-\frac{3K^2}{J(J+1)}\right]\frac{J+1}{2J+3} - J\left[\frac{0.0104K^2}{J(J+1)}+0.0022\right]\right\},$$

$$\delta\nu' = \pm\left\{\frac{3}{4}eqQ\left[1-\frac{3K^2}{J(J+1)}\right]\frac{J}{2J-1} + (J+1)\left[\frac{0.0104K^2}{J(J+1)}+0.0022\right]\right\}.$$

The sign of eqQ cannot be definitely measured experimentally, but is very probably negative, and is assumed negative in the expressions for $\delta\nu$ and $\delta\nu'$. $N^{15}H_3$ shows no hyperfine structure, since the N^{15} quadrupole moment is zero. Intensities of the weak hyperfine components relative to the strong component decrease approximately as $1/J^2$. The rather involved expressions for exact intensities are given by Candler [4c] and (with some typographical errors) in reference [40].

Intensities listed in the table are for the entire fine structure lines (without resolution of hyperfine components) assuming for each line, including the $N^{15}H_3$ lines, the same value of half width $\Delta\nu$ measured for the $N^{14}H_3$ $J=3$, $K=3$ line[50]*. Bleaney et al.[4a] find actually that for a number of NH_3 lines $\Delta\nu$ depends on J and K according to the formula

$$\Delta\nu \alpha \left[\frac{K^2}{J(J+1)}\right]^{1/5}$$

so that intensities should be obtained from those in the table by multiplying by the factor $[3J(J+1)/4K^2]^{1/5}$. The apparent frequencies and values of $\Delta\nu$ at atmospheric and higher pressures differ widely from those given here [4a, 59a, 4b]. See also [33a].

NH_3 (*Ammonia*).

	$N^{14}H_3$	$N^{15}H_3$	
μ	1.45	1.45	
$\Delta\nu$	28.		[50]
A_0	189,000	189,000	[26]
B_0	298,000		[26]
eqQ	−4.10	0	[40]

*Note that in reference [50] the value of $\Delta\nu$ in fig. 3 ($\Delta\nu=29.4$ p mm Hg) is correct and the value of $\tau=1/2\pi\Delta\nu$ on p. 667 is incorrect.

$N^{15}H_3$

J	K	*Frequency*	*Intensity*		*Earlier references by workers other than those already quoted*
7	4	19, 218. 52	2.9×10^{-5}	[45]	
6	3	19, 757. 56	6.8×10^{-5}	[45, 21]	[4]
5	1	19, 829	6.9×10^{-6}	[4]	
5	2	20, 371. 48	3.1×10^{-5}	[45, 21]	[4]
8	6	20, 719. 20	8.8×10^{-5}	[45, 21]	[4]
9	7	20, 735. 46	2.9×10^{-5}	[45, 21]	[4]
7	5	20, 804. 80	6.2×10^{-5}	[45, 21]	[4]
10	8	20, 852. 51	1.7×10^{-5}	[45, 21]	[4]
6	4	20, 994. 62	7.8×10^{-5}	[45, 21]	[4]
11	9	21, 070. 73	1.9×10^{-5}	[45, 21]	[4]
4	1	21, 134. 37	1.6×10^{-5}	[45, 21]	[4]
5	3	21, 285. 30	1.7×10^{-4}	[45, 21]	[4]
12	10	21, 391. 55	4.9×10^{-6}	[45]	
4	2	21, 703. 34	6.9×10^{-5}	[45, 21]	[4]
3	1	22, 234. 51	3.3×10^{-5}	[45, 21]	[4]
14	12	22, 355	2.1×10^{-6}	[56]	
5	4	22, 653. 00	1.9×10^{-4}	[45, 21]	[4]
4	3	22, 688. 24	3.7×10^{-4}	[45, 21, 46]	[4]
6	5	22, 732. 45	1.6×10^{-4}	[45, 21]	[4]
3	2	22, 834. 10	1.5×10^{-4}	[45, 21]	[4, 50]
7	6	22, 924. 91	2.7×10^{-4}	[45, 21]	[4, 50]
15	13	23, 004	4.7×10^{-7}	[56]	
2	1	23, 098. 78	6.7×10^{-5}	[45, 21]	[4, 50]
8	7	23, 232. 20	9.5×10^{-5}	[45, 21]	[4, 50]
9	8	23, 657. 46	6.3×10^{-5}	[45, 21]	[4, 50]
1	1	23, 694. 48	1.6×10^{-4}	[45, 21]	[4, 50]
2	2	23, 722. 61	3.0×10^{-4}	[45, 21]	[4, 50]
3	3	23, 870. 11	7.9×10^{-4}	[45, 21]	[4, 50]
4	4	24, 139. 45	4.3×10^{-4}	[45, 21]	[4, 50]
10	9	24, 205. 25	7.8×10^{-5}	[45, 21]	[4, 50]
5	5	24, 532. 94	4.1×10^{-4}	[45, 21]	[4, 50]
11	10	24, 881. 90	2.2×10^{-5}	[21]	[50]
6	6	25, 056. 04	7.1×10^{-4}	[45, 21]	[4, 50]
12	11	25, 695. 23	1.3×10^{-5}	[21]	
7	7	25, 715. 14	2.8×10^{-4}	[45, 21]	[4]
8	8	26, 518. 91	2.1×10^{-4}	[40]	
13	12	26, 655. 00	1.3×10^{-5}	[40]	
9	9	27, 478. 00	2.9×10^{-4}	[40]	
14	13	27, 772. 52	3.0×10^{-6}	[40]	
10	10	28, 604. 73	9.5×10^{-5}	[40]	
15	14	29, 061. 14	1.4×10^{-6}	[40]	
11	11	29, 914. 66	5.8×10^{-5}	[40]	
12	12	31, 424. 97	6.6×10^{-5}	[40]	
13	13	33, 156. 95	1.8×10^{-5}	[40]	
14	14	35, 134. 44	9.2×10^{-6}	[40]	
15	15	37, 385. 18	8.9×10^{-6}	[40]	
16	16	39, 941. 54	2.0×10^{-6}	[40]	

$N^{15}H_3$

J	K	*Frequency*	*Intensity*	
5	3	20, 272. 04	6.4×10^{-7}	[21]
4	2	20, 682. 87	2.6×10^{-7}	
3	1	21, 202. 30	1.3×10^{-7}	
5	4	21, 597. 86	7.2×10^{-7}	
4	3	21, 637. 91	1.4×10^{-6}	
6	5	21, 667. 93	6.0×10^{-7}	
3	2	21, 783. 98	5.6×10^{-7}	
7	6	21, 846. 41	9.9×10^{-7}	
2	1	22, 044. 28	2.6×10^{-7}	
8	7	22, 134. 89	3.5×10^{-7}	
9	8	22, 536. 26	2.3×10^{-7}	
1	1	22, 624. 96	6.0×10^{-7}	
2	2	22, 649. 85	1.2×10^{-6}	
3	3	22, 789. 41	3.0×10^{-6}	
4	4	23, 046. 10	1.6×10^{-6}	
10	9	23, 054. 97	3.0×10^{-7}	
5	5	23, 421. 99	1.5×10^{-6}	
6	6	23, 922. 32	2.6×10^{-6}	
7	7	24, 553. 42	1.1×10^{-6}	
8	8	25, 323. 51	8.0×10^{-7}	

N_2O (*Nitrous oxide*)

$\Delta\nu = 3.35$ [7b]

$\mu = .16$ [39c]

	$N_2^{14}O^{16}$	$N^{15}N^{14}O^{16}$	
B_0	12, 561. 64	12, 137. 31	[7]
	central	*end*	
$(eqQ)_N =$	−. 27	−1. 03	[7, 43]

$N^{14}N^{14}O^{16}$

	F_i	F_f	*Frequency*	*Intensity*	
$J=0$–1	1	1	25, 123. 03	1.1×10^{-5}	[7]
	1	2	25, 123. 28	1.7×10^{-5}	
	1	0	25, 123. 64	3.4×10^{-5}	

$N^{15}N^{14}O^{16}$

$J=0$–1	1	1	24, 274. 53	3.5×10^{-8}	[7]
	1	2	24, 274. 61	5.8×10^{-8}	
	1	0	24, 274. 73	1.1×10^{-8}	
$N^{14}N^{15}O^{16}$, $J=0$–1			25, 121. 55	1.1×10^{-7}	[7b]
$N^{15}N^{15}O^{16}$, $J=0$–1			24, 274. 78	4.0×10^{-10}	[7b]

O_2 (*Oxygen*). This spectrum is of a fundamentally different nature than the other molecular spectra recorded herein, being due to a magnetic coupling to the electromagnetic field rather than an electric dipole coupling. The theory of the transition has been discussed by Van Vleck [58b].

$\Delta\nu = .8 - 1.3$ [3]

O_2^{16}

Frequency	
Ca. 60,000	[3, 31, 48a]

OCS (*Carbonyl sulfide*).

$\mu(O^{16}C^{12}S^{32}) = .732$ [16, 27]

$\mu_{v_2=1} = .694$ [49c]

$\mu(O^{16}C^{13}S^{32}) = .722$ [16, 27]

$(eqQ)S^{33} = -28.5$ [52]

$\Delta\nu = 6.$ [53]

	$O^{16}C^{12}S^{32}$	$O^{16}C^{12}S^{33}$	$O^{16}C^{12}S^{34}$	$O^{16}C^{13}S^{32}$	$O^{16}C^{13}S^{34}$	$O^{16}C^{14}S^{32}$	$O^{18}C^{12}S^{32}$
B_0	6081. 453	6004. 918	5932. 843	6061. 939	5911. 730	6043. 25	5704. 825
α_1	18. 12						
α_2	−10. 59		−10. 37			−9. 4	
α_3	55. 1		6. 07			6. 7	
q	6. 393		6. 07			6. 7	
	[16]	[52]	[53]	[53]	[53]	[37]	[53]

The B_0's listed above are those for the lowest observed J transition, since they may be expected to increase with J because of centrifugal stretching.

$O^{16}C^{12}S^{32}$

	Frequency	*Intensity*	
$J=1$–2, $v=0$	24, 325. 92	5.5×10^{-5}	[16]
$v_1=1$	24, 253. 44	8.7×10^{-7}	[52]
$v_2=1$, 1_1	24, 355. 50	4.4×10^{-6}	[16]
1_2	24, 380. 84	4.4×10^{-6}	[16]
$v_2=2$	24, 401	1.3×10^{-6}	[39b]
$v_2=3$	24, 411	1×10^{-7}	[39b]
	24, 459	1×10^{-7}	[39b]
$J=2$–3, $v=0$	36, 488. 82	4.6×10^{-5}	[49]
$J=3$–4, $v=0$	48, 651. 64	4.4×10^{-4}	[27]
$J=4$–5, $v=0$	60, 814. 08	8.7×10^{-4}	[27]

$O^{16}C^{12}S^{33}$

	F_i	Ff			
$J=1$–2, $v=0$	1/2	3/2	24, 013. 04	7.2×10^{-8}	[52]
	5/2	5/2			
	1/2	1/2	24, 020. 21	2.9×10^{-7}	[52]
	3/2	5/2			
	5/2	7/2			
	3/2	3/2	24, 025. 39	4.6×10^{-8}	[52]
	3/2	1/2	24, 032. 75	7.2×10^{-9}	[52]

$O^{16}C^{12}S^{34}$

$J=1$–2, $v=0$	23. 731. 33	2.2×10^{-6}	[16]
$v_1=1$	23, 661	4.1×10^{-8}	[32]
$v_2=1$, 1_1	23, 760. 67	1.4×10^{-7}	[52]
1_2	23, 784. 95	1.4×10^{-7}	[52]
$J=3$–4, $v=0$	47, 462. 40	1.9×10^{-5}	[27]

$O^{16}C^{12}S^{36}$

$J=1$–2, $v=0$	23, 198. 66	8×10^{-9}	[32]

$O^{16}C^{13}S^{32}$

	Frequency	Intensity	
$J=1$–2, $v=0$	24, 247. 76	5.9×10^{-7}	[53]
$v_2=1, 1_1$	24, 275. 25	6.6×10^{-8}	[53]
1_2	24, 301. 05	6.6×10^{-8}	[53]

$O^{17}C^{13}S^{34}$

$J=1$–2, $v=0$	23, 646. 92	2.8×10^{-8}	[53]

$O^{16}C^{14}S^{32}$

$J=1$–2, $v=0$	24, 173. 0	5.7×10^{-5} (100% C^{14})	[37]
$v_2=1, 1_1$	24, 197	6.4×10^{-6}	[37]
1_2	24, 224	6.4×10^{-6}	[37]

$O^{17}C^{12}S^{32}$

$J=1$–2, $v=0$	23, 534. 67	2.2×10^{-8}	[32]

$O^{18}C^{12}S^{32}$

$J=1$–2, $v=0$	22, 819. 30	9.6×10^{-8}	[53]

OCSe (*Carbonyl selenide*).

$\mu=.754$
$\mu_{v=1}=.728$ [47]
$\mu_{v=1}=.730$

Molecule	B_{000}	α_1	α_2	q	D_vc/sec	
$O^{16}C^{12}Se^{82}$	3994. 009 ± .005	13. 12 ± .005	−6. 86 ± .005	3. 12 ± .005	875 ± 50	
Se^{80}	4017. 677	13. 27	−6. 92	3. 15	755 ± 20	
Se^{78}	4042. 460	13. 40	−6. 96	3. 19	830 ± 50	
Se^{77}	4055. 300	13. 48	−6. 98	3. 21		
Se^{76}	4068. 465		−7. 00	3. 24		[47]
Se^{74}	4095. 793					
$O^{16}C^{13}Se^{80}$	3980. 045					
Se^{78}	4005. 112					

$O^{16}C^{12}Se^{74}$

	Frequency	Intensity	
$J=2$–3, $v=0$	24, 574. 67	1.3×10^{-7}	

$O^{16}C^{12}Se^{76}$

$J=2$–3, $v=0$	24, 410. 70	1.4×10^{-6}	
$v_2=1, 1_1$	24, 442. 98	1.8×10^{-7}	
$v_2=1, 1_2$	24, 462. 42	1.8×10^{-7}	

$O^{16}C^{12}Se^{77}$

$J=2$–3, $v=0$	24, 331. 71	1.2×10^{-6}	
$v_1=1$	24, 250. 84	5.5×10^{-8}	
$v_2=1, 1_1$	24, 363. 97	1.6×10^{-7}	
$v_2=1, 1_2$	24, 383. 21	1.6×10^{-7}	

$O^{16}C^{12}Se^{78}$

$J=2$–3, $v=0$	24, 254. 67	3.4×10^{-6}	
$v_1=1$	24, 174. 30	1.6×10^{-8}	
$v_2=1, 1_1$	24, 286. 82	4.5×10^{-7}	
$v_2=1, 1_2$	24, 305. 95	4.5×10^{-7}	
$J=5$–6	48, 508. 88	2.8×10^{-5}	
$J=6$–7	56, 593. 16	4.4×10^{-5}	

$O^{16}C^{12}Se^{80}$ [47]

$J=2$–3, $v=0$	24, 105. 98	6.8×10^{-6}	
$v_1=1$	24, 026. 39	3.1×10^{-7}	
$v_2=1, 1_1$	24, 138. 05	9.0×10^{-7}	
$v_2=1, 1_2$	24, 156. 93	9.0×10^{-7}	
$J=5$–6	48, 211. 46	5.6×10^{-5}	
$J=6$–7	56, 246. 47	8.8×10^{-5}	

$O^{16}C^{12}Se^{82}$

$J=2$–3, $v=0$	23, 964. 50	1.3×10^{-6}	
$v_1=1$	23, 885. 76	6.0×10^{-8}	
$v_2=1, 1_1$	23, 996. 26	1.7×10^{-7}	
$v_2=1, 1_2$	24, 014. 97	1.7×10^{-7}	
$J=6$–7	55, 916. 19	1.1×10^{-5}	

$O^{16}C^{13}Se^{78}$

$J=2$–3, $v=0$	24, 030. 58	3.7×10^{-8}	

$O^{16}C^{13}Se^{80}$

$J=2$–3, $v=0$	23, 880. 18	7.5×10^{-8}	

PF_3 (*Phosphorus trifluoride*)

$\mu=1.02$ [39c]
$\Delta\nu=16.$ [19]
$B_0=7819.90$ [19]

PF_3	Frequency	Intensity*	
$J=1-2$, $K=0, 1$	31, 279. 60	2.3×10^{-6}	[19]
$J=2-3$, $K=0, 1$	46, 918. 82	6.7×10^{-6}	[19]
$K=2$	46, 919. 02	1.5×10^{-6}	

*Assuming 80% in ground vibrational state.

excited vibrational states { 46, 940; 47, 010; 47, 033; 47, 040 } [19]

SiH_3Cl (Chlorosilane) $\mu=1.28$

	SiH_3Cl^{35}	SiH_3Cl^{37}	
$A_0=95{,}500$			
B_0	6673.81	6,512.40	[38]
$(eqQ)Cl$	−40.0	−30.8	[38]

SiH_3Cl^{35}	F_i	F_f	Frequency	Intensity*	
$J=1-2$, $K=0$					
	1/2	3/2	26, 685. 25	3.4×10^{-7}	
	5/2	5/2	26, 686. 15	3.7×10^{-7}	
	1/2	1/2	26, 695. 00	3.4×10^{-7}	
	3/2	5/2	26, 696. 10	2.5×10^{-6}	[38]
	5/2	7/2			
	3/2	3/2	26, 703. 34	4.5×10^{-7}	
	3/2	1/2	26, 713. 07	7.0×10^{-8}	

*Assuming 90% of the molecules are in ground vibrational state.

$J=1-2$, $K=1$	F_i	F_f	*Frequency*	*Intensity*	
	3/2	5/2	26, 687. 34	6.6×10^{-7}	[38]
	3/2	3/2	26, 690. 92	3.4×10^{-7}	
	5/2	5/2	26, 692. 66	2.8×10^{-7}	
	5/2	7/2	26, 697. 45	1.3×10^{-6}	
	1/2	3/2	26, 700. 48	2.6×10^{-7}	
	1/2	1/2	26, 705. 02	2.6×10^{-7}	

SiH_3Cl^{37}

$J=1-2$, $K=0$					
	1/2	3/2	26, 042. 41	2.2×10^{-7}	[38]
	5/2	5/2			
	3/2	5/2	26, 050. 26	7.9×10^{-7}	[38]
	5/2	7/2			
	3/2	3/2	26, 055. 86	1.4×10^{-7}	
	3/2	1/2	26, 063. 52	2.2×10^{-8}	
$K=1$	3/2	5/2	26, 043. 29	2.0×10^{-7}	
	3/2	3/2	26, 046. 30	1.0×10^{-7}	
	5/2	5/2	26, 047. 97	8.7×10^{-8}	
	5/2	7/2	26, 051. 09	3.9×10^{-7}	
	1/2	3/2	26, 053. 35	8.1×10^{-8}	
	1/2	1/2	26, 057. 10	8.1×10^{-8}	

SO_2 (*Sulfur dioxide*)

$\mu=1.7$
$A=61{,}100$
$B=10{,}400$ [12]
$C=8{,}870$

$S^{32}O_2^{16}$

Transition	*Frequency*	
$13_{-10}-12_{-8}$	20, 420	[12]
	22, 064	
	22, 225	
	22, 475	
	22, 735	
	22, 904	
	22, 934	
	23, 033	
$6_{-4}-5_{-2}$	23, 413	
	23, 738	
$9_{-8}-8_{-4}$	24, 037	
	24, 083	
	24, 342	
	25, 047	
	25, 170	
$7_{-4}-8_{-6}$	25, 392	
$3_{-2}-4_{-4}$	29, 460	

SPF_2

$B_0=2657.6$

SPF_3

$J=3-4$	21, 262	[37b]
$J=4-5$	26, 574	
Exc. states	21, 283	
	26, 553	

TABLE 2. *Lines listed by frequency*

Frequency	Intensity	Transition	Molecule
6, 684	W	0-1	IC^{37}
6, 980	M	0-1	IC^{35}
10, 278. 99	W	----------	HDO^{16}
17, 961. 2	M	0-1	$B^{10}H_3C^{12}O^{16}$
18, 398. 6	M	0-1	$C^{12}H_3C^{12}N^{14}$
18, 400	M	0-1	$C^{12}H_3C^{12}N^{14}$
18, 402. 1	M	0-1	$C^{12}H_3C^{12}N^{14}$
18, 943. 77	W	0-1	$C^{12}H_3Br^{81}$
18, 992. 36	W	0-1	$C^{12}H_3Br^{79}$
19, 040. 32	M	0-1	$C^{12}H_3Br^{81}$
19, 107. 97	M	0-1	$C^{12}H_3Br^{79}$
19, 160. 82	M	0-1	$C^{12}H_3Br^{81}$
19, 218. 52	S	0-1	$N^{14}H_3$
19, 252. 13	M	0-1	$C^{12}H_3Br^{79}$
19, 700	-------	3-4	$C^{12}H_2N^{14}C^{12}S^{34}$
19, 757. 56	S	----------	$N^{14}H_3$
19, 829	M	----------	$N^{14}H_3$
19, 929	-------	3-4	$C^{12}H_3N^{14}C^{12}S^{34}$
20, 020	-------	3-4	$C^{12}H_3N^{14}C^{12}S^{32}$
20, 140	-------	3-4	$C^{12}H_3N^{14}C^{12}S^{32}$
20, 160	-------	3-4	$C^{12}H_3N^{14}C^{12}$
20, 216	-------	3-4	$C^{12}H_3N^{14}C^{12}S^{32}$
20, 230	-------	3-4	$C^{12}H_3N^{14}C^{12}S^{32}$
20, 241	-------	3-4	$C^{12}H_3N^{14}C^{12}S^{32}$
20, 272. 04	M	----------	$N^{15}H_3$
20, 350	-------	3-4	$C^{12}H_3N^{14}C^{12}S^{32}$
20, 371. 48	S	----------	$N^{14}H_3$
20, 385	-------	----------	CH_3NO_2
20, 413	-------	3-4	$C^{12}H_3N^{14}C^{12}S^{32}$
20, 443	-------	3-4	$C^{12}H_3N^{14}C^{12}S^{32}$
20, 421	-------	----------	SO_2
20, 460. 40	W	----------	HDO^{16}
20, 679. 9	W	1-2	CF_3CH_3
20, 682. 87	W	----------	$N^{15}H_3$
20, 710. 6	M	1-2	CF_3CH_3
20, 719. 20	S	----------	$N^{14}H_3$
20, 735. 46	S	----------	$N^{14}H_3$
20, 742. 3	M	1-2	CF_3CH_3
20, 804. 80	S	----------	$N^{14}H_3$
20, 852. 51	S	----------	$N^{14}H_3$
20, 910	-------	----------	CH_2OH
20, 971	-------	----------	CH_3OH
20, 994. 62	S	----------	$N^{14}H_3$
21, 070. 73	S	----------	$N^{14}H_3$
21, 134. 37	S	----------	$N^{14}H_3$
21, 202. 30	W	----------	$N^{15}H_3$
21, 262	-------	----------	SPF_2
21, 283	-------	----------	SPF_3

TABLE 2. *Lines listed by frequency*—Continued

Frequency	Intensity	Transition	Molecule
21, 285. 30	S	----------	$N^{14}H_3$
21, 350	------	----------	CH_3OH
21, 391. 55	M	----------	$N^{14}H_3$
21, 482	M	----------	CH_2CF_2
21, 549	W	----------	CH_2CF_2
21, 551	------	----------	CH_3OH
21, 573	W	----------	CH_2CF_2
21, 597. 86	M	----------	$N^{15}H_3$
21, 637. 91	M	----------	$N^{15}H_3$
21, 664	------	----------	$C^{12}D_4O^{16}$
21, 667. 93	M	----------	$N^{15}H_3$
21, 689	M	----------	CH_2CF_2
21, 703. 34	S	----------	$N^{14}H_3$
21, 712	------	----------	CH_3NH_2
21, 734	M	----------	CH_2CF_2
21, 783. 98	M	----------	$N^{15}H_3$
21, 839	------	1–2	$DN^{14}C^{13}S^{32}$
21, 846. 41	M	1–2	$DN^{14}C^{13}S^{34}$
21, 897	------	1–2	$DN^{14}C^{12}S^{32}$
21, 930. 2	------	1–2	C_2H_3Cl
21, 935	------	----------	CH_3NH_2
22, 044. 28	W	----------	$N^{15}H_3$
22, 064	------	----------	SO_2
22, 134. 89	W	----------	$N^{15}H_3$
22, 217	------	----------	$CHClF_2$
22, 225	------	----------	SO_2
22, 234. 51	S	----------	$N^{14}H_3$
22, 235. 22	M	----------	H_2O
22, 236	M	----------	CH_2CF_2
22, 247	------	----------	$CHClF_2$
22, 258	------	----------	CH_3NH_2
22, 281	S	----------	CH_2CF_2
22, 305	------	----------	$CHClF_2$, CH_3OH
22, 307. 67	W	----------	HDO
22, 353	------	----------	$CHClF_2$
22, 355	M	----------	$N^{14}H_3$
22, 369. 6	------	1–2	C_2H_3Cl
22, 383	M	----------	CH_2CF_2
22, 386	------	----------	$CHClF_2$
22, 391	M	----------	CH_2CF_2
22, 410	------	----------	$CHClF_2$
22, 436	------	----------	$CHClF_2$
22, 462	------	----------	$CHClF_2$
22, 475	------	----------	SO_2
22, 481	------	----------	$CHClF_2$
22, 485. 9	------	1–2	C_2H_3Cl

TABLE 2. *Lines listed by frequency*—Continued

Frequency	Intensity	Transition	Molecule
22, 535	------	----------	CH_3NH_2
22, 536. 26	W	----------	$N^{15}H_3$
22, 545	------	----------	$CHClF_2$
22, 553	------	----------	$CHClF_2$
22, 590	------	----------	CH_3NH_2
22, 595	------	----------	CH_3NH_2
22, 612	------	----------	CH_3NH_2
22, 624. 96	M	----------	$N^{15}H_3$
22, 649. 85	M	----------	$N^{15}H_3$
22, 653. 00	S	----------	$N^{14}H_3$
22, 660	W	----------	CH_2CF_2
22, 680	------	3–4	$C^{12}H_3S^{32}C^{12}N^{14}$
22, 688. 24	S	----------	$N^{14}H_3$
22, 732	------	----------	CH_3NH_2
22, 732. 45	S	----------	$N^{14}H_3$
22, 735	------	----------	SO_2
22, 740	------	----------	CH_3NH_2
22, 752	S	----------	CH_2CF_2
22, 789. 41	M	----------	$N^{15}H_3$
22, 819. 30	W	1–2	$O^{16}C^{12}S^{32}$
22, 834. 10	S	----------	$N^{14}H_3$
22, 904	------	----------	SO_2
22, 915	------	1–2	$HN^{14}C^{12}S^{34}$
22, 924. 91	S	----------	$N^{14}H_3$
22, 934	------	----------	SO_2
22, 946. 9	------	1–2	C_2H_3Cl
22, 977	------	----------	CH_3NH_2
23, 004	W	----------	$N^{14}H_3$
23, 021	------	----------	CH_3NO_3
23, 033	------	----------	SO_2
23, 046. 10	M	----------	$N^{15}H_3$
23, 054. 97	W	----------	$N^{15}H_3$
23, 055. 0	------	1–2	C_2H_3Cl
23, 098. 78	S	----------	$N^{14}H_3$
23, 115	------	----------	CH^3NH_2
23, 121. 2	------	----------	CH_3OH
23, 134	M	----------	C_2H_4O
23, 181	------	----------	CH_2CF_2
23, 198. 66	W	1–2	$O^{16}C^{12}S^{36}$
23, 205	------	----------	CH_3NH_2
23, 206	W	----------	CH_2CF_2
23, 214	M	----------	CH_2CF_2
23, 220	M	----------	CH_2CF_2
23, 232. 20	S	----------	$N^{14}H_3$
23, 234	W	----------	CH_2CF_2
23, 250	------	----------	CH_3NO_2

TABLE 2. *Lines listed by frequency*—Continued

Frequency	Intensity	Transition	Molecule
23, 295			CH_3NH_2
23, 300			CH_3NH_2
23, 305			CH_3NH_2
23, 308			$CHClF_2$
23, 323	M		CH_2CF_2
23, 335	M		CH_3NH_2
23, 346. 8			CH_3OH
23, 361	M		CH_2CF_2
23, 372. 72	M	1-2	$Cl^{37}C^{12}N^{14}$
23, 389. 00	M	1-2	$Cl^{37}C^{12}N^{14}$
23, 389		1-2	$HN^{14}C^{13}S^{32}$
23, 389. 61	M	1-2	$Cl^{37}C^{12}N^{14}$
23, 390. 53	M	1-2	$Cl^{37}C^{13}N^{14}$
23, 402. 47	M	1-2	$Cl^{37}C^{13}N^{14}$
23, 404			CH_3NH_2
23, 413			SO_2
23, 421. 99	M		$N^{15}H_3$
23, 425			CH_3OH, CH_2NH_2
23, 430			CH_2NH_2
23, 433	S		CH_2CF_2
23, 446			CH_3NH_2
23, 458. 6	W	1-2, $K=0$	AsF_3
23, 463. 0	W	1-2, $K=0$	AsF_3
23, 464		1-2	$HN^{14}C^{12}S^{32}$
23, 467			CH_3NO_2
23, 472. 6	W	1-2, $K=1$	AsF_3
23, 476			CH_2Cl_2
23, 483			CH_3NO_2
23, 494. 2	W	1-2, $K=1$	AsF_3
23, 501. 6	W	1-2, $K=1$	AsF_3
23, 510			CH_3NH_2
23, 512. 9	W		AsF_3
23, 517. 0	W	1-2, $K=0$	AsF_3
23, 522. 4	M	1-2, $K=0$	AsF_3
23, 532. 1	M	1-2, $K=1$	AsF_3
23, 534. 67	W	1-2	$O^{17}C^{12}S^{32}$
23, 538. 9		1-2	C_2H_3Cl
23, 543. 2	W		AsF_3
23, 553. 0	W		AsF_3
23, 564. 6	W	1-2, $K=0$	AsF_3
23, 575. 3	W	1-2, $K=1$	AsF_3
23, 610	M		C_2H_4O
23, 644			$CHClF_2$
23, 646. 92	W	1-2, $v=0$	$O^{16}C^{13}C^{34}$
23, 649	M		CH_2CF_2
23, 657. 46	S		$N^{14}H_3$
23, 661	W	1-2, $v_1=1$	$O^{16}C^{12}S^{34}$
23, 680			$CHClF_2$, CH_3NH_2

TABLE 2. *Lines listed by frequency*—Continued

Frequency	Intensity	Transition	Molecule
23, 694. 48	S		$N^{14}H_3$
23, 706			CH_3NO_2
23, 722. 61	S		$N^{14}H_3$
23, 731. 33	M	1-2, $v=0$	$O^{16}C^{12}S^{34}$
23, 733			$CHClF_2$
23, 738			SO_2
23, 760. 67	W	1-2, $v_2=1$	$O^{16}C^{12}S^{34}$
23, 770	M		CH_2CF_2
23, 784. 95	W	1-2, $v_2=1$	$O^{16}C^{12}S^{34}$
23, 803			$CHClF_2$
23, 812	M		CH_2CF_2
23, 826			$CHClF_2$
23, 845			$CHClF_2$
23, 854. 4			CH_3OH
23, 862. 57	M	1-2, $v=0$	$Cl^{35}C^{12}N^{14}$
23, 863. 5	W	1-2, $v=0$	$Cl^{35}C^{12}N^{14}$
23, 863. 8	W	1-2, $v=0$	$Cl^{35}C^{12}N^{14}$
23, 864. 0	M	1-2, $v=0$	$Cl^{35}C^{12}N^{14}$
23, 864. 2	M	1-2, $v=0$	$Cl^{35}C^{14}N^{14}$
23, 864. 5	M	1-2, $v=0$	$Cl^{35}C^{12}N^{14}$
23, 864. 9	W	1-2, $v=0$	$Cl^{35}C^{12}N^{14}$
23, 865. 1	W	1-2, $v=0$	$Cl^{35}C^{12}N^{14}$
23, 870. 11	S		$N^{14}H_3$
23, 878. 6	M	1-2, $v=0$	$Cl^{35}C^{12}N^{14}$
23, 878. 9	W	1-2, $v=0$	$Cl^{35}C^{13}N^{14}$
23, 879. 7	W	1-2, $v=0$	$Cl^{35}C^{12}N^{14}$
23, 880. 18	W	2-3, $v=0$	$O^{16}C^{12}Se^{80}$
23, 883. 30	M	1-2, $v=0$	$Cl^{35}C^{12}N^{14}$
23, 884. 2	M	1-2, $v=0$	$Cl^{35}C^{12}N^{14}$
23, 884. 8	M	1-2, $v=0$	$Cl^{35}C^{12}N^{14}$
23, 884. 9	S	1-2, $v=0$	$Cl^{35}C^{12}N^{14}$
23, 885. 16	S	1-2, $v=0$	$Cl^{35}C^{12}N^{14}$
23, 885. 3	M	1-2, $v=0$	$Cl^{35}C^{12}N^{14}$
23, 885. 76	W	1-2, $v_1=1$	$O^{16}O^{12}Se^{82}$
23, 886. 0	M	1-2, $v=0$	$Cl^{35}C^{12}N^{14}$
23, 886. 2	M	1-2, $v=0$	$Cl^{35}C^{12}N^{14}$
23, 899. 59	M	1-2, $v=0$	$Cl^{35}C^{12}N^{14}$
23, 900. 20	M	1-2, $v=0$	$Cl^{35}C^{12}N^{14}$
23, 900. 7	M	1-2, $v=0$	$Cl^{35}C^{12}N^{14}$
23, 917. 9	S	1-2, $v_2=1$	$Cl^{35}C^{12}N^{14}$
23, 920. 91	M	1-2, $v=0$	$Cl^{35}C^{12}N^{14}$
23, 922. 32	M		$N^{15}H_3$
23, 925. 5	M	1-2, $v_2=1$	$Cl^{35}C^{12}N^{14}$
23, 928. 7	M	1-2, $v_2=1$	$Cl^{35}C^{12}N^{14}$
23, 938. 6	S	1-2, $v_2=1$	$Cl^{35}C^{12}N^{14}$
23, 944. 4	M	1-2, $v_2=1$	$Cl^{35}C^{12}N^{14}$
23, 948. 2	S	1-2, $v_2=1$	$Cl^{35}C^{12}N^{14}$

TABLE 2. *Lines listed by frequency*—Continued

Frequency	Intensity	Transition	Molecule
23, 954. 5	M	1-2, $v_2=1$	$Cl^{35}C^{12}N^{14}$
23, 958. 4	M	1-2, $v_2=1$	$Cl^{35}C^{12}N^{14}$
23, 964. 50	M	2-3, $v=0$	$O^{16}C^{12}Se^{82}$
23, 968. 6	S	1-2, $v_2=1$	$Cl^{35}C^{12}N^{14}$
23, 974. 4	M	1-2, $v_2=1$	$Cl^{35}C^{12}N^{14}$
23, 984. 6	M	1-2, $v_2=1$	$Cl^{35}C^{12}N^{14}$
23, 986	M	1-2, $v_2=1$	CH_2CF_2
23, 996. 26	W	2-3, $v_2=1$	$O^{16}C^{12}Se^{82}$
24, 013. 04	W	1-2, $v=0$	$O^{16}C^{12}S^{33}$
24, 014. 97	W	2-3, $v_2=1$	$O^{16}C^{12}Se^{82}$
24, 015			CH_3NH_2
24, 017			CH_3NO_2
24, 020. 21	W	1-2, $v=0$	$O^{16}C^{12}S^{33}$
24, 021	M		CH_2CF_2
24, 025. 39	W	1-2, $v=0$	$O^{16}C^{12}S^{33}$
24, 026. 39	W	2-3, $v_1=1$	$O^{16}C^{12}Se^{80}$
24, 030. 58	W	2-3, $v=0$	$O^{16}C^{12}Se^{78}$
24, 032. 75	W	1-2, $v=0$	$O^{16}C^{12}S^{33}$
24, 037			SO_2
24, 055			$C^{12}D_4O^{16}$
24, 078			CH_3NH_2
24, 083			SO_2
24, 105. 98	M	2-3, $v=0$	$O^{16}C^{12}Se^{80}$
24, 138. 05	M	2-3, $v_2=1$	$O^{16}C^{12}Se^{80}$
24, 139. 45	S		$N^{14}H_3$
24, 143		4-5	$C^{13}H_3N^{14}C^{12}S^{32}$
24, 150	W		CH_2CF_2
24, 156. 93	M	2-3, $v_2=1$	$O^{16}C^{12}Se^{80}$
24, 173. 0	W	1-2, $v=0$	$O^{16}C^{14}S^{32}$
24, 174. 30	W	2-3, $v_1=1$	$O^{16}C^{12}Se^{78}$
24, 205. 25	S		$N^{14}H_3$
24, 247. 76	M	1-2, $v=0$	$O^{16}C^{13}S^{32}$
24, 250. 84	W	2-3, $v_1=1$	$O^{16}C^{12}Se^{77}$
24, 253. 44	M	1-2, $v_1=1$	$O^{16}C^{12}S^{32}$
24, 254. 67	M	2-3, $v=0$	$O^{16}C^{12}Se^{78}$
24, 274. 53	W	0-1	$N^{15}N^{14}O^{16}$
24, 274. 61	W	0-1	$N^{15}N^{14}O^{16}$
24, 274. 73	W	0-1	$N^{15}N^{14}O^{16}$
24, 274. 78	W	0-1	$N^{15}N^{15}O^{16}$
24, 275. 25	W	1-2, $v_2=1$	$O^{16}C^{13}S^{32}$
24, 286. 82	W	2-3, $v_2=1$	$O^{16}C^{12}Se^{78}$
24, 294	M		CH_2CF_2
24, 301. 05	W	1-2, $v_2=1$	$O^{16}C^{13}S^{32}$
24, 305. 95	W	2-3, $v_2=1$	$O^{16}C^{12}Se^{78}$
24, 320			CH_3NH_2
24, 323	S		CH_2CF_2
24, 325. 92	S	1-2, $v=2$	$O^{16}C^{12}S^{32}$

TABLE 2. *Lines listed by frequency*—Continued

Frequency	Intensity	Transition	Molecule
24, 331. 71	M	2-3, $v=0$	$O^{16}C^{12}Se^{77}$
24, 342			SO_2
24, 352	M		CH_2CF_2
24, 355. 50	M	1-2, $v_2=1$	$O^{16}C^{12}S^{32}$
24, 357	W		CH_2CF_2
24, 363. 97	W	2-3, $v_2=1$	$O^{16}C^{12}Se^{77}$
24, 380. 84	M	1-2, $v_2=1$	$O^{16}C^{12}S^{32}$
24, 383. 21	W	2-3, $v_2=1$	$O^{16}C^{12}Se^{77}$
24, 401	M	2-3, $v_2=2$	$O^{16}C^{12}S^{32}$
24, 410. 70	M	2-3, $v=0$	$O^{16}C^{12}Se^{76}$
24, 411	W	1-2, $v=3$	$O^{16}C^{12}S^{22}$
24, 428			CH_3NO_2
24, 440			CH_2Cl_2
24, 442. 98	W	2-3, $v_2=1$	$O^{16}C^{12}Se^{76}$
24, 448			CH_3NO_2
24, 450	S		CH_2CF_2
24, 459	W	1-2, $v_2=3$	$O^{16}C^{12}S^{32}$
24, 462. 42	W	2-3, $v_2=1$	$O^{16}C^{12}Se^{76}$
24, 465. 33	M	2-3, $v=0$	$Br^{81}C^{12}N^{14}$
24, 471			CH_2Cl_2
24, 506. 75	M	2-3, $v_1=1$	$Br^{81}C^{12}N^{14}$
24, 507. 38	M	2-3, $v=0$	$Br^{81}C^{12}N^{14}$
24, 528			CH_3NH_2
24, 532. 94	S		$N^{14}H_3$
24, 541. 18	M	2-3, $v_1=1$	$Br^{81}C^{12}N^{14}$
24, 545	M		CH_2CF_2
24, 553. 42	M		$N^{15}H_3$
24, 573. 86	S	2-3, $v=0$	$Br^{81}C^{12}N^{14}$
24, 574. 67	W	2-3, $v=0$	$O^{16}C^{12}Se^{74}$
24, 577			CH_2Cl_2
24, 579	W		CH_2CF_2
24, 583. 00	M	2-3, $v=0$	$Br^{79}C^{12}N^{14}$
24, 599			CH_3NO_2
24, 602	W		CH_2CF_2
24, 608. 92	S	2-3, $v=0$	$Br^{81}C^{12}N^{14}$
24, 609		4-5	$C^{12}H_3N^{14}C^{12}S^{34}$
24, 622. 93	M	2-3, $v_2=1$	$Br^{81}C^{12}N^{14}$
24, 627			CH_2Cl_2
24, 631			CH_2Cl_2
24, 633. 71	M	2-3, $v=0$	$Br^{79}C^{12}N^{14}$
24, 636			CH_2Cl_2
24, 639	M		CH_2CF_2
24, 645. 82	M	2-3, $v_1=1$	$Br^{79}C^{12}N^{14}$
24, 658. 89	M	2-3, $v_2=1$	$Br^{81}C^{12}N^{14}$
24, 668			$C_2{}^{12}D_4O^{16}$
24, 682. 13	M	2-3, $v_2=1$	$Br^{81}C^{12}N^{14}$
24, 687. 11	M	2-3, $v_1=1$	$Br^{79}C^{12}N^{14}$

TABLE 2. *Lines listed by frequency*—Continued

Frequency	Intensity	Transition	Molecule
24, 713. 05	S	2-3, $v=0$	$Br^{79}C^{12}N^{14}$
24, 717. 19	M	2-3, $v=0$	$Br^{81}C^{12}N^{14}$
24, 734	M	----------	CH_2CF_2
24, 755. 22	S	2-3, $v=0$	$Br^{79}C^{12}N^{14}$
24, 760. 76	M	2-3, $v_2=1$	$Br^{79}C^{12}N^{14}$
24, 770	S	----------	CH_2CF_2
24, 784. 02	M	2-3, $v_2=1$	$Br^{79}C^{12}N^{14}$
24, 803. 00	M	2-3, $v_2=1$	$Br^{79}C^{12}N^{14}$
24, 806	W	----------	CH_2CF_2
24, 808	W	----------	CH_2CF_2
24, 824	-------	4-5	$C^{12}H_3N^{14}C^{12}S^{34}$
24, 826. 70	M	2-3, $v_2=1$	$Br^{79}C^{12}N^{14}$
24, 834. 3	S	----------	C_2H_4O
24, 842	-------	----------	CH_2Cl_2
24, 860. 6	M	2-3, $v_2=2$	$Br^{79}C^{12}N^{14}$
24, 881. 90	S	----------	$N^{14}H_3$
24, 884. 57	M	2-3, $v=0$	$Br^{79}C^{12}N^{14}$
24, 890. 0	M	2-3, $v_2=1$	$Br^{79}C^{12}N^{14}$
24, 890	-------	----------	CH_3NH_2
24, 896	-------	----------	CH_3NH_2
24, 910	-------	4-5	$C^{12}H_3N^{14}C^{13}S^{34}$
24, 911	-------	----------	CH_3OH
24, 916	-------	----------	CH_2Cl_2
24, 924. 4	S	----------	C_2H_4O
24, 926	-------	----------	CH_3OH
24, 928. 70	-------	----------	CH_3OH
24, 930	-------	4-5	$C^{12}H_3N^{14}C^{12}S^{33}$
24, 933. 47	-------	----------	CH_3OH
24, 934. 38	-------	----------	CH_3OH
24, 959. 08	-------	----------	CH_3OH
24, 967	-------	----------	CH_2Cl_2
24, 970	-------	----------	CH_2Cl_2
24, 971	-------	4-5	$C^{12}H_3N^{14}C^{12}S^{32}$
24, 976	-------	----------	CH_2Cl_2
24, 981. 5	M	2-3, $v_2=2$	$Br^{79}C^{12}N^{14}$
24, 996	-------	----------	CH_2Cl_2
25, 000	-------	----------	CH_2NH_2
25, 002	-------	4-5	$C^{12}H_3N^{14}C^{13}S^{32}$
25, 006. 0	M	2-3, $v_2=1$	$Br^{79}C^{12}N^{14}$
25, 018	-------	----------	CH_2Cl_2
25, 018. 14	-------	----------	CH_3OH
25, 038	-------	----------	CH_2Cl_2
25, 046	-------	----------	CH_2Cl_2
25, 047	-------	----------	CH_2Cl_2
25, 053	-------	----------	CH_2Cl_2, CH_3OH
25, 056	-------	----------	CH_2Br_2
25, 056. 04	S	----------	$N^{14}H_3$
25, 065	-------	----------	CH_3NH_2

TABLE 2. *Lines listed by frequency*—Continued

Frequency	Intensity	Transition	Molecule
25, 073	-------	----------	CH_2Cl_2
25, 077	-------	4-5	$C^{12}H_2N^{14}C^{12}S^{32}$
25, 099	-------	----------	CH_2Cl_2
25, 100	-------	4-5	$C^{12}H_3N^{14}C^{12}S^{32}$
25, 121. 55	W	0-1	$N^{14}N^{15}O^{16}$
25, 123	-------	----------	CH_2Cl_2
25, 123. 03	M	0-1	$N_2{}^{14}O^{16}$
25, 123. 28	M	0-1	$N_2{}^{14}O^{16}$
25, 123. 61	W	0-1	$N_2{}^{14}O^{16}$
25, 124. 88	-------	----------	CH_3OH
25, 161	-------	4-5	$C^{12}H_3N^{14}C^{12}S^{32}$
25, 167. 4	W	0-1, $K=0$	$C^{13}H_3Cl^{37}$
25, 170	-------	----------	SO_2
25, 183. 0	W	0-1, $K=0$	$C^{13}H_3Cl^{37}$
25, 195	-------	4-5	$C^{12}H_3N^{14}C^{12}S^{32}$
25, 195. 2	W	0-1, $K=0$	$C^{13}H_3Cl^{37}$
25, 200	-------	----------	CH_3NH_2
25, 221	-------	----------	CH_2Cl_2
25, 248	M	----------	CH_2CF_2
25, 269	-------	----------	CH_2Cl_2
25, 269	-------	4-5	$C^{12}H_3N^{14}C^{12}S^{32}$
25, 280	-------	----------	CH_2Cl_2
25, 294. 41	-------	----------	CH_3OH
25, 306	-------	4-5	$C^{12}H_3N^{14}C^{12}S^{32}$
25, 323. 51	M	----------	$N^{15}H_3$
25, 333	-------	4-5	$C^{12}H_3N^{14}C^{12}S^{32}$
25, 350	S	----------	CH_2CF_2
25, 381	-------	----------	CH_3OH
25, 390	-------	4-5	$C^{12}H_3N^{14}C^{12}S^{32}$
25, 392	-------	----------	SO_2
25, 393. 87	M	3-4, $v=0$	$IC^{12}N^{14}$
25, 404	-------	----------	CH_3NO_2
25, 409	-------	4-5	$C^{12}H_3N^{14}C^{12}S^{32}$
25, 414	-------	----------	CH_3NO_2
25, 442	-------	4-5	$C^{12}H_3N^{14}C^{12}S^{32}$
25, 450	M	----------	CH_2CF_2
25, 470	-------	----------	CH_3NH_2
25, 516	S	----------	CH_2CF_2
25, 541. 43	-------	4-5	CH_3OH
25, 550	-------	4-5	$C^{12}H_3N^{14}C^{12}S^{32}$
25, 577. 2	W	0-1, $K=0$	$C^{12}H^3Cl^{35}$
25, 596. 0	W	0-1, $K=0$	$C^{13}H_3Cl^{35}$
25, 611. 2	W	0-1, $K=0$	$C^{13}H^3Cl^{35}$
25, 653	-------	4-5	$C^{12}H_2N^{14}C^{12}S^{32}$
25, 695. 23	S	----------	$N^{14}H_3$
25, 710	-------	----------	CH_2Cl_2
25, 711. 50	S	3-4, $v=0$	$IC^{12}N^{14}$

TABLE 2. *Lines listed by frequency*—Continued

Frequency	Intensity	Transition	Molecule
25, 715. 14	S		$N^{14}H_3$
25, 728. 77	S	3-4, $v=0$	$IC^{12}N^{14}$
25, 729	S		CH_2CF_2
25, 741	M		CH_2CF_2
25, 745			CH_2Cl_2
25, 748			CH_2Cl_2
25, 748. 18	M	3-4, $v_1=1$	$IC^{12}N^{14}$
25, 751			CH_2Cl_2
25, 752. 65	S	3-4, $v=0$	$IC^{12}N^{14}$
25, 763. 23	M	3-4, $v_1=1$	$IC^{12}N^{14}$
25, 783. 50	S	3-4, $v=0$	$IC^{12}N^{14}$
25, 789. 85	S	3-4, $v=0$	$IC^{12}N^{14}$
25,797			CH_3OH
25, 802. 92	M	3-4, $v_2=1$	$IC^{12}N^{14}$
25, 815. 34	M	3-4, $v_2=1$	$IC^{12}N^{14}$
25, 823. 08	S	3-4, $v=0$	$IC^{12}N^{14}$
25, 829. 31	M	3-4, $v_2=1$	$IC^{12}N^{14}$
25, 837. 64	S	3-4, $v=0$	$IC^{12}N^{14}$
25, 848			CH_2Cl_2
25, 850. 78	M	3-4, $v_2=1$	$IC^{12}N^{14}$
25, 872. 24	S	3-4, $v_2=1$	$IC^{12}N^{14}$
25, 878. 18			CH_3OH
25, 893. 73	S	3-4, $v_2=1$	$IC^{12}N^{14}$
25, 906. 28	S	3-4, $v_2=1$	$IC^{12}N^{14}$
25, 927. 66	S	3-4, $v_2=1$	$IC^{12}N^{14}$
24, 954. 36	S	3-4, $v=0$	$IC^{12}N^{14}$
25, 969. 58	M	3-4, $v=0$	$IC^{12}N^{14}$
25, 991. 92	S	3-4, $v=0$	$IC^{12}N^{14}$
26, 007			CH_2Cl_2
26, 042. 41	W	1-2, $K=0$	SiH_2Cl^{37}
26, 043. 29	W	1-2, $K=1$	SiH_3Cl^{37}
26, 046. 30	W	1-2, $K=1$	SiH_3Cl^{37}
26, 046. 32	M	3-4, $v_2=2$	$IC^{12}N^{14}$
26, 047. 97	W	1-2, $K=1$	SiH_3Cl^{37}
26, 050. 26	M	1-2, $K=0$	SiH_2Cl^{37}
26, 051. 09	W	1-2, $K=1$	SiH_3Cl^{37}
26, 053. 35	W	1-2, $K=1$	SiH_3Cl^{37}
26, 055. 86	W	1-2, $K=0$	SiH_3Cl^{37}
26, 057. 10	W	1-2, $K=1$	SiH_3Cl^{37}
26, 063. 52	W	1-2, $K=0$	SiH_3Cl^{37}
26, 118	S		CH_2CF_2
26, 120			CH_3OH
26, 163	M		CH_2CF_2
26, 164. 57	M	0-1, $K=0$	CH_3Cl^{37}
26, 179. 30	M	0-1, $K=0$	CH_3Cl^{37}
26, 181. 6	M	3-4, $v=0$	ICl^{37}
26, 191. 13	M	0-1, $K=0$	CH_3Cl^{37}

TABLE 2. *Lines listed by frequency*—Continued

Frequency	Intensity	Transition	Molecule
26, 295			CH_2Cl_2
26, 310			CH_3OH
26, 328	S		CH_2CF_2
26, 337	M		CH_2CF_2
26, 410	W		CH_2CF_2
26, 466	M		CH_2CF_2
26, 518. 91	S		$N^{14}H_3$
26, 553			SPF_3
26, 562			CH_3OH
26, 565			$C^{12}D_4O^{16}$
26, 570. 77	M	0-1, $K=0$	CH_3Cl^{35}
26, 574			SPF_3
26, 589. 49	M	0-1, $K=0$	CH_3Cl^{35}
26, 604. 57	M	0-1, $K=0$	CH_3Cl^{35}
26, 634	S		CH_2CF_2
26, 649	M		CH_2CF_2
26, 655. 00	S		$N^{14}H_3$
26, 685. 25	W	1-2, $K=0$	SiH_3Cl^{35}
26, 686. 15	W	1-2, $K=0$	SiH_3Cl^{35}
26, 687. 34	W	1-2, $K=1$	SiH_3Cl^{35}
26, 690. 92	W	1-2, $K=1$	SiH_3Cl^{35}
26, 692. 66	W	1-2, $K=1$	SiH_3Cl^{35}
26, 695. 00	W	1-2, $K=0$	SiH_3Cl^{35}
26, 696. 10	M	1-2, $K=0$	SiH_3Cl^{35}
26, 697. 45	M	1-2, $K=1$	SiH_3Cl^{35}
26, 700. 48	W	1-2, $K=1$	SiH_3Cl^{35}
26, 703. 34	W	1-2, $K=0$	SiH_3Cl^{35}
26, 705. 02	W	1-2, $K=1$	SiH_3Cl^{35}
26, 713. 07	W	1-2, $K=0$	SiH_2Cl^{35}
26, 723	W		CH_2CF_2
26, 832	M		CH_2CF_2
26, 865	S		CH_2CF_2
26, 880	M		CH_2CF_2
26, 992	S		CH_2CF_2
27, 014	S		CH_2CF_2
27, 112	M		CH_2CF_2
27, 194. 75	M	3-4, $v=0$	ICl^{35}
27, 202. 64	W	3-4, $v=0$	ICl^{35}
27, 204. 99	M	3-4, $v=0$	ICl^{35}
27, 208. 54	M	3-4, $v=1$	ICl^{35}
27, 216	M		CH_2CF_2
27, 217. 51	M	3-4, $v=0$	ICl^{35}
27, 221. 02	M	3-4, $v=0$	ICl^{35}
27, 225. 32	M	3-4, $v=0$	ICl^{35}
27, 228. 34	M	3-4, $v=0$	ICl^{35}
27, 242. 59	W	3-4, $v=0$	ICl^{35}
27, 254. 90	M	3-4, $v=0$	ICl^{35}
27, 283. 66		3-4, $v=0$	ICl^{35}

TABLE 2. *Lines listed by frequency*—Continued

Frequency	Intensity	Transition	Molecule
27, 286. 25		3-4, $v=0$	IC^{35}
27, 292. 63		3-4, $v=0$	IC^{35}
27, 295. 05		3-4, $v=0$	IC^{35}
27, 297	S		CH_2CF_2
27, 333. 85	M	3-4, $v=0$	IC^{35}
27, 336. 68	M	3-4, $v=0$	IC^{35}
27, 337. 38	M	3-4, $v=0$	IC^{35}
27, 346. 31	M	3-4, $v=0$	IC^{35}
27, 354. 71	M	3-4, $v=0$	IC^{35}
27, 356. 58	M	3-4, $v=0$	IC^{35}
27, 357. 73	M	3-4, $v=0$	IC^{35}
27, 412	M		CH_2CF_2
27, 478	S		$N^{14}H_3$
27, 681	S		CH_2CF_2
27, 772. 52	M		$N^{14}H_3$
27, 818	S		CH_2CF_2
27, 972	S		CH_2CF_2
28, 069. 99	W	1-2, $K=0$	$C^{13}H_3I$
28, 145. 01	W	1-2, $K=0$	$C^{13}H_3I$
28, 174	S		CH_2CF_2
28, 206. 90	W	1-2, $K=1$	$C^{13}H_3I$
28, 253. 84	W	1-2, $K=1$	$C^{13}H_3I$
28, 314	W		CH_2CF_2
28, 339	M		CH_2CF_2
28, 343. 64	W	1-2, $K=0$	$C^{13}H_3I$
28, 380		4-5	$C^{12}H_3S^{32}C^{12}N^{14}$
28, 411. 19	W	1-2, $K=1$	$C^{13}H_3I$
28, 412	S		CH_2CF_2
28, 439	M		CH_2CF_2
28, 458	M		CH_2CF_2
28, 495			$C^{12}D_4O^{16}$
28, 518. 14	W	1-2, $K=0$	$C^{13}H_3I$
28, 550. 86	W	1-2, $K=0$	$C^{13}H_3I$
28, 551	W		CH_2CF_2
28, 575	W		CH_2CF_2
28, 594. 74	W	1-2, $K=1$	$C^{13}H_3I$
28, 604. 73	S		$N^{14}H_3$
28, 615	W		CH_2CF_2
28, 650. 91	W	1-2, $K=0$	$C^{13}H_3I$
28, 687. 21	W	1-2, $K=1$	$C^{13}H_3I$
28, 689	W		CH_2CF_2
28, 852			CH_2CF_2
28, 858			CH_2CF_2
28, 954	S		CH_2CF_2
28, 974. 85			H_2CO

TABLE 2. *Lines listed by frequency*—Continued

Frequency	Intensity	Transition	Molecule
29, 061. 14	M		$N^{14}H_3$
29, 080			$C^{12}D_4O^{16}$
29, 460			SO_2
29, 598. 95	M	1-2, $K=0$	$C^{13}H_3I$
29, 673. 95	M	1-2, $K=0$	$C^{13}H_3I$
29, 688	S		$C_2^{12}H_4O^{16}$
29, 700		5-6	$C^{12}H_3N^{14}C^{12}S^{32}$
29, 735. 71	M	1-2, $K=1$	$C^{13}H_3I$
29, 773. 95	W	1-2, $K=0$	$C^{13}H_3I$
29, 782. 71	M	1-2, $K=1$	$C^{13}H_3I$
29, 872. 52	M	1-2, $K=0$	$C^{13}H_3I$
29, 914. 66	S		$N^{14}H_3$
29, 923. 50	M	1-2, $K=1$	$C^{13}H_3I$
29, 939. 87	M	1-2, $K=1$	$C^{13}H_3I$
29, 986. 84	W	1-2, $K=1$	$C^{13}H_3I$
30, 046. 99	M	1-2, $K=0$	$C^{13}H_3I$
30, 075. 08	M	1-2, $K=1$	$C^{13}H_3I$
30, 079. 72	M	1-2, $K=0$	$C^{13}H_3I$
30, 121. 32	M	1-2, $K=0$	$C^{13}H_3I$
30, 123. 64	M	1-2, $K=1$	$C^{13}H_3I$
30, 179. 71	M	1-2, $K=0$	$C^{13}H_3I$
30, 215. 95	M	1-2, $K=1$	$C^{13}H_3I$
30, 453. 46	M	1-2, $K=0$	$C^{13}H_3I$
31, 020. 7		2-3	CF_3CH_3
31, 066. 8		2-3	CF_3CH_3
31, 114. 4		2-3	CF_3CH_3
31, 279. 60	M	1-2	PF_3
31, 424. 97	S		$N^{14}H_3$
31, 718. 28	M	4-5, $v=0$	$IC^{13}N^{14}$
31, 730. 50	M	4-5, $v=0$	$IC^{13}N^{14}$
31, 741. 50	W	4-5, $v=0$	$IC^{13}N^{14}$
31, 763. 34	M	4-5, $v=0$	$IC^{13}N^{14}$
31, 783. 31	M	4-5, $v=0$	$IC^{13}N^{14}$
31, 793. 46	M	4-5, $v=0$	$IC^{13}N^{14}$
31, 848. 77	M	4-5, $v=0$	$IC^{13}N^{14}$
31, 943			$C^{12}D_4O^{16}$
32, 200. 58	S	4-5, $v=0$	$IC^{12}N^{14}$
32, 203. 57	S	4-5, $v=0$	$IC^{12}N^{14}$
32, 215. 56	S	4-5, $v=0$	$IC^{12}N^{14}$
32, 226. 85	S	4-5, $v=0$	$IC^{12}N^{14}$
32, 248. 52	S	4-5, $v=0$	$IC^{12}N^{14}$
32, 268. 33	S	4-5, $v=0$	$IC^{12}N^{14}$
32, 278. 55	S	4-5, $v=0$	$IC^{12}N^{14}$
32, 386. 29	S	4-5, $v=0$	$IC^{12}N^{14}$
32, 392. 59	M	3-4, $v=0$	$Br^{81}C^{12}N^{14}$
32, 409. 06	M	3-4, $v=0$	$Br^{81}C^{13}N^{14}$
32, 581. 73	M	3-4, $v=0$	$Br^{79}C^{12}N^{14}$

TABLE 2. *Lines listed by frequency*—Continued

Frequency	Intensity	Transition	Molecule
32, 601. 46	M	3-4, $v=0$	$Br^{79}C^{12}N^{14}$
32, 643. 13	M	3-4, $v=0$	$Br^{81}C^{12}N^{14}$
32, 720. 28	M	3-4, $v=0$	$Br^{81}C^{12}N^{14}$
32, 770. 13	S	3-4, $v=0$	$Br^{81}C^{12}N^{14}$
32, 786. 65	M	3-4, $v=0$	$Br^{81}C^{12}N^{14}$
32, 804. 56	M	3-4, $v=0$	$Br^{79}C^{12}N^{14}$
32, 913. 24	M	3-4, $v=0$	$Br^{81}C^{12}N^{14}$
32, 956. 68	M	3-4, $v=0$	$Br^{79}C^{12}N^{14}$
32, 976. 40	S	3-4, $v=0$	$Br^{79}C^{12}N^{14}$
33, 156. 95	S	----------	$N^{14}H_3$
33, 285	-------	----------	$C^{12}D_4O^{16}$
34, 150	-------	----------	$C^{12}H_4O^{16}$
34, 158	-------	----------	$C^{12}H_4O^{16}$
34, 627. 24	M	1-2, $K=1$	$B^{11}H_3C^{12}O^{16}$
34, 627. 50	M	1-2, $K=1$	$B^{11}H_3C^{12}O^{16}$
34, 627. 73	M	1-2, $K=1$	$B^{11}H_3C^{12}O^{16}$
34, 627. 89	M	1-2, $K=1$	$B^{11}H_3C^{12}O^{16}$
34, 628. 62	M	1-2, $K=0$	$B^{11}H_3C^{12}O^{16}$
34, 628. 90	S	1-2, $K=0$	$B^{11}H_3C^{12}O^{16}$
34, 629. 32	M	1-2, $K=0$	$B^{11}H_3C^{12}O^{16}$
34, 889. 05	W	2-3, $v=0$	$Cl^{37}C^{12}N^{14}$
35, 067. 99	M	2-3, $v=0$	$Cl^{37}C^{12}N^{14}$
35, 068	-------	----------	$C^{12}D_4O^{16}$
35, 080. 39	S	2-3, $v=0$	$Cl^{37}C^{12}N^{14}$
35, 084. 15	S	2-3, $v=0$	$Cl^{37}C^{12}N^{14}$
35, 091. 97	M	2-3, $v=0$	$Cl^{37}C^{12}N^{14}$
35, 134. 44	M	2-3, $v=0$	$N^{14}H_3$
35, 341	-------	----------	$C^{12}D_4O^{16}$
35, 618. 81	W	2-3, $v=0$	$Cl^{35}C^{12}N^{14}$
35, 634. 85	M	2-3, $v=0$	$Cl^{35}C^{12}N^{14}$
35, 639. 78	M	2-3, $v=0$	$Cl^{35}C^{12}N^{14}$
35, 649. 56	W	2-3, $v=0$	$Cl^{35}C^{12}N^{14}$
35, 805. 09	S	2-3, $v=0$	$Cl^{35}C^{12}N^{14}$
35, 820. 65	S	2-3, $v=0$	$Cl^{35}C^{12}N^{14}$
35, 825. 95	S	2-3, $v=0$	$Cl^{35}C^{12}N^{14}$
35, 835. 74	S	2-3, $v=0$	$Cl^{35}C^{12}N^{14}$
35, 917. 62	M	1-2, $K=1$	$B^{10}H_3C^{12}O^{16}$
35, 917. 88	M	1-2, $K=1$	$B^{10}H_3C^{12}O^{16}$
35, 918. 20	W	1-2, $K=1$	$B^{10}H_3C^{12}O^{16}$
35, 918. 50	M	1-2, $K=1$	$B^{10}H_3C^{12}O^{16}$
35, 919. 02	W	1-2, $K=0$	$B^{10}H_3C^{12}O^{16}$
35, 919. 53	M	1-2, $K=0$	$B^{10}H_3C^{12}O^{16}$
35, 919. 86	M	1-2, $K=0$	$B^{10}H_3C^{12}O^{16}$
35, 920. 14	M	1-2, $K=0$	$B^{10}H_3C^{12}O^{16}$

TABLE 2. *Lines listed by frequency*—Continued

Frequency	Intensity	Transition	Molecule
36, 488. 82	S	2-3, $v=0$	$O^{16}C^{12}S^{32}$
36, 632	M	----------	CH_2CF_2
36, 791	S	----------	$C_2^{12}H_4O^{16}$
36, 793. 64	-------	0-1	$C^{12}H_3C^{12}N^{14}$
36, 794. 26	-------	0-1	$C^{12}H_3C^{12}N^{14}$
36, 794. 88	-------	0-1	$C^{12}H_3C^{12}N^{14}$
36, 795. 38	-------	0-1	$C^{12}H_3C^{12}N^{14}$
36, 796. 27	-------	0-1	$C^{12}H_3C^{12}N^{14}$
36, 797. 52	-------	0-1	$C^{12}H_3C^{12}N^{14}$
36, 870. 94	-------	0-1	$C^{12}H_3C^{12}N^{14}$
36, 903. 40	-------	0-1	$C^{12}H_3C^{12}N^{14}$
36, 942. 15	-------	0-1	$C^{12}H_3C^{12}N^{14}$
37, 329	S	----------	$C_2^{12}H_4O^{16}$
37, 385. 18	M	----------	$N^{14}H_3$
37, 781	S	----------	$C_2^{12}H_4O^{16}$
38, 006. 47	W	1-2, $K=1$	CH_3Br^{81}
38, 030. 77	M	1-2, $K=0$	CH_3Br^{81}
38, 066. 72	W	1-2, $K=1$	CH_3Br^{81}
38, 097. 45	M	1-2, $K=1$	CH_3Br^{81}
38, 116. 65	M	1-2, $K=0$	CH_3Br^{81}
38, 126. 97	M	1-2, $K=0$	CH_3Br^{81}
38, 128. 40	W	1-2, $K=1$	$C^{12}H_3Br^{79}$
38, 157. 30	M	1-2, $K=0$	$C^{12}H_3Br^{79}$
38, 157. 70	W	1-2, $K=1$	$C^{12}H_3Br^{81}$
38, 175. 08	M	1-2, $K=1$	$C^{12}H_3Br^{81}$
38, 200. 52	W	1-2, $K=1$	$C^{12}H_3Br^{79}$
38, 218. 21	M	1-2, $K=1$	$C^{12}H_3Br^{81}$
38, 237. 14	M	1-2, $K=1$	$C^{12}H_3Br^{79}$
38, 247. 77	M	1-2, $K=0$	$C^{12}H_3Br^{81}$
38, 260. 10	M	1-2, $K=0$	$C^{12}H_3Br^{79}$
38, 272. 40	M	1-2, $K=0$	$C^{12}H_3Br^{79}$
38, 309. 45	W	1-2, $K=1$	$C^{12}H_3Br^{79}$
38, 330. 25	M	1-2, $K=1$	$C^{12}H_3Br^{79}$
38, 381. 70	M	1-2, $K=1$	$C^{12}H_3Br^{79}$
38, 404. 49	M	1-2, $K=0$	$C^{12}H_3Br^{79}$
38, 417. 09	M	1-2, $K=0$	$C^{12}H_3Br^{79}$
38, 702	S	----------	$C_2^{12}H_4O^{16}$
38, 782. 21	-------	1-2, $K=1$	$C^{12}H_3N^{14}C^{13}$
38, 783. 21	-------	1-2, $K=0$	$C^{12}H_3N^{14}C^{13}$
39, 582	M	----------	$C_2^{12}H_4O^{16}$
39, 592	-------	----------	$C^{12}D_4O^{16}$
39, 677	S	----------	$C_2^{12}H_4O^{16}$
39, 941. 54	M	----------	$N^{14}H_3$
40, 210. 27	-------	1-2, $K=1$	$C^{12}H_3N^{14}C^{13}$

TABLE 2. *Lines listed by frequency*—Continued

Frequency	Intensity	Transition	Molecule
40, 211. 16	.....	1-2, $K=0$	$C^{12}H_2N^{14}C^{12}$
40, 313. 37	.....	1-2, $K=0$	$C^{12}H_2N^{14}C^{12}$
40, 364. 07	.....	.....	$C^{12}H_2N^{14}C^{12}$
40, 366. 55	.....	.....	$C^{12}H_2N^{14}C^{12}$
40, 424. 49	.....	.....	$C^{12}H_2N^{14}C^{13}$
41, 394. 95	S	1-2	$HC^{12}F_3$
41, 581	.....	.....	$C_2{}^{13}H_4O^{16}$
43, 398	.....	.....	$C^{12}H_4O^{16}$
45, 324. 24	.....	0-1	CH_3NH_2
46, 918. 82	M	2-3, $K=0, 1$	PF_3
46, 919. 02	M	2-3, $K=2$	PF_3
46, 940	.....	.....	PF_3
47, 010	.....	.....	PF_3
47, 033	.....	.....	PF_3
47, 040	.....	.....	PF_3
45, 324. 94	.....	0-1	CH_3NH_2
47, 052	.....	.....	$C^{12}H_3OD$
47, 266	.....	.....	$C^{12}H_3OD$
47, 346	.....	.....	$C^{12}H_3OD$
47, 462. 40	S	3-4, $v=0$	$O^{16}C^{12}S^{34}$
47, 840	.....	.....	CH_3OH
48, 010	.....	.....	CH_3OH
48, 211. 46	S	5-6	$O^{16}C^{12}Se^{80}$
48, 284. 60	.....	.....	H_2CO
48, 357	.....	.....	CH_3OH
48, 363	.....	.....	CH_3OH
48, 396	.....	.....	CH_3OH
48, 404	.....	.....	CH_3OH
48, 508. 88	S	5-6	$O^{16}C^{12}Se^{78}$
48, 700	.....	.....	CH_3OH

TABLE 2. *Lines listed by frequency*—Continued

Frequency	Intensity	Transition	Molecule
49, 724. 73	M	0-1, $K=0$	$C^{13}H_3F$
50, 236. 90	W	.....	HDO^{16}
51, 071. 69	S	.....	$C^{12}H_3F$
51. 260	.....	2-3	$C^{12}H_3C^{12}C^{12}H$
51, 264	.....	2-3	$C^{12}H_3C^{12}C^{12}H$
51, 266	.....	2-3	$C^{12}H_3C^{12}C^{12}H$
51, 296	.....	2-3	$C^{12}H_3C^{12}C^{12}H$
51, 313	.....	2-3	$C^{12}H_3C^{12}C^{12}H$
51, 314	.....	2-3	$C^{12}H_3C^{12}C^{12}H$
51, 318	.....	2-3	$C^{12}H_3C^{12}C^{12}H$
51, 319	.....	2-3	$C^{12}H_3C^{12}C^{12}H$
51, 334	.....	2-3	$C^{12}H_3C^{12}C^{12}H$
51, 363	.....	2-3	$C^{12}H_3C^{12}C^{12}H$
51, 410	.....	2-3	$C^{12}H_3C^{12}C^{12}H$
51, 416	.....	2-3	$C^{12}H_3C^{12}C^{12}H$
51, 418	.....	2-3	$C^{12}H_3C^{12}C^{12}H$
51, 419	.....	2-3	$C^{12}H_3C^{12}C^{12}H$
51, 464	.....	2-3	$C^{12}H_2C^{13}C^{12}H$
55, 916. 19	S	6-7	$O^{16}C^{12}Se^{82}$
56, 246. 47	S	6-7	$O^{16}C^{12}Se^{80}$
56, 593. 16	S	6-7	$O^{16}C^{12}Se^{78}$
60, 814. 08	S	4-5, $v=0$	$O_{16}C^{12}S^{32}$
72, 409. 35	.....	.....	H_2CO
72, 838. 14	.....	.....	H_2CO
73, 742	S	8-9, $v=0$	$Br^{81}C^{12}N^{14}$
74, 165	S	8-9, $v=0$	$Br^{79}C^{12}N^{14}$
77, 413	S	11-12, $v=0$	$IC^{12}N^{14}$
81, 936	S	9-10, $v=0$	$Br^{81}C^{12}N^{14}$
82, 405	S	9-10, $v=0$	$Br^{79}C^{12}N^{14}$
83, 864	S	12-13, $v=0$	$IC^{12}N^{14}$
88, 671	S	0-1	$HC^{12}N^{14}$

TABLE 3. *Values of* $[\frac{3}{4}C(C+1)-I(I+1)J(J+1)]/2I(2I-1)(2J-1)(2J+3)$, *where* $C=F(F+1)-I(I+1)-J(J+1)$

J	F \ I	1	3/2	2	5/2	3	7/2	4	9/2
1	11/2								0.050000
	5							0.050000	
	9/2						0.050000		−0.133333
	4					0.050000		−0.137500	
	7/2				0.050000		−0.142857		0.091667
	3			0.050000		−0.150000		0.098214	
	5/2		0.050000		−0.160000		0.107143		
	2	0.050000		−0.175000		0.120000			
	3/2		−0.200000		0.140000				
	1	−0.250000		0.175000					
	1/2		0.250000						
	0	0.500000							
2	13/2								0.071429
	6							0.071429	
	11/2						0.071429		−0.083333
	5					0.071429		−0.089286	
	9/2				0.071429		−0.096939		−0.083333
	4			0.071429		−0.107142		−0.082908	
	7/2		0.071429		−0.121428		−0.081633		0.005952
	3	0.071429		−0.142857		−0.078571		0.014031	
	5/2		−0.178571		−0.071429		0.025510		0.130952
	2	−0.250000		−0.053571		0.042857		0.140306	
	3/2		0		0.071429		0.153061		
	1	0.250000		0.125000		0.171429			
	1/2		0.250000		0.200000				
	0			0.250000					
3	15/2								0.083333
	7							0.083333	
	13/2						0.083333		−0.055556
	6					0.083333		−0.062500	
	11/2				0.083333		−0.071429		−0.091667
	5			0.083333		−0.083333		−0.094643	
	9/2		0.083333		−0.100000		−0.097619		−0.061111
	4	0.083333		−0.125000		−0.100000		−0.055952	
	7/2		−0.166667		−0.100000		−0.047619		0.005556
	3	−0.250000		−0.091667		−0.033333		0.017857	
	5/2		−0.050000		−0.006667		0.035714		0.083333
	2	0.200000		0.050000		0.063333		0.098214	
	3/2		0.200000		0.110000		0.119048		0.152777
	1			0.200000		0.150000		0.163690	
	1/2				0.200000		0.178571		
	0					0.200000			

883124—50——6

TABLE 3. *Values of* $[\frac{3}{4}C(C+1)-I(I+1)J(J+1)]/2I(2I-1)(2J-1)(2J+3)$, *where* $C=F(F+1)-I(I+1)-J(J+1)-$ Continued

	I	1	3/2	2	5/2	3	7/2	4	9/2
J	F								
4	17/2								0.090909
	8							0.090909	
	15/2						0.090909		−0.037879
	7					0.090909		−0.045455	
	13/2				0.090909		−0.055195		−0.086580
	6			0.090909		−0.068182		−0.091721	
	11/2		0.090909		−0.086364		−0.097403		−0.079545
	5	0.090909		−0.113636		−0.103246		−0.077110	
	9/2		−0.159091		−0.107792		−0.071892		−0.037879
	4	−0.250000		−0.105519		−0.061039		−0.026670	
	7/2		−0.071429		−0.037662		−0.009276		0.020563
	3	0.178571		0.017857		0.019481		0.038729	
	5/2		0.178571		0.071429		0.065399		0.081169
	2			0.178571		0.107143		0.102389	
	3/2				0.178571		0.132653		0.132576
	1					0.178571		0.151786	
	1/2						0.178571		0.166667
	0							0.178571	
5	19/2								0.096154
	9							0.096154	
	17/2						0.096154		−0.025641
	8					0.096154		−0.033654	
	15/2				0.096154		−0.043956		−0.080128
	7			0.096154		−0.057692		−0.086767	
	13/2		0.096154		−0.076923		−0.094322		−0.085470
	6	0.096154		−0.105769		−0.102564		−0.085165	
	11/2		−0.153846		−0.110256		−0.082418		−0.057692
	5	−0.250000		−0.112179		−0.074571		−0.048077	
	9/2		−0.083333		−0.053846		−0.032051		−0.010684
	4	0.166667		0		−0.003846		0.008013	
	7/2		0.166667		0.050000		0.036630		0.043803
	3			0.166667		0.083333		0.069368	
	5/2				0.166667		0.107143		0.096154
	2					0.166667		0.125000	
	3/2						0.166667		0.138889
	1							0.166667	
	1/2								0.166667
6	21/2								0.100000
	10							0.100000	
	19/2						0.100000		−.016667
	9					0.100000		−.025000	
	17/2				0.100000		−.035174		−.074242
	8			0.100000		−.050000		−.081981	
	15/2		0.100000		−.070000		−.090909		−.087121
	7	0.100000		−.100000		−.100909		−.088474	
	13/2		−.150000		−.110909		−.087662		−.068182
	6	−.250000		−.115909		−.081818		−.060065	
	11/2		−.090909		−.063636		−.045455		−.028788
	5	.159091		−.011364		−.018182		−.001039	
	9/2		.159091		.036364		.018831		.021212
	4			.159091		.068182		.048864	
	7/2				.159091		.090909		.073485
	3					.159091		.107955	
	5/2						.159091		.121212
	2							.159091	
	3/2								.159091

TABLE 3. *Values of* $[\frac{3}{4}C(C+1)-I(I+1)J(J+1)]/2I(2I-1)(2J-1)(2J+3)$, *where* $C=F(F+1)-I(I+1)-J(J+1)$—Continued

	I	1	3/2	2	5/2	3	7/2	4	9/2
J	F								
	23/2								.102941
	11							.102941	
	21/2						.102941		−.009804
	10					.102941		−.018382	
	19/2				.102941		−.029412		−.069193
	9			.102941		−.044118		−.077771	
	17/2		.102941		−.064746		−.087750		−.087104
	8	.102941		−.095588		−.099095		−.090417	
7	15/2		−.147059		−.110859		−.090498		−.074284
	7	−.250000		−.118212		−.086425		−.067469	
	13/2		−.096154		−.070136		−.054137		−.040347
	6	.153846		−.019231		−.027828		−.022503	
	11/2		.153846		.026923		.006787		.006222
	5			.153846		.057692		.034947	
	9/2				.153846		.079670		.058069
	4					.153846		.096154	
	7/2						.153846		.108974
	3							.153846	
	5/2								.153846
	25/2								0.015263
	12							0.105263	
	23/2						0.105263		−.004386
	11					0.105263		−.013158	
	21/2				0.105263		−.024436		−.064912
	10			0.105263		−.039474		−.074154	
	19/2		0.105263		−.060526		−.084962		−.086404
	9	0.105263		−.092105		−.097368		−.090132	
8	17/2		−.144737		−.110526		−.092105		−.078070
	8	−.250000		−.119737		−.089474		−.072368	
	15/2		−.100000		−.074737		−.060150		−.048246
	7	.150000		−.025000		−.034737		−.031015	
	13/2		.150000		.020000		−.001880		−.004386
	6			.150000		.050000		.024906	
	11/2				.150000		.071429		.046930
	5					.150000		.087500	
	9/2						.150000		.100000
	4							.150000	
	7/2								.150000
	27/2								.107143
	13							.107143	
	25/2						.107143		0
	12					.107143		−.008929	
	23/2				.107143		−.020408		−.061275
	11			.107143		−.035714		−.071053	
	21/2		.107143		−.057143		−.082533		−.085434
	10	.107143		−.089286		−.095798		−.090036	
	19/2		−.142857		−.110084		−.093037		−.080532
9	9	−.250000		−.120798		−.091597		−.075780	
	17/2		−.102941		−.078151		−.064526		−.053922
	8	.147059		−.029412		−.039916		−.037290	
	15/2		.147059		.014706		−.008403		−.012255
	7			.147059		.044118		.017332	
	13/2				.147059		.065126		.038515
	6					.147059		.080882	
	11/2						147059		.093137
	5							.147059	
	9/2								.147059

TABLE 3. *Values of* $[\frac{3}{4}C(C+1)-I(I+1)J(J+1)]/2I(2I-1)(2J-1)(2J+3)$, *where* $C=F(F+1)-I(I+1)-J(J+1)$—Continued

	I	1	3/2	2	5/2	3	7/2	4	9/2
J	F								
	29/2								0. 108696
	14							0. 108696	
	27/2						0. 018696		−. 003623
	13					0. 108696		−. 005435	
	25/2				0. 108696		−. 017081		−. 058162
	12			0. 108696		−. 032609		−. 068384	
	23/2		0. 108696		−. 054348		−. 080418		−. 084382
	11	0. 108696		−. 086957		−. 094394		−. 089715	
	21/2		−. 141304		−. 109610		−. 093576		−. 082189
	10	−. 250000		−. 121568		−. 093135		−. 078253	
10	19/2		−. 105263		−. 080778		−. 067833		−. 058162
	9	. 144737		−. 032895		−. 043936		−. 042089	
	17/2		. 144737		. 010526		−. 013485		−. 018307
	8			. 144737		. 039474		. 001142	
	15/2				. 144737		. 060150		. 031941
	7					. 144737		. 075658	
	13/2						. 144737		. 087719
	6							. 144737	
	11/2								. 144737

References

[1] C. I. Beard and B. P. Dailey, J. Chem. Phys. **15,** 762 (1947).

[1a] C. I. Beard and B. P. Dailey, MITRLE Tech. Report #79 (1948).

[2] G. E. Becker and S. H. Autler, Phys. Rev. **70,** 300 (1946).

[3] R. Beringer, Phys. Rev. **70,** 53 (1946).

[4] B. Bleaney and R. P. Penrose, Proc. Roy. Soc. **A189,** 358 (1947).

[4a] B. Bleaney and R. P. Penrose, Proc. Phys. Soc. (London) **60,** 540 (1947).

[4b] B. Bleaney and J. H. N. Loubser, Nature **161,** 522 (1948).

[4c] A. C. Candler, Atomic spectra and the vector model (Cambridge Univ. Press, Cambridge, Mass., 1937).

[5] H. B. G. Casimir, On the interaction between atomic nuclei and electrons (DeErven F. Bohn, Haarlem, 1936).

[6] D. K. Coles, Phys. Rev. **74,** 1194 (1948).

[7] D. K. Coles, E. S. Elyash, and J. G. Gorman, Phys. Rev. **72,** 973 (1947).

[7a] D. K. Coles and W. E. Good, Phys. Rev. **70,** 979 (1946).

[7b] D. K. Coles and R. H. Hughes, private communication.

[8] E. U. Condon and G. H. Shortley, The theory of atomic spectra (Macmillan and Co., New York, N. Y., 1935).

[9] P. C. Cross, R. M. Hainer, and G. W. King, J. Chem. Phys. **12,** 210 (1944).

[10] G. L. Cunningham, W. I. LeVan, and W. D. Gwinn, Phys. Rev. **74,** 1537 (1948).

[10a] G. L. Cunningham, A. W. Boyd, W. D. Gwinn, and W. I. LeVan, private communication.

[11] B. P. Dailey, private communication.

[12] B. P. Dailey, S. Golden, and E. B. Wilson, Jr., Phys. Rev. **72,** 871 (1947).

[12a] B. P. Dailey, R. L. Kyhl, M. W. P. Strandberg, J. H. VanVleck, and E. B. Wilson, Jr., Phys. Rev. **70,** 984 (1946).

[13] B. P. Dailey, K. Rusinow, R. G. Shulman, and C. H. Townes, Phys. Rev. **74,** 1245 (1948); also private communication.

[14] B. P. Dailey and E. B. Wilson, Jr., Phys. Rev. **72,** 84 (1947).

[15] B. P. Dailey and E. B. Wilson, Jr., Phys. Rev. **72,** 522 (1947).

[16] T. W. Dakin, W. E. Good, and D. K. Coles, Phys. Rev. **71,** 640 (1947).

[17] W. F. Edgell and A. Roberts, J. Chem. Phys. **16,** 1002 (1948).

[18] H. D. Edwards, O. R. Gilliam, and W. Gordy, to be published.

[19] O. R. Gilliam, H. D. Edwards, and W. Gordy, Phys. Rev. **75,** 1014 (1949)

[20] S. Golden, T. Wentink, Jr., R. E. Hillger, and M. W. P. Strandberg, Phys. Rev. **73,** 92 (1948).

[20a] J. H. Goldstein and J. K. Bragg, Phys. Rev. **75,** 1453 (1949).

[21] W. E. Good and D. K. Coles, Phys, Rev. **71,** 383 (1947).

[22] W. Gordy, H. Ring, and A. B. Burg, Phys. Rev. **74,** 1191 (1948).

[23] W. Gordy, J. W. Simmons, and A. G. Smith, Phys. Rev. **74,** 243 (1948).

[23a] W. D. Gwinn, private communication.

[24] R. M. Hainer, G. W. King, and P. C. Cross, Phys. Rev. **70,** 108 (1948).

[24a] R. S. Henderson, Phys. Rev. **74,** 107 and **74,** 626 (1948).

[25] W. D. Hershberger and J. Turkevitch, Phys. Rev. **71,** 554 (1947); and private communication.
[26] G. Herzberg, Molecular spectra and molecular structure; II infrared and Raman spectra of polyatomic molecules (D. VanNostrand & Co., New York, N. Y., 1945).
[27] R. E. Hillger, M. W. P. Strandberg, T. Wentink, Jr., and R. L. Kyhl, Phys. Rev. **72,** 157 (1947).
[27a] J. M. Jauch, Phys. Rev. **72,** 715 (1947).
[27b] R. Karplus and A. H. Sharbaugh, Phys. Rev. **75,** 889 (1949).
[28] M. Kessler, H. Ring, and W. Gordy, quoted by H. H. Nielsen. Phys. Rev. **75,** 1961 (1949) and private communication.
[29] G. W. King, R. M. Hainer, and P. C. Cross, J. Chem. Phys. **11,** 27 (1943).
[30] J. Klein, W. Low, and C. H. Townes, private communication.
[31] H. R. L. Lamont, Phys. Rev. **74,** 353 (1948).
[32] W. Low and C. H. Townes, Phys. Rev. **75,** 529 (1949).
[33] C. H. Millar, thesis, McGill University (1947).
[33a] M. Mizoshima, Phys. Rev. **74,** 705 (1948).
[34] H. H. Nielsen and D. M. Dennison, Phys. Rev. **72,** 1101 (1947).
[35] H. Ring, H. D. Edwards, W. Gordy, and O. R. Gilliam, to be published.
[36] H. Ring, H. D. Edwards, M. Kessler, and W. Gordy, Phys. Rev. **72,** 1262 (1947).
[37] A. Roberts, Phys. Rev. **73,** 1405 (1948).
[37a] A. Roberts and W. F. Edgell, J. Chem. Phys. **17,** 742 (1949).
[37b] A. Roberts, private communication.
[38] A. H. Sharbaugh, Phys. Rev. **74,** 1870 (1948); and private communication.
[38a] A. H. Sharbaugh and J. Mattern, Phys. Rev. **75,** 1102 (1949).
[39] R. G. Shulman, B. P. Dailey, and C. H. Townes, Phys. Rev. **74,** 846 (1948).
[39a] R. G. Shulman and H. Minden, private communication.
[39b] R. G. Shulman and C. H. Townes, private communication.
[39c] R. G. Shulman, private communication.
[40] J. W. Simmons and W. Gordy, Phys. Rev. **73,** 713 (1947).
[41] A. G. Smith, W. Gordy, J. W. Simmons, and W. V. Smith, Phys. Rev. **75,** 260 (1949).
[42] A. G. Smith, H. Ring, W. V. Smith, and W. Gordy, Phys. Rev. **74,** 370 (1948).
[43] A. G. Smith, H. Ring, W. V. Smith, and W. Gordy, Phys. Rev. **73,** 635 (1948).
[44] M. W. P. Strandberg, paper delivered at Washington meeting of the American Physical Society (1948).
[45] M. W. P. Strandberg, R. L. Kyhl, R. E. Hillger, and T. Wentink, Jr., Phys. Rev. **71,** 326 (1947).
[46] M. W. P. Strandberg, R. L. Kyhl, R. E. Hillger, and T. Wentink, Jr., Phys. Rev. **71,** 639 (1947).
[47] M. W. P. Strandberg, T. Wentink, Jr., and A. G. Hill, Phys. Rev. **75,** 827 (1949).
[48] M. W. P. Strandberg, T. Wentink, Jr., R. E. Hillger, G. H. Wannier, and M. L. Deutsch, Phys. Rev. **73,** 188 (1948).
[48a] M. W. P. Strandberg, C. Y. Meng, and J. G. Ingersoll, Phys. Rev. **75,** 1524 (1949).
[49] M. W. P. Strandberg, T. Wentink, Jr., and R. L. Kyhl, MITRLE Rept. 59 (1948).
[49a] M. W. P. Strandberg, private communication.
[49b] M. W. P. Strandberg, MITRLE Report #85 (1948).
[49c] M. W. P. Strandberg, et al., MITRLE Quarterly Progress Report (Oct. 15, 1948).
[49d] M. W. P. Strandberg, C. S. Pearsall, and M. T. Weiss, J. Chem. Phys. **17,** 429 (1949).
[50] C. H. Townes, Phys. Rev. **70,** 665 (1946).
[51] C. H. Townes and J. Bardeen, Phys. Rev. **73,** 97 (1948).
[52] C. H. Townes and S. Geschwind, Phys. Rev. **74,** 626 (1948).
[53] C. H. Townes, A. N. Holden, and F. R. Merritt, Phys. Rev. **74,** 1113 (1948).
[54] C. H. Townes, A. N. Holden, and F. R. Merritt, Phys. Rev. **73,** 1334 (1948).
[55] C. H. Townes and F. R. Merritt, Phys. Rev. **70,** 558 (1946).
[57] T. E. Turner, thesis, McGill University (1948).
[58] J. H. Van Vleck and V. Weisskopf, Rev. Mod. Phys. **17,** 227 (1945).
[58a] J. H. Van Vleck, Phys. Rev. **71,** 468 (1947).
[58b] J. H. Van Vleck, Phys. Rev. **71,** 413 (1947).
[59] R. T. Weidner, Phys. Rev. **73,** 254 and **72,** 1268 (1947–48).
[59a] I. R. Weingarten, The absorption of microwaves by gases at high pressure, thesis, Columbia University (1948).
[60] H. E. White, Introduction to atomic spectra (McGraw Hill Book Co., Inc., New York, N. Y., 1948).
[61] T. Y. Wu, Vibrational spectra and the structure of polyatomic molecules (J. W. Edwards, Ann Arbor, Mich., 1946).

Index

By Chemical Symbol

	Page
1. AsF_3	614
2. BH_3CO	614
3. BrCN	615
4. CF_2CH_2	616
5. CF_3CH_3	616
6. $CHClF_2$	616
7. CH_2Br_2	616
8. CH_2CF_2	616
9. CH_2Cl_2	617
10. CH_3Br	617
11. CH_3CCH	618
12. CH_3Cl	618
13. CH_3CN	618
14. CH_3F	618
15. CH_3I	618
16. CH_3NC	619
17. CH_3NCS	619
18. CH_3NH_2	619
19. CH_3NO_2	620
20. CH_3OH	620
21. CH_3SCN	620
22. C_2H_3Cl	620
23. C_2H_4O	621
24. C_3H_4	618
25. ClCN	621
26. COS	626
27. COSe	627
28. HCF_3	622
29. HCN	622
30. H_2CO	622
31. H_2O	622
32. HNCS	622
33. ICl	623
34. ICN	623
35. NH_3	624
36. N_2O	626
37. O_2	626
38. OCS	626
39. OCSe	627
40. PF_3	627
41. SiH_3Cl	627
42. SO_2	628
43. SPF_3	628

By Name

	Page
Ammonia	624
Arsenic trifluoride	614
Borine carbonyl	614
Carbonyl selenide	627
Carbonyl sulfide	626
Chlorodifluoromethane	616
Chlorosilane	627
Cyanogen bromide	615
Cyanogen chloride	621
Cyanogen iodide	623
Difluorochloroform	616
Difluoroethylene (Uns.)	616
Ethylene oxide	621
Fluoroform	622
Formaldehyde	622
Hydrocyanic acid	622
Iodine chloride	623
Isothiocyanic acid	622
Methanol	620
Methyl acetylene	618
Methyl alcohol	620
Methyl bromide	617
Methyl chloride	618
Methyl cyanide	618
Methyl fluoride	618
Methyl fluoroform	616
Methyl iodide	618
Methyl isocyanide	619
Methyl isothiocyanate	619
Methyl thiocyanate	620
Methylamine	619
Methylene bromide	616
Methylene chloride	617
Nitromethane	620
Nitrous oxide	626
Oxygen	626
Phosphorus trifluoride	627
Phosphorus sulfatrifluoride	628
Propyne	618
Sulfur dioxide	628
Vinyl chloride	620
Water	622

WASHINGTON, February 14, 1949.

INDEX TO VOLUME 44

A

Page

Acetylglycosyl halides, stabilization, RP2068 ... 173
Acquista, N., Earle K. Plyler, W. Harold Smith, Infrared spectra of bromochloromethane, dibromomethane, tribromochloromethane, and tetrabromomethane, RP2097 ... 503
Alloys of phosphorus with nickel and cobalt, electrodeposition, RP2061 ... 109
Alloys, magnesium, stress corrosion, RP2074 ... 233
Antenna, multiple-wire delta, for ionosphere studies, RP2094 ... 475

B

Back-scatter observation by the Central Radio Propagation Laboratory, RP2071 ... 199
Barceló, José F., Infrared absorption spectra of hexafluoroethane and of chloropentafluoroethane, P P2099 ... 521
Behrent, Lewis F., Myron C. Selby, A bolometer bridge for standardizing radio-frequency voltmeters, RP2055 ... 15
Belknap, Marion A., Deane B. Judd, Lorenzo Plaza, A suggested relocation and respacing of the Union colorimeter scale for lubricating oil and petrolatum, RP2103 ... 559
—, *Kasson S. Gibson*, Permanence of glass standards of spectral transmittance, RP2093 ... 463
Benzene, alkyl derivatives, refractive index, RP2085 ... 373
Benzene, bis(trifluoromethyl), heats of reaction with cobaltic fluoride, RP2092 ... 457
Bernoulli polynomials, modified, table of, RP2060 ... 103
Bernoulli polynomials used in conjunction with solution of the telegrapher's equation, RP2059 ... 89
Blanch, Gertrude, Roselyn Siegel, Table of modified Bernoulli polynomials, RP2060 ... 103
Bloom, Evelyn G., Fred L. Mohler, Laura Williamson, C. Edward Wise, Edmund J. Wells, Helen M. Dean, Mass spectra of nonanes, RP2078 ... 291
Brass, corrosion in soils, RP2077 ... 259
Brenner, Abner, Dwight E. Couch, Eugenia Kellogg Williams, Electrodeposition of alloys of phosphorus with nickel or cobalt, RP2061 ... 109
Brickwedde, F. G., Ralph S. Jessup, Martin T. Wechsler, Heat of fluorination of cobaltous fluoride, and the heats of reaction of cobaltic fluoride with hydrogen and with bis(trifluoromethyl) benzene (α, α, α, α', α', α'-hexafluoroxylene), RP2092 ... 457
Burnett, Jr., Harry C., Herbert C. Vacher, A note on the formation and structure of iron dendrites in a magnesium alloy, RP2090 ... 443

C

Carter, J., C. E. Weir, Rate of shrinkage of tendon collagen: Further effects of tannage and liquid environment on the activation constants of shrinkage, RP2106 ... 599
Cast iron, corrosion in soils, RP2057 ... 47
Cellulose and nitrocellulose, heats of combustion and formation, RP2086 ... 387
Cellulose, infrared spectrum, effect of hydrogen-bonding on, RP2080 ... 313
Chromaticity, incandescent lamp standards, RP2053 ... 1
Cleek, Giten W., Donald Hubbard, Gerald F. Rynders, Electrode function (pH response), hygroscopicity, and chemical durability of Na_2O-CaO-SiO_2 glasses, RP2076 ... 247
Cobalt and nickel, alloys of phosphorus with, electrodeposition, RP2061 ... 109
Cobalt-60, concrete as a protective barrier for gamma rays from, RP2066 ... 157
Cobaltic fluoride, heats of reaction, RP2092 ... 457
Cobaltous fluoride, heat of fluorination, RP2092 ... 457
Collagen, influence of temperature on adsorption of water vapor by, RP2056 ... 31
Collagen, tendon shrinkage, RP2106 ... 599
Color of petroleum products, revision of Union scale, RP2103 ... 549
Color temperature, 1949 scale, RP2053 ... 1
Colorimetry, standard illuminants, RP2053 ... 1
Cones, M. N., H. V. Cottony, J. M. Watts, A 600-ohm multiple-wire delta antenna for ionosphere studies, RP2094 ... 475
Cooter, Irvin L., Pulse packing in magnetic recording wire, RP2067 ... 163
Copper, corrosion in soils, RP2077 ... 259
Corrosion of metals in soils:
RP2057 ... 47
RP2077 ... 259
Corrosion, stress, of magnesium alloys, RP2074 ... 233
Cottony, H. V., H. N. Cones, J. M. Watts, A 600-ohm multiple-wire delta antenna for ionosphere studies, RP2094 ... 475
Couch, Dwight E., Abner Brenner, Eugenia Kellogg Williams, Electrodeposition of alloys of phosphorus with nickel or cobalt, RP2061 ... 109
Crystal growth in glasses, and liquidus temperature of, RP2096 ... 495
Crystallization and second-order transitions in silicone rubbers, RP2084 ... 367
Current distribution within a waveguide, field generated by, RP2070 ... 193
Curtis, Harvey L., Determination of curvature by an osculometer, RP2063 ... 131
Curvature, determination by an osculometer, RP2063 ... 131
Cyclohexane, alkyl derivatives, refractive index, RP2085 ... 373
Cyclopentane, alkyl derivatives, refractive index, RP2085 ... 373
Cyclopentanes, separation from fraction of petroleum:
RP2065 ... 141
RP2088 ... 411

D

Dean, Helen M., Fred L. Mohler, Laura Williamson, C. Edward Wise, Edmund J. Wells, Evelyn G. Bloom, Mass spectra of nonanes, RP2078 ... 291
Dendrites in magnesium, alloy formation and structure, RP2090 ... 443
Denison, Irving A., Melvin Romanoff, Soil-corrosion studies, 1946 and 1948: Copper alloys, lead, and zinc, RP2077 ... 259
—, —, Soil-corrosion studies: Ferrous metals and alloys, RP2057 ... 47
Deuteration, effect on infrared spectrum of cellulose, RP2080 ... 313
Dibeler, Vernon H., Reduction of halomethanes with lithium aluminum hydride, RP2083 ... 363
—, *Fred L. Mohler, Laura Williamson*, Mass spectra of diborane-d_8 and ethane-d_6, RP2095 ... 489
—, *C. Edward Wise, Robert M. Reese, Fred L. Mohler*, Introduction of measured liquid samples into the mass spectrometer, RP2072 ... 215
Diborane-d_8 and ethane-d_6, mass spectra, RP2095 ... 489
Differential equations, note on numerical integration, RP2101 ... 549
Donsker, M. D., M. Kac, A sampling method for determining the lowest eigenvalue and the principal eigenfunction of Schrödinger's equation, RP2102 ... 551
Driscoll, Raymond L., Harold A. Thomas, John A. Hipple, Measurement of the proton moment in absolute units, RP2104 ... 569
Dussinger, Cecil S., Thomas W. Mears, Abraham Fookson, Philip Pomerantz, Edwin H. Rich, Frank L. Howard, Syntheses and properties of two olefins, six paraffins, and their intermediates, RP2079 ... 299

E

Eigenvalue and eigenfunction of Schrödinger's equation, RP2102 ... 551
Electrodeposition of phosphides of nickel and cobalt, RP2061 ... 109
Electron micrographs of disintegrated wool, RP2054 ... 9
Emerson, Walter R., Chauncey G. Peters, Interference methods for producing and calibrating end standards, RP2089 ... 419
End standards, production and calibration, RP2089 ... 419
Energy levels and g-values of tantalum, RP2075 ... 245
Esters, stabilization by addition of alkaline earth carbonate, RP2068 ... 173

Page

Ethane-d_6 and diborane-d_6, mass spectra, RP2095 489
Eubank, William R., Phase-equilibrium studies of the high-lime portion of the quinary system Na_2O-CaO-Al_2O_3-Fe_2O_3-SiO_2, RP2069 .. 175
Expansion, thermal and moisture, of granite, RP2087 395

F

Fibers, disintegration of wool in abrasion tests, RP2054 9
Fluorocarbons, absorption spectra of two, RP2099 521
Fookson, Abraham, Thomas W. Mears, Philip Pomerantz, Edwin H. Rich, Cecil S. Dussinger, Frank L. Howard, Syntheses and properties of two olefins, six paraffins, and their intermediates, RP2079 299
Forsythe, George E., Solution of the telegrapher's equation with boundary conditions on only one characteristic, RP2059 89
Forziati, Alphonse F., Refractive index as a function of wavelengths for sixty API-NBS hydrocarbons, RP2085 373
Fractionation, separation of hydrocarbons from petroleum by:
RP2065 141
RP2088 411
Freeman, J. J., The field generated by an arbitrary current distribution within a waveguide, RP2070 193
Frush, Harriet L., Horace S. Isbell, Note on the stabilization of acetylglycosyl halides and sugar acetates, RP2068 173

G

Gamma rays from cobalt-60, concrete as a protective barrier, RP2066 .. 157
Gas analyses of carburetted water-gas, RP2098 509
Gibson, Kasson S., Marion A. Belknap, Permanence of glass standards of spectral transmittance, RP2093 463
Glasgow, Jr., Augustus R., Charles B. Willingham, Frederick D. Rossini, Hydrocarbons in the 108° to 116° C fraction of petroleum, RP2065 .. 141
—, —, —, Separation of 2,3-dimethylpentane, 1,*cis*-3-dimethylcyclopentane, and 3-ethylpentane from petroleum, RP2088 411
Glass standards of spectral transmittance, RP2093 463
Glasses, determination of liquidus temperature and rates of crystal growth, RP2096 495
Glasses, soda-lime-silica, electrode function, chemical durability, and hygroscopicity, RP2076 247
Gloss, specular, measurement, RP2105 585
Granites, expansion, thermal and moisture, RP2087 395
Grauer, Oscar H., Edgar H. Hamilton, An improved apparatus for the determination of liquidus temperature and rates of crystal growth in glasses, RP2096 495
Greene, Frank M., Influence of the ground on the calibration and use of VHF field-intensity meters, RP2062 123
—, *Max Solow*, Development of very high frequency field-intensity standards, RP2100 527
Ground influence on the calibration and use of VHF field-intensity meters, RP2062 123
g-values and energy levels of tantalum, RP2075 245
Gyromagnetic ratio of proton, RP2104 569

H

Halides, acetylglycosyl, stabilization by use of alkaline earth carbonate, RP2068 173
Halomethanes, reduction with lithium aluminum hydride, RP2083 ... 363
Hamilton, Edgar H., Oscar H. Grauer, An improved apparatus for the determination of liquidus temperature and rates of crystal growth in glasses, RP2096 495
Hammond, III, Harry K., Isadore Nimeroff, Measurement of sixty-degree specular gloss, RP2105 585
Harrison, G. R., C. C. Kiess, W. J. Hitchcock, Preliminary list of levels and *g*-values for Ta II, RP2075 245
Hartsfield, W. L., S. M. Ostrow, R. Silberstein, Back-scatter observations by the Central Radio Propagation Laboratory—August 1947 to March 1948, RP2071 199
Heat of fluorination of cobaltous fluoride and the heats of reaction of cobaltic fluoride, RP2092 457
Heat of permeation of leather, RP2082 347
Heats of combustion and formation of cellulose and nitrocellulose, RP2086 387
Heats of polymerization, published values, RP2073 221
Hessing, Harold, Hugh L. Logan, Stress corrosion of wrought magnesium base alloys, RP2074 233

Page

Hexafluoroethane and chloropentafluoroethane, absorption spectra, RP2099 521
Hexafluoroxylene, heat of reaction with cobaltic fluoride, RP2092 457
Hippel, John A., Harold A. Thomas, Raymond L. Driscoll, Measurement of the proton moment in absolute units, RP2104 569
Hitchcock, W. J., C. C. Kiess, G. R. Harrison, Preliminary list of levels and *g*-values for Ta II, RP2075 245
Hockman, Arthur, Daniel W. Kessler, Thermal and moisture expansion studies of some domestic granites, RP2087 395
Hoge, Harold J., Vapor pressure and fixed points of oxygen and heat capacity in the critical region, RP2081 321
Howard, Frank L., Thomas W. Mears, Abraham Fookson, Philip Pomerantz, Edwin H. Rich, Cecil S. Dussinger, Syntheses and properties of two olefins, six paraffins, and their intermediates, RP2079 .. 299
Hubbard, Donald, Given W. Cleek, Gerald F. Rynders, Electrode function (pH response), hygroscopicity, and chemical durability of Na_2O-CaO-SiO_2 glasses, RP2076 247
Hydrocarbons, refractive index, RP2085 373
Hydrocarbons, separation from petroleum:
RP2065 141
RP2088 411
Hydrocarbons, syntheses and properties, RP2079 299
Hydrogen-bonding, effect on infrared spectrum of cellulose, RP2080 .. 313
Hydrogen, heat of reaction with cobaltic fluoride, RP2092 457

I

Infrared spectra of cellulose, RP2080 313
Infrared spectra of four methane derivatives, RP2097 503
Infrared spectra of hexafluoroethane and chloropentafluoroethane, RP2099 521
Interference methods for producing and calibrating end standards, RP2089 419
Ionosphere studies, multiple-wire delta antenna for, RP2094 475
Iron and steel, corrosion in soils, RP2057 47
Iron dendrites in a magnesium alloy, formation and structure, RP2090 .. 443
Isbell, Horace S., Harriet L. Frush, Note on the stabilization of acetylglycosyl halides and sugar acetates, RP2068 173

J

Jessup, Ralph S., Edward J. Prosen, Heats of combustion and formation of cellulose and nitrocellulose (cellulose-nitrate), RP2086 387
—, *F. G. Brickwedde, Martin T. Wechsler*, Heat of fluorination of cobaltous fluoride, and the heats of reaction of cobaltic fluoride with hydrogen and with bis(trifluoromethyl)benzene ($\alpha, \alpha, \alpha, \alpha', \alpha', \alpha'$-hexafluoroxylene), RP2092 457
Judd, Deane B., Lorenzo Plaza, Marion A. Belknap, A suggested relocation and respacing of the Union colorimeter scale for lubricating oil and petrolatum, RP2103 559
—, The 1949 scale of color temperature, RP2053 1

K

Kac, M., M. D. Donsker, A sampling method for determining the lowest eigenvalue and the principal eigenfunction of Schrodinger's equation, RP2102 551
Kanagy, Joseph R., Influence of temperature on the adsorption of water by collagen and leather, RP2056 31
—, *Robert A. Vickers, III*, Factors affecting the water vapor permeability of leather, RP2082 347
Kennedy, Robert J., Harold O. Wyckoff, William A. Snyder, Concrete as a protective barrier for gamma rays from cobalt-60, RP2066 157
Kessler, Daniel W., Arthur Hockman, Thermal and moisture expansion studies of some domestic granites, RP2087 395
Kiess, C. C., G. R. Harrison, W. J. Hitchcock, Preliminary list of levels and *g*-values for Ta II, RP2075 245
Kisliuk, Paul, Charles M. Townes, Molecular microwave spectra tables, RP2107 611
Krasny, John F., Herbert F. Schiefer, Note on the disintegration of wool in abrasion tests, RP2054 9

L

Page

Lamps and wavelengths of mercury 198, RP2091 447
Lead, corrosion in soils, RP2077 259
Leather, influence of temperature on adsorption of water vapor by, RP2056 31
Leser, W. H., C. E. Weir, L. A. Wood, Crystallization and second-order transitions in silicone rubbers, RP2084 367
Levels and *g*-values of tantalum, RP2075 245
Liquidus temperature of and rate of crystal growth in glasses, RP2096 495
Lithium aluminum hydride, reaction with halomethanes, RP2083 363
Logan, Hugh L., Harold Hessing, Stress corrosion of wrought magnesium base alloys, RP2074 233
London, Albert, Transmission of reverberant sound through double walls, RP2058 77

M

Modorsky, Samuel L., A multicolumn countercurrent molecular still, RP2064 135
Magnesium alloy containing iron dendrites, formation and structure, RP2090 443
Magnesium alloys, wrought, stress corrosion, RP2074 233
Magnetic recording wire, pulse packing in, RP2067 163
Mass spectra of diborane-d_8 and ethane-d_6, RP2095 489
Mass spectrometer, introduction of liquid samples into, RP2072 215
Mass spectrometric analysis of carburetted water-gas, RP2098 509
Mears, Thomas W., Abraham Fookson, Philip Pomerantz, Edwin H. Rich, Cecil S. Dussinger, Frank L. Howard, Syntheses and properties of two olefins, six paraffins, and their intermediates, RP2079 299
Meggers, William F., F. Oliver Westfall, Lamps and wavelengths of mercury 198, RP2091 447
Mercury 198, spectra, RP2091 447
Metals and alloys, underground corrosion:
RP2057 47
RP2077 259
Methane derivatives, absorption spectra, RP2097 503
Methane, preparation by reaction of lithium aluminum hydride and halomethanes, RP2083 363
Microwave, molecular, spectra tables, RP2107 611
Milne, W. E., Note on the Runge-Kutta method, RP2101 549
Mohler, Fred L., Vernon H. Dibeler, Laura Williamson, Mass spectra of diborane-d_8 and ethane-d_6, RP 2095 489
—, *Laura Williamson, C. Edward Wise, Edmund J. Wells, Helen M. Dean, Evelyn G. Floom*, Mass spectra of nonanes, RP2078 291
—, *C. Edward Wise, Robert M. Reese, Vernon H. Dibeler*, Introduction of measured liquid samples into the mass spectrometer, RP2072 215
Molecular still, a multicolumn countercurrent, RP2064 135
Multiple-wire delta antenna for ionosphere studies, RP2094 475

N

Nickel and cobalt, alloys of phosphorus with, electrodeposition, RP2061 109
Nimeroff, Ladore, Harry K. Hammond, III, Measurement of sixty-degree specular gloss, RP2105 585
Nitrocellulose, heats of combustion and formation, RP2086 387
Nonanes, mass spectra, RP2078 291
Numerical analysis, integration of differential equations, RP2101 549

O

Oil, lubricating, revision of color scale for, RP2103 559
Oscillatory pressures, attenuation of, in instrument lines, RP2108 643
Osculometer, determination of curvature by, RP2063 131
Ostrow, S. M., W. L. Hartsfield, R. Silberstein, Back-scatter observations by the Central Radio Propagation Laboratory—August 1947 to March 1948, RP2071 199
Oxygen, vapor pressure, heat capacity, triple point, critical constants, and transition temperatures, RP2081 321

P

Paraffins, refractive index, RP2085 373
Paraffins, separation from fraction of petroleum:
RP2065 141
RP2088 411
Permeability of leather to water vapor, RP2082 347
Peters, Chauncey G., Walter B. Emerson, Interference methods for producing and calibrating end standards, RP2089 419
Petroleum products, revision of color scale, RP2103 559
Petroleum, separation of hydrocarbons from:
RP2065 141
RP2088 411
Phase-equilibrium, Na_2O-CaO-Al_2O_3-Fe_2O_3-SiO_2, RP2069 175
Phosphorus alloys with cobalt and nickel, electrodeposition, RP2061 109
Plaza, Lorenzo, Deane B. Judd, Marion A. Belknap, A suggested relocation and respacing of the Union colorimeter scale for lubricating oil and petrolatum, RP2103 559
Plyler, Earl K., John W. Rowen, Effect of deuteration, oxidation, and hydrogen bonding on the infrared spectrum of cellulose, RP2080 313
—, *W. Harold Smith, N. Acquista*, Infrared spectra of bromochloromethane, dibromomethane, tribromochloromethane, and tetrabromomethane, RP2097 503
Pomerantz, Philip, Thomas W. Mears, Abraham Fookson, Edwin H. Rich, Cecil S. Dussinger, Frank L. Howard, Syntheses and properties of two olefins, six paraffins, and their intermediates, RP2079 299
Polymerization, heats of, published values, RP2073 221
Polynomials, Bernoulli, used in conjunction with solution of the telegrapher's equation, RP2059 89
Polynomials, table of modified Bernoulli, RP2060 103
Portland cement, phase-equilibrium, RP2069 175
Prosen, Edward J., Ralph S. Jessup, Heats of combustion and formation of cellulose and nitrocellulose (cellulose nitrate), RP2086 387
Proton moment, measurement, RP2104 569
Pulse packing in magnetic recording wire, RP2067 163

Q, R

Quinary system, Na_2O-CaO-Al_2O_3-Fe_2O_3-SiO_2, phase equilibrium, RP2069 175
Radiant flux, spectral distribution, standards, RP2053 1
Radio field-intensity measurements, RP2100 527
Radio field-intensity meters (VHF), calibration, RP2062 123
Radio-frequency voltmeters, standardizing, RP2055 15
Radio ionosphere studies, multiple-wire delta antenna for, RP2094 475
Radio Propagation Laboratory, Central, back-scatter observations, RP2071 199
Reese, Robert M., C. Edward Wise, Vernon H. Dibeler, Fred L. Mohler, Introduction of measured liquid samples into the mass spectrometer, RP2072 215
Refractive index of hydrocarbons, RP2085 373
Rich, Edwin H., Thomas W. Mears, Abraham Fookson, Philip Pomerantz, Cecil S. Dussinger, Frank L. Howard, Syntheses and properties of two olefins, six paraffins, and their intermediates, RP2079 299
Roberts, Donald E., Heats of polymerization. A summary of published values and their relation to structure, RP2073 221
Romanoff, Melvin, Irving A. Denison, Soil-corrosion studies, 1946: Ferrous metals and alloys, RP2057 47
—, —, Soil-corrosion studies, 1946 and 1948: Copper alloys, lead, and zinc, RP2077 259
Rossini, Frederick D., Augustus R. Glasgow, Jr., Charles B. Willingham, Hydrocarbons in the 108° to 116° C fraction of petroleum, RP2065 141
—, —, —, Separation of 2,3-dimethylpentane, 1, *cis*-3-dimethylcyclopentane, and 3-ethylpentane from petroleum, RP2088 411
Rowen, John W., Earle K. Plyler, Effect of deuteration, oxidation, and hydrogen bonding on the infrared spectrum of cellulose, RP2080 313
Rubbers, silicone, crystallization and second-order transitions, RP2084 367
Runge-Kutta method, note on, RP2101 549
Rynders, Gerald F., Donald Hubbard, Given W. Cleek, Electrode function (pH response), hygroscopicity, and chemical durability of Na_2O-CaO-SiO_2 glasses, RP2076 247

S

Schiefer, Herbert F., John F. Krasny, Note on the disintegration of wool in abrasion tests, RP2054 9
Schrödinger's equation, determination of lowest eigenvalue and principal eigenfunction, RP2102 551
Selby, Myron C., Lewis F. Behrent, A bolometer bridge for standardizing radio-frequency voltmeters, RP2055 15

Page

Shepherd, Martin, Mass spectrometric analysis of a standard sample of carburetted water-gas by laboratories cooperating with the American Society for Testing Materials, RP2098 ... 509
Shrinkage of tendon collagen, RP2106 ... 599
Siegel, Roselyn, Gertrude Blanch, Table of modified Bernoulli polynomials, RP2090 ... 103
Silberstein, R., W. L. Hartsfield, S. M. Ostrow, Back-scatter observations by the Central Radio Propagation Laboratory—August 1947 to March 1948, RP2071 ... 199
Silicone rubbers, crystallization and second-order transitions, RP2084 ... 367
Smith, W. Harold, Earle K. Plyler, N. Acquista, Infrared spectra of bromochloromethane, dibromomethene, tribromochloromethane, and tetrabromomethane, RP2097 ... 503
Snyder, William A., Robert J. Kennedy, Harold O. Wyckoff, Concrete as a protective barrier for gamma rays from cobalt-60, RP2066 ... 157
Soda-lime-silica, electrode function, chemical durability, and hygroscopicity, RP2076 ... 247
Soil corrosion of metals and alloys:
RP2057 ... 47
RP2077 ... 259
Solow, Max, Frank M. Greene, Development of very high frequency field-intensity standards, RP2100 ... 527
Sound, transmission through double walls, RP2058 ... 77
Spectra, infrared, of cellulose, RP2080 ... 313
Spectra, infrared, of four methane derivatives, RP2097 ... 503
Spectra, infrared, of hexafluoroethane and of chloropentafluoroethane, RP2099 ... 521
Spectra, mass, of diborane-d_6 and ethane-d_6, RP2095 ... 489
Spectra, mass, of nonanes, RP2078 ... 291
Spectra of mercury 198, RP2091 ... 447
Spectra tables, molecular microwave, RP2107 ... 611
Spectra distribution of radiant flux, standards, RP2053 ... 1
Spectral transmittance, glass standards of, RP2093 ... 463
Spectrometer, mass, introduction of liquid samples into, RP2072 ... 215
Standards, glass, of spectral transmittance, RP2093 ... 463
Steel, corrosion in soils, RP2057 ... 47
Still, molecular, multicolumn countercurrent, RP2064 ... 135
Stress corrosion of wrought magnesium base alloys, RP2074 ... 233
Syntheses and properties of eight hydrocarbons, RP2079 ... 299

T, U

Tantalum, energy levels and g-values, RP2075 ... 245
Telegrapher's equation, solution, RP2059 ... 89
Temperature, influence on adsorption of water vapor by collagen and leather, RP2056 ... 31
Textiles, disintegration of wool, in abrasion tests, RP2054 ... 9
Thermal expansion of granite, RP2087 ... 395
Thomas, Harold A., Raymond L. Driscoll, John A. Hipple, Measurement of the proton moment in absolute units, RP2104 ... 569
Townes, Charles M., Paul Kisliuk, Molecular microwave spectra tables, RP2107 ... 611
Transmittance, spectral, glass standards, RP2093 ... 463
Union colorimeter scale, revision of, RP2103 ... 559

V

Page

Vacher, Herbert C., Harry C. Burnett, Jr., A note on the formation and structure of iron dendrites in a magnesium alloy, RP2090 ... 443
Vapor pressure, heat capacity, triple point, critical constants, and transition temperatures of oxygen, RP2081 ... 321
Vickers, III, Robert A., Joseph R. Kanagy, Factors affecting the water permeability of leather, RP2082 ... 347
Voltmeters, radio-frequency, a bolometer bridge for standardizing, RP2055 ... 15

W, Z

Walls, double, transmission of sound, RP2058 ... 77
Water gas, carburetted, mass spectrometric analysis, RP2098 ... 509
Water vapor, adsorption by collagen and leather, effect of temperature on, RP2056 ... 31
Water-vapor, permeability of leather, RP2082 ... 347
Watts, J. M., H. N. Cones, H. V. Cottony, A 600-ohm multiple-wire delta antenna for ionosphere studies, RP2094 ... 475
Waveguide, field generated by an arbitrary current distribution within, RP2070 ... 193
Wechsler, Martin T., Ralph S. Jessup, F. G. Brickwedde, Heat of fluorination of cobaltous fluoride, and the heats of reaction of cobaltic fluoride with hydrogen and with bis(trifluoromethyl)benezene ($\alpha, \alpha, \alpha, \alpha', \alpha', \alpha'$-hexafluoroxylene), RP2092 ... 457
Wells, Edmund J., Fred L. Mohler, Laura Williamson, C. Edward Wise, Helen M. Dean, Evelyn G. Bloom, Mass spectra of nonanes, RP2078 ... 291
Weir, C. E., J. Carter, Rate of shrinkage of tendon collagen: Further effects of tannage and liquid environment on the activation constants of shrinkage, RP2106 ... 599
—, *W. H. Leser, L. A. Wood*, Crystallization and second-order transitions in silicone rubbers, RP2084 ... 367
Westfall, F. Oliver, William F. Meggers, Lamps and wavelengths of mercury 198, RP2091 ... 447
Williams, Eugenia Kellogg, Abner Brenner, Dwight E. Couch, Electrodeposition of alloys of phosphorus with nickel or cobalt, RP2061 ... 109
Williamson, Laura, Fred L. Mohler, C. Edward Wise, Edmund J. Wells, Helen M. Dean, Evelyn G. Bloom, Mass spectra of nonanes, RP2078 ... 291
—, *Vernon H. Dibeler, Fred L. Mohler*, Mass spectra of diborane-d_6 and ethane-d_6, RP2095 ... 489
Willingham, Charles B., Augustus R. Glasgow, Jr., Frederick D. Rossini, Hydrocarbons in the 108° to 116° C fraction of petroleum, RP2065 ... 141
—, —, —, Separation of 2,3-dimethylpentane, 1, *cis*-3-dimethylcyclopentane, and 3-ethylpentane from petroleum, RP2088 ... 411
Wire, magnetic recording, pulse packing in, RP2067 ... 163
Wise, C. Edward, Fred L. Mohler, Laura Williamson, Edmund J. Wells, Helen M. Dean, Evelyn G. Bloom, Mass spectra of nonanes, RP2078 ... 291
—, *Robert M. Reese, Vernon H. Dibeler, Fred L. Mohler*, Introduction of measured liquid samples into the mass spectrometer, RP2072 ... 215
Wood, L. A., C. E. Weir, W. H. Leser, Crystallization and second-order transitions in silicone rubbers, RP2084 ... 367
Wool, abrasion tests, RP2054 ... 9
Wyckoff, Harold O., Robert J. Kennedy, William A. Snyder, Concrete as a protective barrier for gamma rays from cobalt-60, RP2066 ... 157
Zinc, corrosion in soils, RP2077 ... 259

U. S. GOVERNMENT PRINTING OFFICE: 1950

Engineering Library

JUL 5 '50

Journal of Research

of the

National Bureau of Standards

JUNE 1950

VOLUME 44 NUMBER 6

PERIODICALS OF THE NATIONAL BUREAU OF STANDARDS

As the principal agency of the Federal Government for fundamental research in physics, chemistry, mathematics, and engineering, the National Bureau of Standards conducts projects in fifteen fields: electricity, optics, metrology, heat and power, atomic and radiation physics, chemistry, mechanics, organic and fibrous materials, metallurgy, mineral products, building technology, applied mathematics, commodity standards, electronics, and radio propagation. The Bureau has custody of the national standards of measurement and conducts research leading to the improvement of scientific and engineering standards and of techniques and methods of measurement. Testing methods and instruments are developed; physical constants and properties of materials are determined; and technical processes are investigated.

Journal of Research

Internationally known as a leading scientific periodical, the Journal presents research papers by authorities in the specialized fields of physics, mathematics, chemistry, and engineering. Complete details of the work are presented, including laboratory data, experimental procedures, and theoretical and mathematical analyses. Each of the monthly issues averages 100 two-column pages; illustrated. Annual subscription: domestic, $4.50; foreign, $5.50.

Technical News Bulletin

Summaries of current research at the National Bureau of Standards are published each month in the Technical News Bulletin. The articles are brief, with emphasis on the results of research, chosen on the basis of their scientific or technologic importance. Lists of all Bureau publications during the preceding month are given, including Research Papers, Handbooks, Applied Mathematics Series, Building Materials and Structures Reports, and Circulars. Each issue contains 12 or more two-column pages; illustrated. Annual subscription: domestic, $1.00; foreign $1.35.

Basic Radio Propagation Predictions

The Predictions provide the information necessary for calculating the best frequencies for communication between any two points in the world at any time during the given month. The data are important to all users of long-range radio communications and navigation, including broadcasting, airline, steamship, and wireless services, as well as to investigators of radio propagation and ionosphere. Each issue, covering a period of one month, is released three months in advance and contains 16 large pages, including pertinent charts, drawings, and tables. Annual subscription: domestic, $1.00; foreign, $1.25.

Order all publications from the Superintendent of Documents,
U. S. Government Printing Office, Washington 25, D. C.

The printing of this publication has been approved by the Director of the Bureau of the Budget, April 6, 1950.